Combined Armature And Field Voltage Control Of DC Motor

التحكم المشترك لمحركات التيار المباشر باستخدام ملفي عضو الانتاج والمجال

By

Khalid Mohamed Ali Tahsoun Alshehhi

Student ID number 120164

Dissertation submitted in partial fulfillment of

MSc Systems Engineering

Faculty of Engineering & IT

Dissertation Supervisor

Professor Robert Whalley

December -2014-

Abstract

In this research work a multivariable feedback control system for the separately excited DC motor is presented. The control inputs are the motor armature and the motor field voltages, while the controlled outputs are the motor angular speed and the motor field current. Three different multivariable control systems were designed and compared. The first control system uses the new advances in the multivariable control theory, namely, the least effort controller, developed by Whalley, R. and Ebrahimi, M. The performance of the system with this controller is compared with the performance of the system with other two controllers. One from the classical control school, using the Inverse Nyquist Array approach, and the other from the modern control school, using the Optimal Control approach. The comparison between the three types of controllers includes the general control performance, suitability and applicability, disturbance recovery capability and the energy consumed by the control system itself. This work concludes that the new least effort control technique provides the simplest controller with superior performance and disturbance recovery capability.

This should promote the implementation of this new type of controllers for general multivariable applications.

Keyword : least effort control, inverse Nyquist array, optimal control, separately excited DC motor.

ملخص

يتضمن هذا البحث تصميم نظام تحكم بتغذية راجعة وبمتغيرات متعددة لمحرك تيار مباشر ذو تهيج مستقل. مداخل التحكم للنظام هي جهد الجزء الدوار وجهد ملف المجال للمحرك. بينما المخارج التي يتم التحكم بها فهي سرعة دوران المحرك وتيار المجال له.

تم تصميم ومقارنة أداء ثلاثة أنواع من أنظمة التحكم متعددة المتغيرات. النوع الأول من أنظمة التحكم هذه يستخدم نظرية حديثة تنميز باستراتيجية تقليل استهلاك الطاقة، حيث يتم فيها التركيز على تقليل الطاقة المستهلكة بواسطة نظام التحكم نفسه. وتم مقارنة أداء نظام التحكم هذا مع أداء نظامي تحكم أخرين مختلفين. الأول من المدرسة التقليدية للتحكم، ويستخدم مجموعة نايكويست العكسية، والثاني من المدرسة الحديثة للتحكم ، ويستخدم مبدأ التحكم المثالي.

شملت مقارنة أنظمة التحكم الثلاث المختلفة نواح مختلفة مثل الأداء العام لنظام التحكم، الصعوبات والتحديات التي تواجه تطبيقه، كفاءة النظام في مواجهة الاضطرابات التي تقابله وكذلك الطاقة المستهلكة من نظام التحكم نفسه.

لقد بينت نتائج هذه الدراسة أن التقنية الأولى، والتي يتم فيها تصميم نظام تحكم يتميز باستراتيجية تقليل استهلاك الطاقة، تؤدي لانتاج نظام تحكم بسيط وأقل تعقيداً وبأداء عالي الجودة وذو كفاءةعالية في مواجهة الاضطرابات، مما يجعل هذا النوع من أنظمة التحكم مؤهلاً لاستخدامه للتحكم في الأنظمة متعددة المتغيرات المختلفة.

Acknowledgments

I would like to show my gratitude, thanks, respect and appreciation to Professor Dr. Robert Walley, who has been a great advisor for me. Thank you Dr. Walley for encouraging me during my study and for allowing me to grow as a research scientist. Your advices have been priceless. They are the main reason for my success.

I would like also to thank Dr. Alaa Ameer for his brilliant comments and suggestions, thanks to you.

Dedication

I dedicate this work to my family for nursing me with affection and love and their dedicated partnership for success in my life.

List of Notations and Abbreviations:

The definitions of all the variables that are used in this thesis are given below:

A – System state matrix

$A(s)$ – Numerator of $G(s)$

B – System input matrix

C – System output matrix

D – System feedforward matrix

$E(t)$ – Control energy

F – Outer loop feedback array

$G(s)$ – Transfer function array

$G_N(s)$ – Transfer function array for percentage changes

$H(s)$ – Feedback path matrix model

$H(s)$ – Closed loop transfer function matrix

I – Identity matrix

J – Performance index

J – System inertia

K – State feedback matrix

$K(s)$ – Forward path matrix model

$L(s)$ – Left (row) factor array

L_f – Self inductance of the motor field winding.

P – Precompensator array

P – Solution of Riccati matrix equation

Q – Coefficient matrix

Q – State weighting matrix

$Q(s)$ – Open loop transfer function matrix

R – Input weighting matrix

$R(s)$ – Right (column) factor array

R_a – Resistance of the motor armature circuit.

R_f – Resistance of the motor field winding.

S – Controllability matrx

$S(s)$ – Sensitivity array

$T(t)$ – Motor shaft torque

$U(t)$ – System input vector

V – Observability matrix

$X(t)$ – System state vector

$Y(t)$ – System output vector

$\hat{G}$, $\hat{K}$, $\hat{Q}$, $\hat{H}$ – Inverse of G , K , Q , H matrices, respectively

$a_{i,j}$, $b_{i,j}$,…, $\gamma_{i,j}$ – Coefficient of the Q matrix

$a_{i,j}(s)$ – Elements of $A(s)$ matrix

$b(s)$ – Polynomial function

b_0 , b_1 ,…, b_{m-1} – Coefficient of $b(s)$

C – Viscous friction coefficient.

$d(s)$ – Denominator of $G(s)$

d_i – Diameter of Gershgorin circle for column i

$e(s)$ – Error signal between reference input and output

$f_1, f_2, ..., f_m$ – Outer loop feedback gains

$g_{i,j}$ – Elements of $G(s)$

$h(s)$ – Transformed measurement elements

h_1, h_2, …, h_m – Gains of $h(s)$ elements

$i_a(t)$ – Motor armature current.

$i_f(t)$ – Motor field current.

k – Forward path gain

$k(s)$ – Transformed forward path elements

k_a – Motor torque-armature current proportionality constant.

k_F – Motor torque-field current proportionality constant.

k_1 – Motor back emf-angular speed proportionality constant

k_1, k_2, …, k_m – Gains of $k(s)$ elements

m – Dimension of $A(s)$

m – Number of system inputs and outputs

n, n_1, n_2, …, n_{m-1} – Gain ratios

$r(s)$ – Transformed reference input

$\bar{r}(s)$ - transformed reference input of the inner loop

s – Laplace variable

t – Tim

$u(t)$ – System input

$u(s)$ – Transformed input

$v_a(t)$ – Motor armature voltage

$v_B(t)$ – Motor back emf voltage.

$v_f(t)$ – Motor field voltage.

$y(s)$ – Transformed output.

$y(t)$ – System output.

$\hat{g}_{ij}$, $\hat{k}_{ij}$, $\hat{q}_{ij}$, $\hat{h}_{ij}$ – Elements of the inverse of G, K, Q, H matrices, respectively

$k \times h$ – Outer product of vectors k and h

$< k, h >$ – Inner product of vectors k and h

$\Gamma(s)$ – Finite time delay array

$\delta(s)$ – Transformed disturbance input

$\delta(t)$ – Disturbance input

λ – Eigen value

$\omega(t)$ – Motor angular speed

ARE – Algebriac Riccati equration

INA – Inverse Nyquist array

L.E.C – Least effort control

LQR – Linear Quadratic Rgulator

LTI – Linear Time-invarient

MIMO – Multi-input Multi-output

O.C – Optimal Control

PID – Proportional-Integral-Derivative

SEDM – Separately Excited DC Motor

SISO – Single-input Single-output

List of Figures:

Contents:

Chapter (1)

Introduction

1.1 Research Background

Due to their excellent control characteristics, DC motors have been widely used in industrial applications. Generally, the DC motor has two windings. These are the armature winding and the field winding. In order to produce a unidirectional torque, the armature winding is supplied through brushes and a commutator that switches the direction of the current in the armature winding. Figure 1.1 shows the construction of the DC motor.

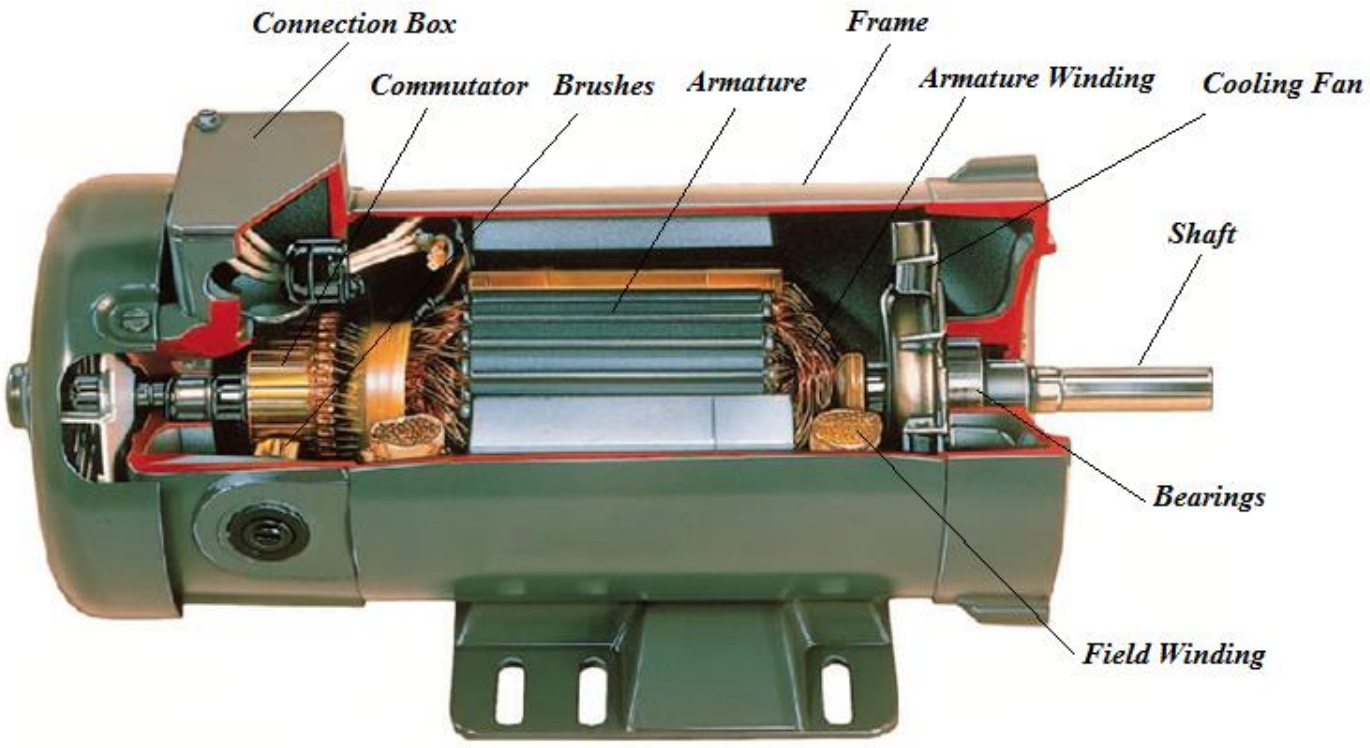

Figure 1.1: Construction of the DC motor.

To produce different characteristics, the two motor windings are usually connected in different configurations, such as, series, shunt or separately excited. In terms of the control theory, series or shunt connection of the two motor windings produces a

system with single degree of freedom, as in this case the system will have only a single input, which is the motor supply voltage. Motors with separated armature and field windings have two degrees of freedom as they have two control inputs, which are the motor armature voltage V_a and the motor field voltage V_f. These two voltages are usually supplied to the motor by two controlled DC voltage sources. The figure below shows the schematic diagram of the separately excited DC motor (SEDM).

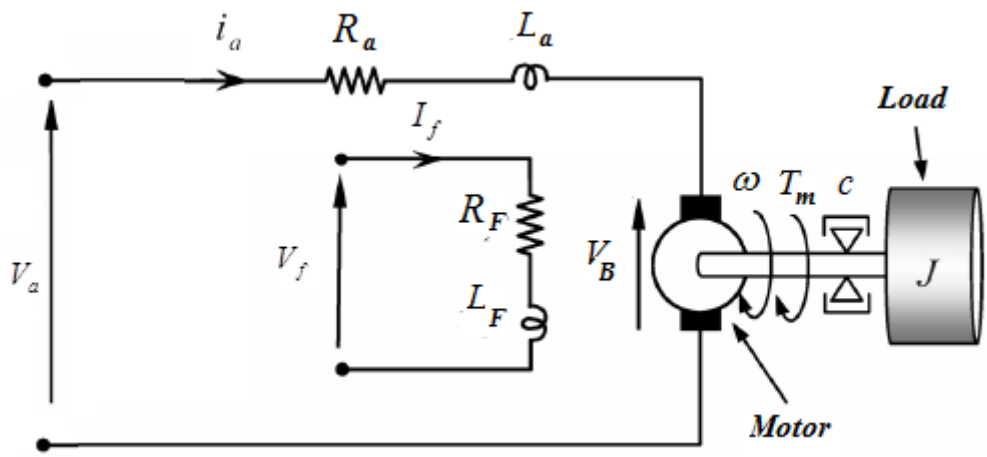

Figure 1.2: Schematic diagram of the separately-excited DC motor.

The interaction of the motor armature current and the magnetic field, produced by the current in the motor field winding, produces the motor torque. When the armature of the DC motor rotates, a voltage is induced in the armature winding. This voltage is called the back emf voltage, V_B, and it is proportional to the motor angular speed.

As a multi-input, multi-output (MIMO) system, different approaches can be used to design the controller of the separately excited DC motor. In this thesis three approaches are used. These are the least effort approach (Whalley, R. and Ebrahimi, M., 1999), the Inverse Nyquist Array approach (Rosenbrock, 1969) and the optimal control approach (Kalman R.E., 1960).

The least effort approach is based on minimizing a performance index. The controller, in this approach, has two loops; the inner loop ensures stable dynamics of the closed loop system, while the outer loop provides specified disturbance suppression conditions and provides specified steady state output decoupling (R Whalley, and M Ebrahimi, 1999).

In the inverse Nyquist array approach, developed by Rosenbrock in 1969, and in order to decrease the system output interaction, a diagonally-dominant closed-loop transfer function has to be found. This will reduce the design process to the design of a set of independent single loops, in which single-input single- output (SISO) control methods can be used. Gershgorin's band theorem will be used to test the diagonal dominance of the closed loop transfer function matrix.

In the optimal control approach, state feedback is used. The design problem is to find a state feedback matrix that will minimize a quadratic performance index, whilst simultaneously providing acceptable performance conditions.

1.2 Research Problem Statement:

This research covers the control of the separately-excited DC motor, using different control techniques. The motor is modeled as a two-input, two-output multivariable system. The armature voltage V_a and the field voltage V_f are the system input variables, while the motor shaft speed ω and the motor field current I_f are the system output variables. The output interaction, in this multivariable system, provides new restrictions on the classical control theory, as if any input is changed, it would affect all outputs.

Rrandom disturbances, that would affect the performance of the system, are expected. These disturbances may be caused by different sources as changes in the supply voltages or changes in the motor shaft loading. The control system should be designed such that the effect of these disturbances on the system performance is limited.

1.3 Research Aims and Objectives

In this research, the recent advances in the multivariable controller design approaches, namely the least effort approach, presented by Whalley, R. and Ebrahimi, M, will be applied to the case of the combined armature and field control of the separately-excited DC motor. The objective will be to design a multivariable feedback

controller, to control the angular speed and the field current of the DC motor. The armature voltage V_a and the field voltage V_f will be the control inputs, while the controlled outputs will be the motor angular speed ω and the motor field current, I_f. The above stated approach will be compared with two other approaches from the British and the American schools, these are the Inverse Nyquist Array approach and the Optimal Control approach, respectively. The comparison will include the difficulties of each approach and the complexity of the controller, the general control performance, disturbance recovery and the energy consumed by the controller.

1.4 Dissertation Organization

This Dissertation is organized in seven chapters that will include the following:
Chapter one: this chapter is the introduction to this research work. It includes the theoretical background of DC motors and their control problems. The problem statement as well as the aims and objectives, of this research work, are clearly defined in this chapter.

Chapter two: this chapter contains the summary of the literature review that was made. The literature, that has been reviewed for this research, include that covering the control methods used for DC motors, as well as the fundamentals of the multivariable feedback control theory as in the British and in the American schools.

Chapter three: this chapter forms the core of this research work. It covers modeling the DC motor as an open-loop two-input, two-output system. The motor system is modeled using state-space and transfer function representations. The characteristics and the open loop response of the DC motor are studied. The study was done by simulating the performance of the open-loop DC motor system using MATLAB®/SIMULINK®.

Chapter four: in this chapter, a feedback controller using the first approach, namely, the Least Effort approach, is designed to reach certain performance characteristics for the closed-loop system. The designed feedback controller was simulated and its performance was analyzed.

Chapter five: in this chapter a feedback controller, using the second approach, namely, the Nyquist Array approach is designed. The designed feedback controller has been also simulated and its performance has been analyzed.

Chapter six: this chapter includes the design of a feedback controller using the third approach, namely, the Optimal Control approach. The designed feedback controller has been simulated and its performance has been analyzed.

Chapter seven: this chapter includes the comparison between the performances of the feedback control systems built using the three previously mentioned approaches. It also contains the conclusions and the recommendations that have been obtained from this research work.

In addition to the above, this dissertation includes an abstract in both Arabic and English languages.

Chapter (2)

Literature Review

2.1 Introduction

The main advantage of DC motors is the speed control. As the motor angular speed, ω, is directly proportional to armature voltage and inversely proportional to the magnetic flux produced by the field current, adjusting the armature voltage and/or the field current will change the rotor angular speed.

The seperately excited DC motor (SEDM) is usually supplied by two controlled voltage sources, that can be controlled rectifiers or choppers. One source is supplying the motor armature winding with the armature voltage, V_a, and the other is supplying the motor field winding by the field voltage V_f. The speed of the SEDM can be controlled by controlling either the armature voltage V_a or the field voltage V_f, or both of them.

Usually, the voltage speed control method is used to control the speed of the SEDM below its rated speed. In this method, the field voltage V_f is kept constant, while the armature voltage V_a is varied. A constant field voltage V_f produces a constant field current I_f, which in turn, produces a constant magnetic flux in the motor air-gap. Hence, the torque produced on the motor shaft remains constant, as the armature current remains constant. The motor angular speed ω and the power on the motor shaft are linearly proportional to the armature voltage V_a.

To run the SEDM above its rated speed, the field speed control method is used. Here, the field current I_f is reduced by reducing the field voltage V_f. The magnetic flux in the motor air gap will be reduced, causing reduction of the back emf V_B. The motor armature current will increase, resulting in increasing the motor speed. As a result of that, the back emf V_B will increase and a new equilibrium will be established at a higher speed. Or

with decreasing the field voltage V_f, the motor angular speed ω increases, while the motor torque decreases and the motor shaft power remains constant.

The figure below shows the mechanical power and the torque on the shaft of the SEDM, as a function of the angular motor speed, in the two previously described control methods.

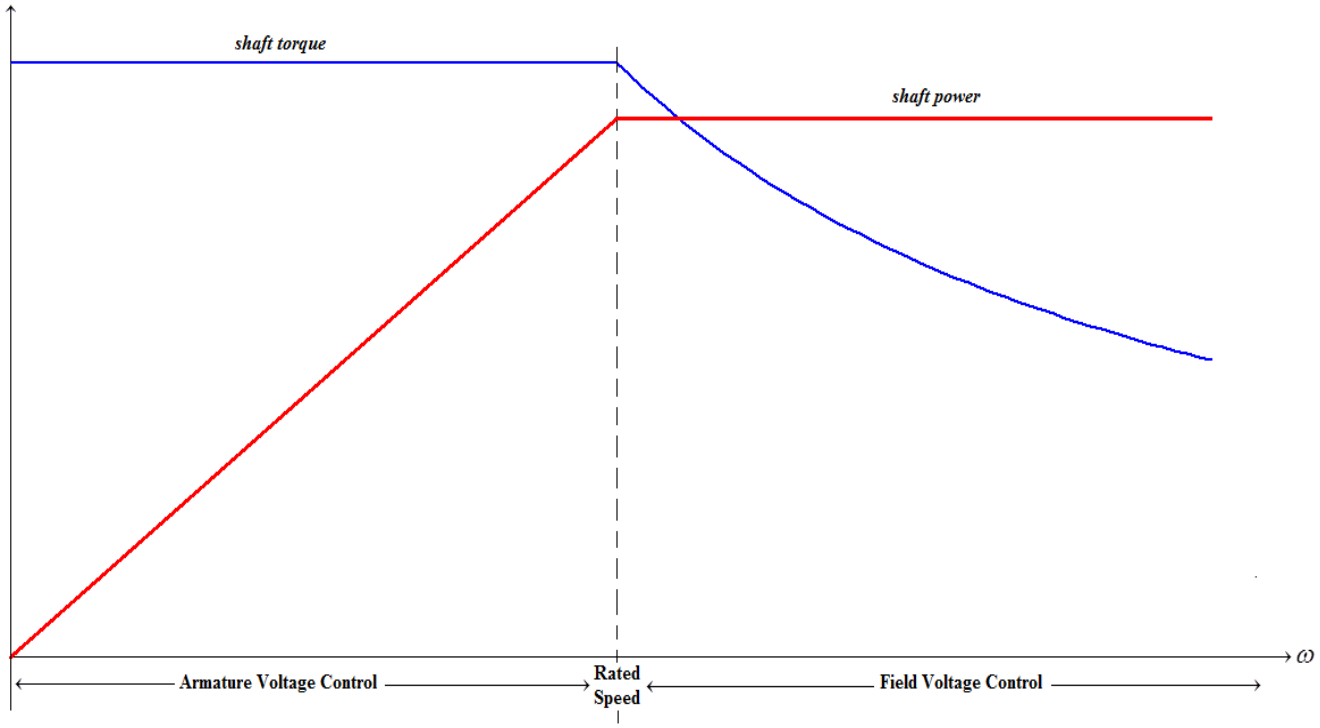

Figure 2.1: Armature voltage control and field voltage control of the separately-excited DC motor.

It has to be noted that in these two control methods, the SEDM is usually represented as a single-input single-output (SISO) system. As only one input (V_a or V_f) and only one output (ω or T) are of interest.

In this research work, the SEDM will be treated as multi-input multi-output (MIMO) system, having two control inputs and two outputs. The control inputs are the armature voltage V_a and the field voltage V_f, while the outputs are the motor angular speed ω and the motor field current I_f.

Many researches covering the therory of the multivariable control systems and the control of the SEDM have been previously done. This chapter contains a summary review of the published literature regarding these two subjects, from both the classical and the modern control schools.

2.2 Development of the Control Theory

As known, controlling a system is the process of regulating or managing the behavior of the system, in the required manner. There are two common classes of control systems; open-loop control systems and closed-loop or feedback control systems. In open loop control systems, the output is controled by the inputs only. While, in closed-loop control systems, feedback control is used. In feedback control systems, the difference between the desired and the actual values of the system variables, is used to control the system. As the system output, or part of it, is returned back to its input, the system is usually called a closed-loop system.

According to reference [28], differential equations were the early tools for the analysis of control systems. In 1868, J.C Maxwell studied the stability of Watt's fly-ball governor, as a closed-loop system, used in the feedback speed control of the steam engines. In his work, Maxwell linearized the differential equations of motion to build the characteristic equation of the system. He showed that the system is stable if the roots of the characteristic equation have negative real parts. It can be said that with the work of Maxwell the fundamentals of control theory were established. During this time, E.J. Routh and A. Hurwitz found a numerical technique for determining when a characteristic equation is describing a stable system.

In 1892, A.M Lyapunov studied the stability of nonlinear control systems. In his study, he used a generalized notion of energy. During the same year, Operational calculus was invented by Heaviside. He analyzed the transient behavior of systems, using a notion equivalent to that of the transfer function. In 1893, A.B Stodola studied the regulation of the water turbine. The notion of system time constant was firstly mentioned by him, when he studied the control of the hydro turbine.

The frequency domain approach in studying control systems was developed by J. Fourier, P. S. Laplace, A. L. Cauchy and others at Bell Telephone Laboratories. This approach was firstly applied for the analysis and design of filters for long telephone lines.

During the First World War, ships became more complicated in their design. The problem of their control and navigation came to light. Sensors were required for their closed-loop control. The gyroscope was invented by E.A. Sperry in 1910. He used it in the stabilization and guiding of ships, and later in aircraft control. The three-term controller for guiding of ships were introduced by N. Minorsky in 1922. He was the first to apply the proportional-integral-derivative (PID) controller.

In 1927, H.S. Black implemented the negative feedback to improve the stability of amplifiers. Five years later, in 1932, the stability criterion based on the polar plot of a complex function was derived by H. Nyquist. The magnitude and phase frequency plots of a complex function were used by H.W Bode, in 1938. He used the notions of gain and phase margins to investigate the stability of the closed-loop system.

Nichols Chart for the design of feedback systems was developed by N.B. Nichols in 1947. One year later, W.R. Evans presented his root locus method. This method provided a direct way to determine the closed-loop pole locations in the s-plane. During the 1950's, much controls work was focused on the s-plane, and on obtaining desirable closed-loop step-response characterictics in terms of rise time, percent overshoot, steady-state error and so on.

The period after the Second World War may be called the classical period of control theory. This period was distiguished by publishing the first books on control theory [MacColl 1945; Lauer, Lesnick, and Matdon 1947; Brown and Campbell 1948; Chestnut and Mayer 1951; Truxall 1955], and by inventing of tools that provided great intuition and simplifies the solutions of design problems. These tools were applied using hand calculations, or slide rules with graphical techniques.

With the arrival of the space age, in the USA, controls design techniques turned away from the frequency-domain, of classical control theory, to time domain, of modern control theory. The reason for this development is that the frequency-domain techniques were appropriate for linear time-invariant (LTI) systems. They are at their best when dealing with single-input/single-output (SISO) systems.

Three significant papers were published by R. Kalman in 1960. The first one supported the work of Lyapunov in the time-domain control of nonlinear systems. The second, described the optimal control theory and the design of the linear quadratic regulator (LQR). Optimal filtering and estimation theory were discussed in the third paper. In this paper, the design equations for the discrete Kalman filter were provided. In 1961, Kalman and Bucy founded the theory of the continuous Kalman filter. It can be brifly said that in the period of 1960 and 1961, the constraints of the classical control theory were overcome, new theoretical techniques for the analysis and the design of control systems were introduced, and the era of the modern control theory had started.

The focal point of Kalman's publications is that they are discussing the time-domain approach, making it more suitable for linear time-varying systems as well as nonlinear systems. Kalman used matrices and linear algebra to describe control systems, so that multi-input multi-output (MIMO) systems could easily be studied. He introduced the concept of the internal system state; hence, his approach covers the system internal dynamics as well as the system input/output relationship. In optimal control theory, Kalman formalized the concept of optimality by minimizing a generalized quadratic energy function.

In Great Britain, in the 1970's, H.H. Rosenbrock, A.G.J. MacFarlane, I. Postlethwaite and others extended the classical frequency-domain and the root locus techniques to multi-input multi-output (MIMO) systems. New concepts like the characteristic locus, diagonal dominance, and the inverse Nyquist array were introduced.

2.3 The Classical Control School

In the classical control school, system description was conventionally formulated in the frequency domain and the s-plane. Relying on transform methods, this description is primarily applicable for linear time-invariant (LTI) systems.
An exact description of the internal system dynamics is not required for classical design; that is, only the input/output behavior of the system is of importance. The transfer function is used to describe the system input-output relation. The system description required for controls design using the methods of Bode or Nyquist is the magnitude and phase of the frequency response. This is advantageous as the frequency response can be found experimentally. The transfer function can then be computed. For root locus design, the transfer function is required. The block diagram is used to find the transfer functions of composite systems.

In the classical control school, the design may be done by hand using graphical techniques. These methods introduce a great deal of intuition and provide the control system designer with a range of design solutions, so that the resulting control systems are not unique. The design process is an engineering art. Compensators as lead-lag or proportional-integral-derivative (PID) are usually used in the control structure. The effects of these compensators on the Bode, Nyquist, and root locus plots are easy to be understood, so that an appropriate compensator structure can be chosen.

As the open-loop properties, of the system to be controlled, are usually known or can be measured easily, an essential concept in the classical control is the ability to depict the system closed-loop properties in terms of its open-loop properties. For example, the Bode, Nyquist and root locus plots for the open-loop system are usually available, the steady-state error and disturbance rejection properties, for the closed-loop system, can be described in terms of the return difference and sensitivity.

Due to the interaction of the control loops, generally, classical control theory is difficult to be applied for multi-input multi-output (MIMO) systems. In these systems, a single-input single-output (SISO) transfer function may have acceptable properties, but when combined with the other transfer functions, relating the rest of the system inputs and outputs, the entire performance of the system may fail to be

acceptable. Hence, traditional design, using the approach of closing a single loop at a time, may be used. But this approach requires many iterations and is a painstaking effort.

For example, if the root-locus method is used to design a controller for a given system, the root locus for each gain element, should be plotted taking into consideration the gains previously selected. However, this requires multiple attempts, and may not reach the required closed-loop system performance or even system stability.

During 1970's different approaches, using the multivariable frequency-domain, have been developed to overcome many of these limitation.

Obtaining the transient response of a system from frequency response data was one of Rosenbrock's interests. His work includes the theory of linear systems, the transformations of linear system equations and the reduction of system matrices. He presented the Nyquist and Inverse Nyquist Array method for multivariable control systems design which was done by reducing the system coupling assuring the diagonally dominance of the transfer function matrix model in 1969. Gershgorin's band theorem was used to investigate the stability and the diagonal dominance for the system transfer function matrix (Gershgorin, 1931). In the last decades, the conventional Inverse Nyquist Array (INA) method was used by many engineers for the improvement of controllers for many processes (Koudstaal *et al.* 1981) and (Grujic, 1995).

Model predictive and adaptive control, as described in Whalley et al. (2009), have also been proposed, for MIMO systems with significant non-linearities. An approach based on the consumption of minimum control energy was propsed by Whalley, R. and Ebrahimi, M. This approach can be used to design a multivariable robust and low gain controllers with acceptable response characteristics and disturbance rejection, with minimum consumption of energy.

2.4 The Modern Control School

Modern control design is, in general, a time-domain technique. In modern control, the system to be controlled, is required to be represented in a state-space form, as suggested by Kalman. The State-space model of a system is a set of first-order differential equations having the form:

$$\dot{X}(t) = A.X(t) + B.U(t)$$

$$Y(t) = C.X(t) + D.U(t)$$

In these equations, $X(t)$ is a vector of the system states, $U(t)$ is a vector of the control inputs, and $Y(t)$ is a vector of the controlled outputs. Matrices A, B, C and D describe the dynamical interconnections between the inputs, the states and the outputs of the system. State-space model can be used to describe a MIMO system as well as a SISO system.

The properties of controllability and observability, of the open-loop system, provide insight on what it is possible to be achieved using feedback control. As by Kalman, a state is controllable if it could be varied by an input signal, in a finite time. And, if all the system states are controllable, then the system is said to be completely controllable. Meanwhile, a state is said to be observable if it could be found from the input signals and the measured output signals, in a finite time. And, if all the system states are observable, then the system is said to be completely observable. Controllability and the observability of a given system could be tested by checking the ranks of special matrices, called the controllability and the observability matrices, respectively.

Generally, to achieve the required closed-loop properties, a feedback control of the form:

$$U(t) = -K.X(t)$$

is usually used. The elements of the feedback gain matrix, K, are the control gains in the system. As the system states are used for feedback, this control method is usually called state-variable feedback control.

In the standard linear quadratic regulator (LQR), as an example from the modern control school, a quadratic time-domain performance index, J , like:

$$J = \int_0^\infty \left(X^T Q.X + U^T R.U \right) dt$$

is used. The feedback gain matrix, K , is selected such that this index is minimized.

Matrices Q and R , used in the definition of the performance index, J , are the design parameters. They are the weighting matrices for the states and the inputs, respectively. The elements of these two matrices are chosen to achieve the required performance. In modern controls design, the engineering art is in the selection of these two weighting matrices. The value of the feedback gain matrix, K , that minimizes the performance index, J , is defined as:

$$K = R^{-1}.B^T.P$$

In this equation, P is an nxn matrix satisfying the Algebriac Riccati Equation,

$$A^T P + PA - PBR^{-1}B^T P + Q = 0$$

The use of the Ricatti equation for finding the state feedback gain matrix, K , was firstly introduced by Kalman. Its use in control theory was new.

It can be noted that the Algebriac Riccati Equation is not suitable for hand calculations. Thus, computer-aided design (CAD) is an essential tool for modern controls.

In some practical designs, an output feedback of the form:

$$U(t) = -K.Y(t).$$

is applied. In this case, this output feedback control law regains much of the intuition of classical controls design.

It can be stated that, the developments in digital control theory and discrete-time systems, make modern control more applicable for the design of control systems using microcontrollers or microprocessors.

2.5 Control of DC Motors

Many researches dealing with the control of DC motors have be done. In reference [29], a winder for a deep shaft mining is presented. This winder is driven by a Ward-Leondard system having a minimum control effort regulation strategy. A linear model of the system is derived. The proposed control strategy enables regulation of the motor angular speed and the motor armature current. The responses for both the closed-loop and the open-loop systems are presented and compared. The control energy consumed and the regenerative braking performance of the system are also discussed.

A model of speed controller for a separately excited DC motor is provided in [30]. The controller has two control loops, one for controlling the motor angular speed and the other for controlling the motor armature current. The controller implemented is Proportional-Integral (PI) type which minimizes the delay and provides fast control. The optimization of the speed controller is done by using modulus hugging approach, that provides stable and fast control of the DC motor. Simulation results under varying speed and varying load torque conditions are shown.

Reference [31] describes DC motor speed control system using the pole assignment feedback technique, in which all closed-loop poles are specified. The objective of the controller is to regulate the motor angular speed. Results obtained were compared with another controller applied to the DC motor based on Proportional Integral Derivative (PID) control.

References [32] and [33] present a comparison of time response specification between the Linear Quadratic Regulator (LQR) and the conventional Proportional-Integral-Derivatives (PID) controller for a speed control of a separately excited DC motor. The performances of these two types of controllers have been verified through simulations. It has been shown, in these two references, that the linear quadratic regulator method provides the better performance, in terms of settling time, steady state error and overshoot, compared to conventional PID controller.

Refrence [34] describes the principle of DC motor speed control using nonlinear combined control and proportional-integral-derivative (PID) controller. The control

inputs are both the armature voltage and the field current. Simulation results have been obtained using MATLAB®/Simulink®.

Reference [35] investigates the design and implementation of nonlinear control schemes for a separately excited DC motor operating in the field-weakening region. A linearized feedback controller, and two other nonlinear controllers are designed and implemented. The stability of the closed-loop system is proved using Lyapunov theory. A hardware test model is constructed to experimentally verify the designed controllers.

The application of artificial neural network-based model reference controller (MRC) for the speed control of the separately-excited DC motor is presented in reference [36]. This reference proposes the speed control of the motor (SEDM) in the constant torque region. The reference also discusses and compares the speed control systems of SEDM using PI-controlled and fuzzy logic-controlled chopper circuit with MRC. The performance of the system has been modeled using MATLAB® /SIMULINK® .

Comparative studies between the different control strategies, used to control the angular speed of the separately-excited DC motor, are provided in references [37], [38] and [39]. In reference [37], PID and FUZZY Controllers are represented. Their performance are simulated and compared. In reference [38], Proportional, Integral, and Proportional-Integral controllers are represented and their performances are also compared. In reference [39] , the performance of motor speed controllers of different types as proportional, integral, derivative, proportional and integral, PID controller, phase lag compensator, lead integral compensator, lead lag compensator, and the linear quadratic regulator (LQR) are presented and compared.

References [40] and [41] provide mathematical models of separately excited DC motors. In reference [41] Three different mathematical models of the separately excited DC motor are considered: (i) a precise nonlinear model, (ii) a piecewise linear model, and (iii) a second-order linear model. Experimental results are presented comparing the various models, and the range of applications for each is suggested.

Chapter (3)

Modeling of the DC Motor

In this chapter the separately-excited DC motor is modeled as a linear two-input, two-output system. The model of this motor is represented in both state-space and transfer function forms. The model inputs are the armature and the field supply voltages, i,e., v_a and v_f, respectively. The model outputs are the motor angular speed ω and the motor field current i_f. The system states are the same as the system outputs, i.e the system states are the motor angular speed ω and the motor field current i_f.

The characteristics and the open loop response of the motor are also studied.

The figure below shows the equivalent circuit of the separately-excited DC motor. As shown in the figure, and for simplifying the mathematical model that describes the operation of the separately-excited DC motor, the leakage inductance of the motor armature circuit is neglected, as usually its value is very small, as compared to other motor parameters.

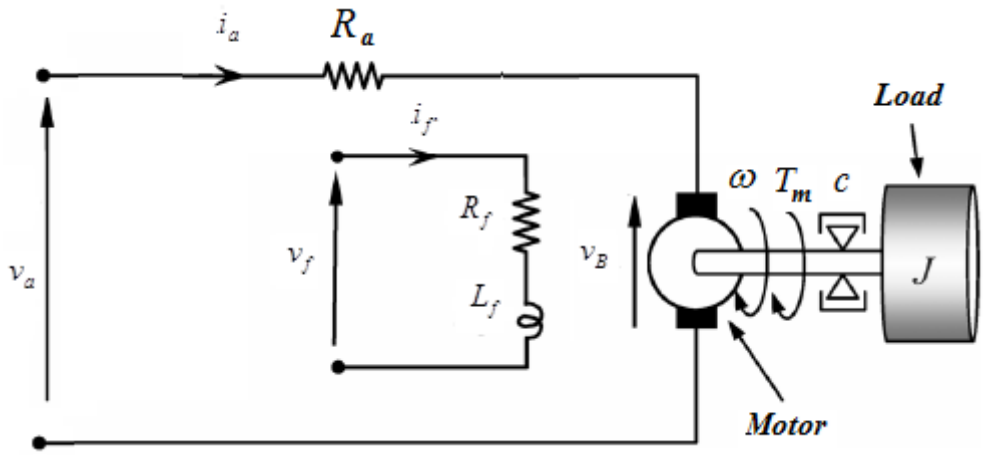

Figure 3.1: Equivalent circuit of the separately-excited DC motor.

3.1 System Governing Equations

Upon analyzing the system, the armature input voltage is equal to the sum of the voltage drop on the armature resistance and the back electromotive force, or:

$$v_a(t) = R_a.i_a(t) + v_B(t) \tag{3.1}$$

As the back electromotive force is proportional to the motor angular speed, then:

$$v_B(t) = k_1.\omega(t) \tag{3.2}$$

Substituting (3.2) in (3.1), it is found that:

$$v_a(t) = R_a.i_a(t) + k_1.\omega(t) \tag{3.3}$$

The motor shaft torque is proportional to both the armature and the field currents, or:

$$T(t) = k_a.i_a(t) + k_f.i_f(t) \tag{3.4}$$

Also, the equation that describes the dynamics of the motor shaft is:

$$T(t) = J.\dot{\omega}(t) + c.\omega(t) \tag{3.5}$$

Where:

$$\dot{\omega}(t) = \frac{d\omega(t)}{dt} \tag{3.6}$$

For the field circuit, the field input voltage is equal to the sum of the voltage drops on the resistance and the inductance of the field circuit, or:

$$v_f(t) = R_f.i_f(t) + L_f.\dot{i}_f(t) \tag{3.7}$$

Where:

$$\dot{i}_f(t) = \frac{di_f(t)}{dt} \tag{3.8}$$

Equation (3.1)-(3.8) are the governing equations that describe the operation of the separately-excited DC motor.

3.2. System Equations in PQR Form

Equating the right-hand sides of equations (3.4) and (3.5), it is found that:

$$J.\dot{\omega}(t) + c.\omega(t) = k_a.i_a(t) + k_f.i_f(t) \tag{3.9}$$

Or:

$$J.\dot{\omega}(t) = k_a.i_a(t) + k_f.i_f(t) - c.\omega(t) \tag{3.10}$$

From equation (3.3), it is found that:

$$i_a(t) = \frac{v_a(t) - k_1.\omega(t)}{R_a} \tag{3.11}$$

Substituting (3.11) in (3.10), then:

$$J.\dot{\omega}(t) = -\left(\frac{k_a.k_1}{R_a} + c\right).\omega(t) + k_f.i_f(t) + \frac{k_a}{R_a}v_a(t) \tag{3.12}$$

Equation (3.7) can be written in the form:

$$L_f.\dot{i}_f(t) = -R_f.i_f(t) + v_f(t) \tag{3.13}$$

Substituting (3.11) in (3.4), it is found that:

$$T = -\frac{k_a.k_1}{R_a}.\omega(t) + k_f.i_f(t) + \frac{k_a}{R_a}.v_a(t) \tag{3.14}$$

Equation (3.11) can be written as:

$$i_a(t) = -\frac{k_1}{R_a}\omega(t) + \frac{1}{R_a}v_a(t) \tag{3.15}$$

Equations (3.12)-(3.15) with the identities $\omega(t) = \omega(t)$ and $i_f(t) = i_f(t)$, can be written in the PQR form as:

$$\begin{bmatrix} J & 0 & 0 & 0 & 0 & 0 \\ 0 & L_f & 0 & 0 & 0 & 0 \\ 0 & 0 & 1 & 0 & 0 & 0 \\ 0 & 0 & 0 & 1 & 0 & 0 \\ 0 & 0 & 0 & 0 & 1 & 0 \\ 0 & 0 & 0 & 0 & 0 & 1 \end{bmatrix}.\begin{bmatrix} \dot{\omega} \\ \dot{i}_f \\ T \\ i_a \\ \omega \\ i_f \end{bmatrix} = \begin{bmatrix} -\left(\frac{k_a.k_1}{R_a} + c\right) & k_f \\ 0 & -R_f \\ -\frac{k_a.k_1}{R_a} & k_f \\ -\frac{k_1}{R_a} & 0 \\ 1 & 0 \\ 0 & 1 \end{bmatrix}.\begin{bmatrix} \omega \\ i_f \end{bmatrix} + \begin{bmatrix} \frac{k_a}{R_a} & 0 \\ 0 & 1 \\ \frac{k_a}{R_a} & 0 \\ \frac{1}{R_a} & 0 \\ 0 & 0 \\ 0 & 0 \end{bmatrix}.\begin{bmatrix} v_a \\ v_f \end{bmatrix} \tag{3.16}$$

Or in abbreviated form as:

$$P.\begin{bmatrix} \dot{X} \\ \dots \\ Y \end{bmatrix} = Q.[X] + R.[U] \tag{3.17}$$

Here, the matrices P , Q and R are respectively:

$$P = \begin{bmatrix} J & 0 & 0 & 0 & 0 & 0 \\ 0 & L_f & 0 & 0 & 0 & 0 \\ 0 & 0 & 1 & 0 & 0 & 0 \\ 0 & 0 & 0 & 1 & 0 & 0 \\ 0 & 0 & 0 & 0 & 1 & 0 \\ 0 & 0 & 0 & 0 & 0 & 1 \end{bmatrix} \tag{3.18}$$

$$Q = \begin{bmatrix} -\left(\frac{k_a.k_1}{R_a} + c\right) & k_f \\ 0 & -R_f \\ -\frac{k_a.k_1}{R_a} & k_f \\ -\frac{k_1}{R_a} & 0 \\ 1 & 0 \\ 0 & 1 \end{bmatrix} \tag{3.19}$$

$$R = \begin{bmatrix} \frac{k_a}{R_a} & 0 \\ 0 & 1 \\ \frac{k_a}{R_a} & 0 \\ \frac{1}{R_a} & 0 \\ 0 & 0 \\ 0 & 0 \end{bmatrix} \tag{3.20}$$

The state vector is:

$$X = \begin{bmatrix} \omega & i_f \end{bmatrix}^T \tag{3.21}$$

The output vector is:

$$Y = \begin{bmatrix} T & i_a & \omega & i_f \end{bmatrix}^T \tag{3.22}$$

The input vector is:

$$U = \begin{bmatrix} v_a & v_f \end{bmatrix}^T \tag{3.23}$$

And the required system output are the same as the system states, or the vector of the required system outputs is $\begin{bmatrix}\omega & i_f\end{bmatrix}^T$.

3.3. State-Space Representation of the System

As mentioned before, the system inputs are $v_a(t)$ and $v_f(t)$, while the system states are $\omega(t)$ and $i_f(t)$. The required system outputs are the same as the system states, i.e., the required system outputs are $\omega(t)$ and $i_f(t)$. The state-space form of the system equations can be derived from the PQR form, equations (3.16) – (3.23), by matrix inversion or by carrying out row-operation methods.

Multiplying the two sides of equation (3.17) by the inverse of matrix P, it is found that:

$$\begin{bmatrix}\dot{X}\\ \dots\\ Y\end{bmatrix} = P^{-1}.Q.[X] + P^{-1}.R.[U] \tag{3.24}$$

The inverse of matrix P can be found by using the equation:

$$P^{-1} = \frac{1}{|P|}\begin{bmatrix}P_{11} & P_{12} & \dots & P_{1n}\\ P_{21} & P_{22} & \dots & P_{2n}\\ \dots & \dots & \dots & \dots\\ P_{n1} & P_{n2} & \dots & P_{nn}\end{bmatrix}^T \tag{3.25}$$

Here $|P|$ is the determinant of matrix P and P_{ij} are the cofactors of its elements.

The inverse of matrix P can also be found by performing row operations, after augmenting P with an identity matrix having a dimension as that of matrix P, as shown below.

$$\tilde{P} = \begin{bmatrix}J & 0 & 0 & 0 & 0 & 0. & 1 & 0 & 0 & 0 & 0 & 0\\ 0 & L_f & 0 & 0 & 0 & 0. & 0 & 1 & 0 & 0 & 0 & 0\\ 0 & 0 & 1 & 0 & 0 & 0. & 0 & 0 & 1 & 0 & 0 & 0\\ 0 & 0 & 0 & 1 & 0 & 0. & 0 & 0 & 0 & 1 & 0 & 0\\ 0 & 0 & 0 & 0 & 1 & 0. & 0 & 0 & 0 & 0 & 1 & 0\\ 0 & 0 & 0 & 0 & 0 & 1. & 0 & 0 & 0 & 0 & 0 & 1\end{bmatrix} \tag{3.26}$$

Dividing the first row of the augmented matrix by J and the second row by L_f, then:

$$\tilde{P}^{(1)} = \begin{bmatrix} 1 & 0 & 0 & 0 & 0 & 0. & \frac{1}{J} & 0 & 0 & 0 & 0 & 0 \\ 0 & 1 & 0 & 0 & 0 & 0. & 0 & \frac{1}{L_f} & 0 & 0 & 0 & 0 \\ 0 & 0 & 1 & 0 & 0 & 0. & & & & & & \\ 0 & 0 & 0 & 1 & 0 & 0. & 0 & 0 & 1 & 0 & 0 & 0 \\ 0 & 0 & 0 & 0 & 1 & 0. & 0 & 0 & 0 & 1 & 0 & 0 \\ 0 & 0 & 0 & 0 & 0 & 1. & 0 & 0 & 0 & 0 & 1 & 0 \\ & & & & & & 0 & 0 & 0 & 0 & 0 & 1 \end{bmatrix} \tag{3.27}$$

Hence the inverse of matrix P is:

$$P^{-1} = \begin{bmatrix} \frac{1}{J} & 0 & 0 & 0 & 0 & 0 \\ 0 & \frac{1}{L_f} & 0 & 0 & 0 & 0 \\ 0 & 0 & 1 & 0 & 0 & 0 \\ 0 & 0 & 0 & 1 & 0 & 0 \\ 0 & 0 & 0 & 0 & 1 & 0 \\ 0 & 0 & 0 & 0 & 0 & 1 \end{bmatrix} \tag{3.28}$$

Substituting equation (3.28) in equation (3.24), it is found that:

$$\begin{bmatrix} \dot{\omega} \\ \dot{i}_f \\ T \\ i_a \\ \omega \\ i_f \end{bmatrix} = \begin{bmatrix} -\left(\frac{k_a.k_1}{J.R_a} + \frac{c}{J}\right) & \frac{k_f}{J} \\ 0 & -\frac{R_f}{L_f} \\ -\frac{k_a.k_1}{R_a} & k_f \\ -\frac{k_1}{R_a} & 0 \\ 1 & 0 \\ 0 & 1 \end{bmatrix} \cdot \begin{bmatrix} \omega \\ i_f \end{bmatrix} + \begin{bmatrix} \frac{k_a}{J.R_a} & 0 \\ 0 & \frac{1}{L_f} \\ \frac{k_a}{R_a} & 0 \\ \frac{1}{R_a} & 0 \\ 0 & 0 \\ 0 & 0 \end{bmatrix} \cdot \begin{bmatrix} v_a \\ v_f \end{bmatrix} \tag{3.29}$$

From this equation, the system state and output equations can be deduced.

The system state equation is:

$$\begin{bmatrix} \dot{\omega} \\ \dot{i}_f \end{bmatrix} = \begin{bmatrix} -\left(\frac{k_a.k_1}{J.R_a} + \frac{c}{J}\right) & \frac{k_f}{J} \\ 0 & -\frac{R_f}{L_f} \end{bmatrix} \cdot \begin{bmatrix} \omega \\ i_f \end{bmatrix} + \begin{bmatrix} \frac{k_a}{J.R_a} & 0 \\ 0 & \frac{1}{L_f} \end{bmatrix} \cdot \begin{bmatrix} v_a \\ v_f \end{bmatrix} \tag{3.30}$$

and the system output equation is:

$$\begin{bmatrix} \omega \\ i_f \end{bmatrix} = \begin{bmatrix} 1 & 0 \\ 0 & 1 \end{bmatrix} \cdot \begin{bmatrix} \omega \\ i_f \end{bmatrix} \tag{3.31}$$

Or, in the abbreviated form:

$$\dot{X} = A.X + B.U \tag{3.32}$$

$$Y = C.X + D.U \tag{3.33}$$

Where A, B, C, D, X, Y and U are defined as below:

$$A = \begin{bmatrix} -\left(\frac{k_a.k_1}{J.R_a} + \frac{c}{J}\right) & \frac{k_f}{J} \\ 0 & -\frac{R_f}{L_f} \end{bmatrix} \tag{3.34}$$

$$B = \begin{bmatrix} \frac{k_a}{J.R_a} & 0 \\ 0 & \frac{1}{L_f} \end{bmatrix} \tag{3.35}$$

$$C = \begin{bmatrix} 1 & 0 \\ 0 & 1 \end{bmatrix} \tag{3.36}$$

$$D = \begin{bmatrix} 0 & 0 \\ 0 & 0 \end{bmatrix} \tag{3.37}$$

$$X = Y = \begin{bmatrix} \omega \\ i_f \end{bmatrix} \tag{3.38}$$

$$U = \begin{bmatrix} v_f \\ v_a \end{bmatrix} \tag{3.39}$$

3.4. System Transfer Function

Laplace transforms, with zero initial conditions, for each of the state equation (3.32) and the output equation (3.33) are, respectively:

$$s.X(s) = A.X(s) + B.U(s) \tag{3.40}$$

and:

$$Y(s) = C.X(s) \tag{3.41}$$

From these two equations, it can be concluded that:

$$Y(s) = C.(s.I - A)^{-1}.B.U(s) \tag{3.42}$$

Or:

$$Y(s) = G(s).U(s) \tag{3.43}$$

Where:

$$G(s) = C.(s.I - A)^{-1}.B \tag{3.44}$$

In this equation, matrix I is the identity matrix of order as that of the order of matrix A.

Substituting matrices A, B and C as found in (3.34), (3.35) and (3.36) into equation (3.44), it is found that the system transfer function $G(s)$ is:

$$G(s) = \frac{1}{\left(J.R_a.s + R_a.c + k_a.k_1\right).\left(L_f.s + R_f\right)}\begin{bmatrix} k_a.\left(L_f.s + R_f\right) & k_f.R_a \\ 0 & J.R_a.s + R_a.c + k_a.k_1 \end{bmatrix} \tag{3.45}$$

As:

$$U(s) = \begin{bmatrix} v_a(s) & v_f(s) \end{bmatrix}^T \tag{3.46}$$

$$Y(s) = \begin{bmatrix} \omega(s) & i_f(s) \end{bmatrix}^T \tag{3.47}$$

Hence:

$$\begin{bmatrix} \omega(s) \\ i_f(s) \end{bmatrix} = \frac{1}{\left(J.R_a.s + R_a.c + k_a.k_1\right).\left(L_f.s + R_f\right)}\begin{bmatrix} k_a.\left(L_f.s + R_f\right) & k_f.R_a \\ 0 & J.R_a.s + R_a.c + k_a.k_1 \end{bmatrix}.\begin{bmatrix} v_a(s) \\ v_f(s) \end{bmatrix} \tag{3.48}$$

For the DC motor with the following parameters: $P = 200hp$, $V_a = 400V$, $V_f = 400V$, $R_f = 50\Omega$, $L_f = 23.25H$, $R_a = 0.24\Omega$, $k_1 = 26.96V/(rad/\sec)$, $k_a = 16.33N.m/A$, $k_f = 613.36N.m/A$, $J = 555.kg.m^2$, $c = 1200.24N.m/(rad/\sec)$, and after substituting these parameters in equations (3.34) and (3.35), the state and the input matrices of the system become:

$$A = \begin{bmatrix} -54.68 & 11.05 \\ 0 & -2.15 \end{bmatrix} \tag{3.49}$$

$$B = \begin{bmatrix} 1.23 & 0 \\ 0 & 0.043 \end{bmatrix} \tag{3.50}$$

Or the system state equation is:

$$\begin{bmatrix} \dot{\omega} \\ \dot{i}_f \end{bmatrix} = \begin{bmatrix} -54.68 & 11.05 \\ 0 & -2.15 \end{bmatrix} . \begin{bmatrix} \omega \\ i_f \end{bmatrix} + \begin{bmatrix} 1.23 & 0 \\ 0 & 0.043 \end{bmatrix} . \begin{bmatrix} v_a \\ v_f \end{bmatrix} \tag{3.51}$$

and the system output equation is:

$$\begin{bmatrix} y_1 \\ y_2 \end{bmatrix} = \begin{bmatrix} 1 & 0 \\ 0 & 1 \end{bmatrix} . \begin{bmatrix} \omega \\ i_f \end{bmatrix} \tag{3.52}$$

The tansfer function of system is found by substtituting the motor parameters in equation (3.45), hence:

$$G(s) = \begin{bmatrix} \dfrac{1.226s + 2.64}{s^2 + 56.83s + 117.6} & \dfrac{0.475}{s^2 + 56.83s + 117.6} \\ 0 & \dfrac{0.043s + 2.35}{s^2 + 56.83s + 117.6} \end{bmatrix} \tag{3.53}$$

As:

$$U(s) = \begin{bmatrix} v_a(s) & v_f(s) \end{bmatrix}^T \tag{3.54}$$

$$Y(s) = \begin{bmatrix} \omega(s) & i_f(s) \end{bmatrix}^T \tag{3.55}$$

Thus, the input-output description of the system becomes:

$$\begin{bmatrix} \omega(s) \\ i_f(s) \end{bmatrix} = \begin{bmatrix} \dfrac{1.226s + 2.64}{s^2 + 56.83s + 117.6} & \dfrac{0.475}{s^2 + 56.83s + 117.6} \\ 0 & \dfrac{0.043s + 2.35}{s^2 + 56.83s + 117.6} \end{bmatrix} . \begin{bmatrix} v_a(s) \\ v_f(s) \end{bmatrix} \tag{3.56}$$

3.5. Scaling the Model

The base values used for scaling of the model are the maximum values of the input and the output signals. The maximum values of the input signals are $u_{1\max} = v_{a\max} = 400V$ and $u_{2\max} = v_{f\max} = 400V$. While, the maximum values of the output signals are $y_{1\max} = \omega_{\max} = 10.96 rad/\sec.$ and $y_{2\max} = i_{f\max} = 8A.$ Hence:

$$u_1 = \frac{u_{1\max}}{100}.\tilde{u}_1(\%) = 4\tilde{u}_1(\%) \tag{3.57}$$

$$u_2 = \frac{u_{2\max}}{100}.\tilde{u}_2(\%) = 4\tilde{u}_2(\%) \tag{3.58}$$

Or in matrix form:

$$\begin{bmatrix} u_1 \\ u_2 \end{bmatrix} = \begin{bmatrix} 4 & 0 \\ 0 & 4 \end{bmatrix}.\begin{bmatrix} \tilde{u}_1(\%) \\ \tilde{u}_2(\%) \end{bmatrix} \tag{3.59}$$

In these equations:

- u_1 and u_2 are the actual values of the input signals, which are the motor armature and field voltages, respectively,
- $\tilde{u}_1(\%)$ and $\tilde{u}_2(\%)$ are the percentage change of u_1 and u_2, respectively.

In the same way, for the output signals:

$$y_1 = \frac{y_{1\max}}{100}.\tilde{y}_1(\%) = 0.1096 y_1(\%) \tag{3.60}$$

$$y_2 = \frac{y_{2\max}}{100}.\tilde{y}_2(\%) = 0.08\tilde{y}_2(\%) \tag{3.61}$$

Or in matrix form:

$$\begin{bmatrix} y_1 \\ y_2 \end{bmatrix} = \begin{bmatrix} 0.1096 & 0 \\ 0 & 0.08 \end{bmatrix}.\begin{bmatrix} \tilde{y}_1(\%) \\ \tilde{y}_2(\%) \end{bmatrix} \tag{3.62}$$

Here:

- y_1 and y_2 are the actual values of the output signals, which are the motor angular speed and the motor field current, respectively.
- $\tilde{y}_1(\%)$ and $\tilde{y}_2(\%)$ are the percentage change of y_1 and y_2, respectively.

Substituting equations (3.59) and (3.62) in equation (3.56), we find:

$$\begin{bmatrix} 0.1096 & 0 \\ 0 & 0.08 \end{bmatrix}.\begin{bmatrix} \tilde{y}_1(\%) \\ \tilde{y}_2(\%) \end{bmatrix} = \begin{bmatrix} \frac{1.226s + 2.64}{s^2 + 56.83s + 117.6} & \frac{0.475}{s^2 + 56.83s + 117.6} \\ 0 & \frac{0.043s + 2.35}{s^2 + 56.83s + 117.6} \end{bmatrix}.\begin{bmatrix} 4 & 0 \\ 0 & 4 \end{bmatrix}.\begin{bmatrix} \tilde{u}_1(\%) \\ \tilde{u}_2(\%) \end{bmatrix}$$

or:

$$\begin{bmatrix}\tilde{y}_1(\%)\\ \tilde{y}_2(\%)\end{bmatrix}=\begin{bmatrix}0.1096 & 0\\ 0 & 0.08\end{bmatrix}^{-1}.\begin{bmatrix}\dfrac{1.226s+2.64}{s^2+56.83s+117.6} & \dfrac{0.475}{s^2+56.83s+117.6}\\ 0 & \dfrac{0.043s+2.35}{s^2+56.83s+117.6}\end{bmatrix}.\begin{bmatrix}4 & 0\\ 0 & 4\end{bmatrix}.\begin{bmatrix}\tilde{u}_1(\%)\\ \tilde{u}_2(\%)\end{bmatrix}$$

or:

$$\begin{bmatrix}\tilde{y}_1(\%)\\ \tilde{y}_2(\%)\end{bmatrix}=\begin{bmatrix}\dfrac{44.74s+96.35}{s^2+56.83s+117.6} & \dfrac{17.35}{s^2+56.83s+117.6}\\ 0 & \dfrac{2.15s+117.6}{s^2+56.83s+117.6}\end{bmatrix}.\begin{bmatrix}\tilde{u}_1(\%)\\ \tilde{u}_2(\%)\end{bmatrix} \tag{3.63}$$

i.e, the transfer function of the system for percentage changes is:

$$G_N(s)=\begin{bmatrix}\dfrac{44.74s+96.35}{s^2+56.83s+117.6} & \dfrac{17.35}{s^2+56.83s+117.6}\\ 0 & \dfrac{2.15s+117.6}{s^2+56.83s+117.6}\end{bmatrix} \tag{3.64}$$

3.6. Modelling the System Using MATLAB®/Simulink®

System state equations (3.12) and (3.13), can be written in the form:

$$\omega(t)=\int\left[\frac{k_a}{J.R_a}v_a(t)+\frac{k_f}{J}.i_f(t)-\left(\frac{k_a.k_1}{J.R_a}+\frac{c}{J}\right).\omega(t)\right].dt \tag{3.65}$$

$$i_f(t)=\int\left[\frac{1}{L_f}v_f(t)-\frac{R_f}{L_f}.i_f(t)\right].dt \tag{3.66}$$

The block diagram of the separately-excited DC motor as described by these two state equations is shown in figure 3.2 below.

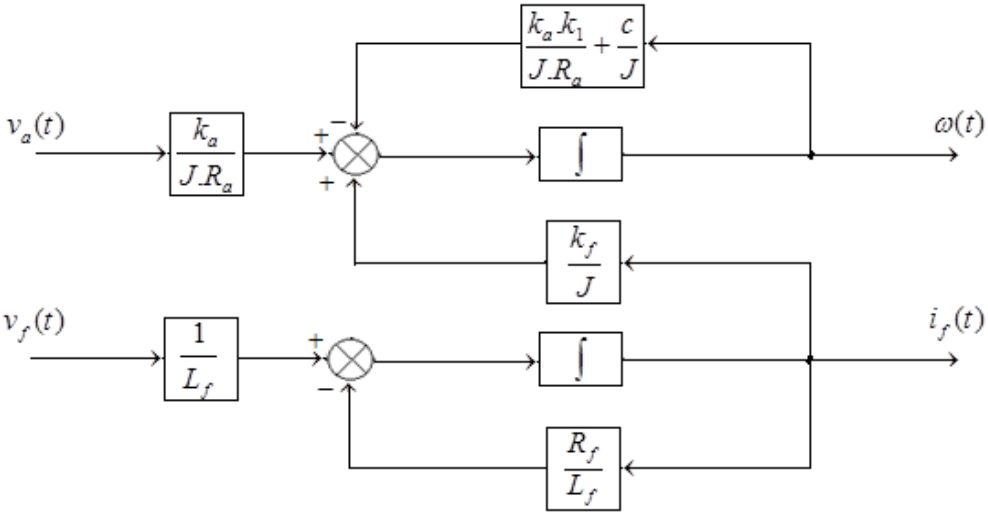

Figure 3.2: Block diagram of the separately-excited DC motor, as desribed by the state equations.

For the purpose of simulating the operation of the DC motor system, a MATLAB®/Simulink® model, using equations (3.65) and (3.66), was built. This model is shown in figure A.1.

Other MATLAB®/Simulink® model, using the state-space representation of the DC motor system, equations (3.30) and (3.31), is also built. This model is shown in figure A.2.

Block diagrams of the separetly-excited DC motor, using the transfer function, equation (3.56), and the transfer function for pecent changes, equation (3.63), are shown in figures 3.3 and 3.4, respectively.

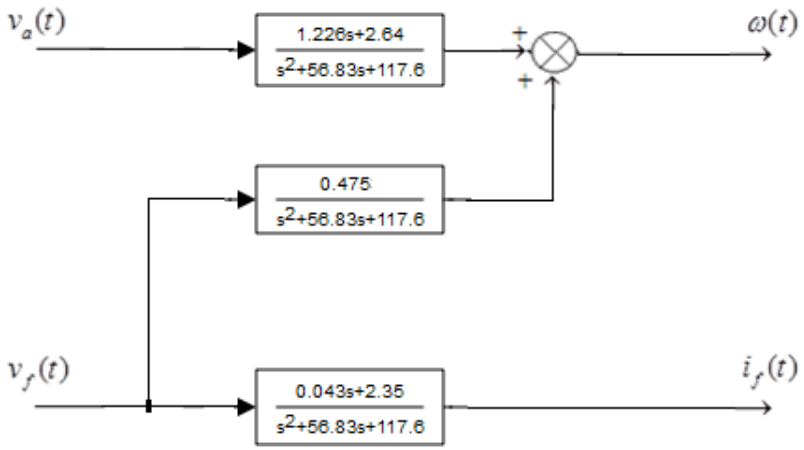

Figure 3.3: Block diagram of the separately-excited DC motor, as described by the tranfser function.

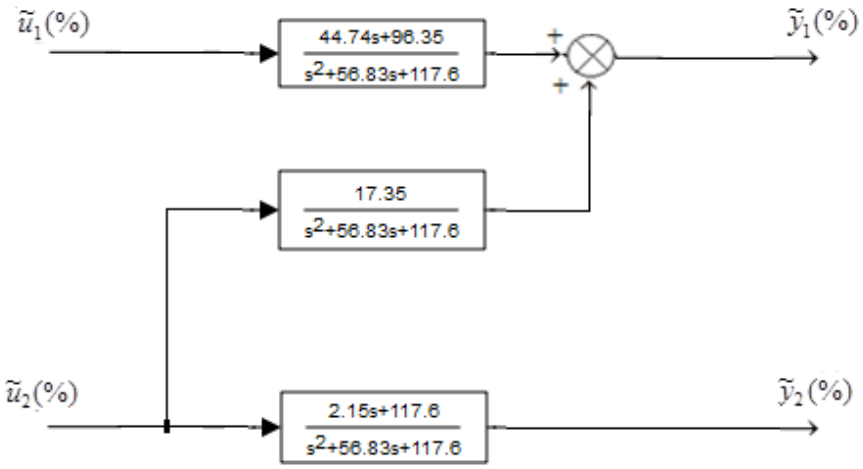

Figure 3.4: Block diagram of the separately-excited DC motor, as described by the tranfser function for percentage changes.

MATLAB®/Simulink® models, using the transfer function and the transfer function for percentage changes, were also built. These models are shown in figures A.3 and A.4, respectively.

3.7 Open Loop Response Analysis and Control Objectives

3.7.1 System Poles and Zeros

System poles are the zeros of the denominator of the transfer functions $G(s)$ or $G_N(s)$ defined by equations (3.53), and (3.64), respectively. Or system poles are the roots of the equation $s^2 + 56.83s + 117.6 = 0$, which are: $p_1 = -2.15$ and $p_2 = -54.68$.

As system poles are also the eigenvalues of the state matrix A, in the state equation of the system, system poles can also be found by solving the equation $|s.I - A| = 0$.

The system poles are shown in the diagram in figure 3.5.

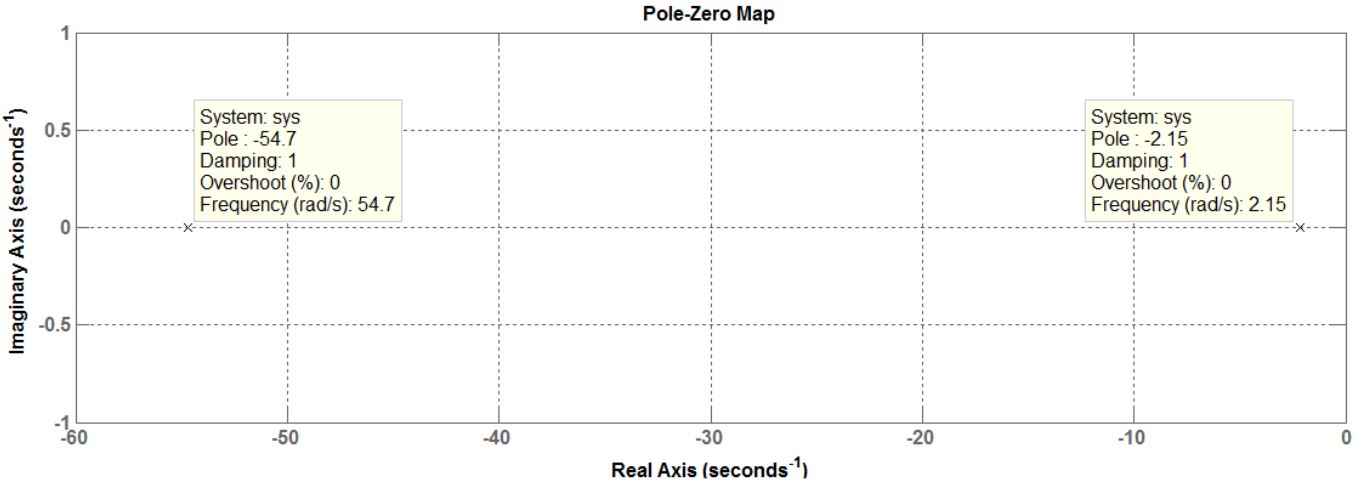

Figure 3.5: Poles of the open-loop DC motor system.

System zeros are found from each of the two system inputs to each of the two system outputs, defined by the zeros of the numerators of the respective elements of the transfer functions $G(s)$ or $G_N(s)$. Or system zeros are as follows:

- from input 1 to output 1: two zeros at infinity.
- from input 2 to output 1: $z_1 = -2.15$, in addition to a zero at infinity..
- from input1 to output 2: $z_1 = -54.68$, in addition to a zero at infinity.
- from input 2 to output 2: two zeros at infinity.

As the system poles are negative and real, it can be concluded that this system is stable and will have no oscillations.

3.7.2 Output Responses For One Percent Change On Each Input, In Turn

The output responses of the system, for one percent change on each of the two inputs, in turn, can be obtained from the MATLAB/Simulink model, which simulates the system using the transfer function for percent changes, $G_N(s)$, shown in figure A.4.

As from equation (3.63), when $\tilde{u}_2(\%) = 0$:

$$\tilde{y}_1(\%) = \frac{44.74s + 96.35}{s^2 + 56.83s + 117.6}.\tilde{u}_1(\%) \tag{3.67}$$

$$\tilde{y}_2(\%) = 0.\tilde{u}_1(\%) \tag{3.68}$$

In the same way, when $\tilde{u}_1(\%) = 0$

$$\tilde{y}_1(\%) = \frac{17.35}{s^2 + 56.83s + 117.6}.\tilde{u}_2(\%) \tag{3.69}$$

$$\tilde{y}_2(\%) = \frac{2.15s + 117.5}{s^2 + 56.83s + 117.6}.\tilde{u}_2(\%) \tag{3.70}$$

These responses are shown in the figures below.

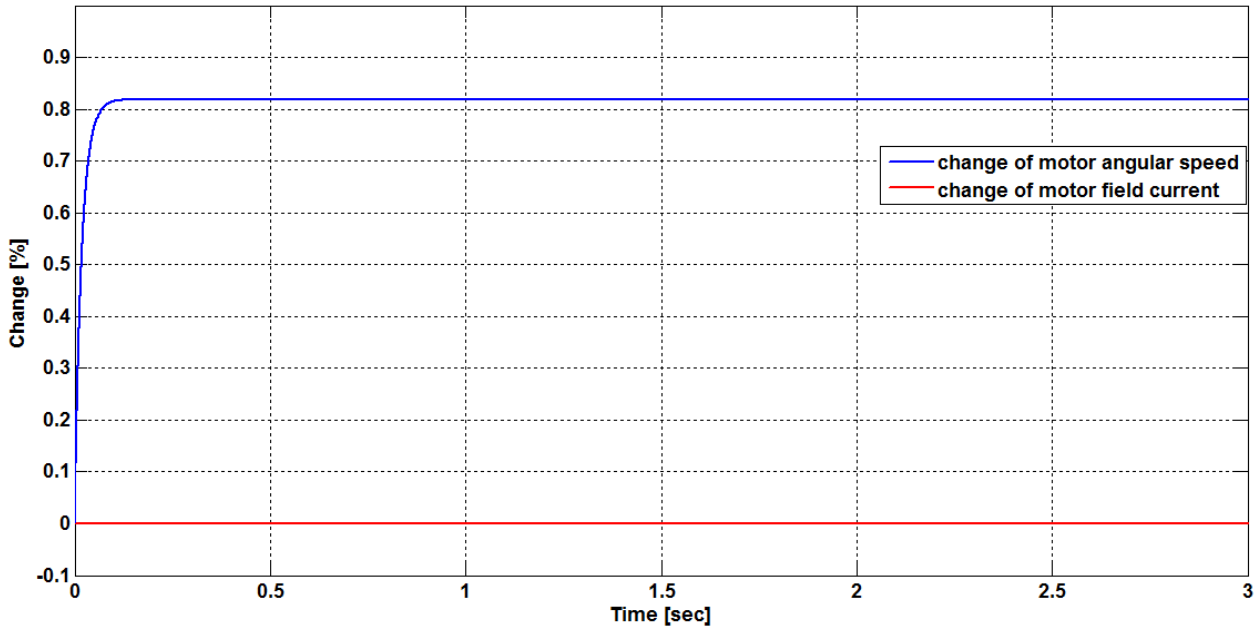

Figure 3.6: Open-loop system response for a unit step change in the motor armature voltage, $u_1(t)$, with no change in the motor field voltage, $u_2(t) = 0$.

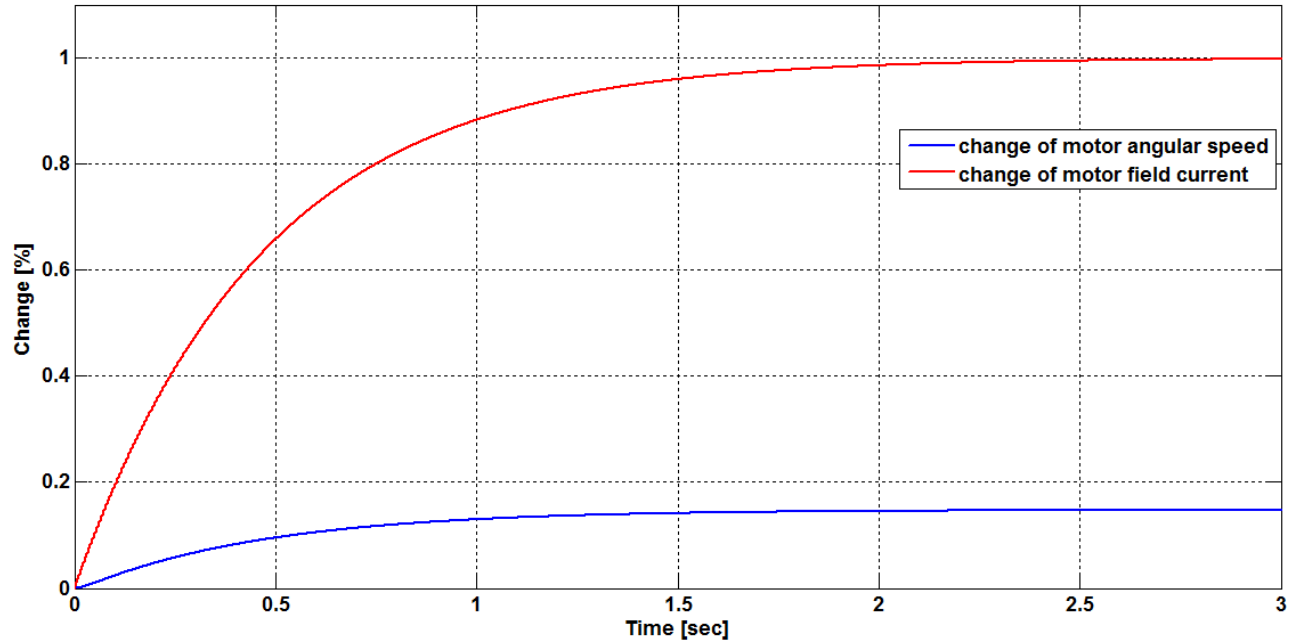

Figure 3.7: Open-loop system response for a unit step change in the motor field voltage, $u_2(t)$, with no change in the motor armature voltage $u_1(t) = 0$.

3.7.3 System Steady State Interaction

System steady-state interaction can be derived using the final-value theorem, which states that:

$$\lim_{t\to\infty} y(t) = \lim_{s\to 0} s.Y(s) = \lim_{s\to 0}\left[s.G(s).U(s)\right] \tag{3.71}$$

Where $G(s)$, $U(s)$ and $Y(s)$ are, as described before:

$$G(s) = \begin{bmatrix} \dfrac{1.226s + 2.64}{s^2 + 56.83s + 117.6} & \dfrac{0.475}{s^2 + 56.83s + 117.6} \\ 0 & \dfrac{0.043s + 2.35}{s^2 + 56.83s + 117.6} \end{bmatrix} \tag{3.72}$$

$$U(s) = \begin{bmatrix} V_a(s) & V_f(s) \end{bmatrix}^T \tag{3.73}$$

And:

$$Y(s) = \begin{bmatrix} \omega(s) & I_f(s) \end{bmatrix}^T \tag{3.74}$$

Hence:

$$y(t)\big|_{Steady-State} = \lim_{s\to 0}\left\{ s.\begin{bmatrix} \dfrac{1.226s + 2.64}{s^2 + 56.83s + 117.6} & \dfrac{0.475}{s^2 + 56.83s + 117.6} \\ 0 & \dfrac{0.043s + 2.35}{s^2 + 56.83s + 117.6} \end{bmatrix} \right\}.U(s) \tag{3.75}$$

In the same manner, system steady state interaction, in percentage changes, can be found by applying the final-value theorem to the system transfer function description using percentage changes of inputs and outputs, given by equation (3.63).

or:

$$\begin{bmatrix} \tilde{y}_1(\%) \\ \tilde{y}_2(\%) \end{bmatrix}_{Steady-State} = \lim_{s\to 0}\left\{ s.\begin{bmatrix} \dfrac{44.74s + 96.35}{s^2 + 56.83s + 117.6} & \dfrac{17.35}{s^2 + 56.83s + 117.6} \\ 0 & \dfrac{2.15s + 117.6}{s^2 + 56.83s + 117.6} \end{bmatrix} \right\}.\begin{bmatrix} \tilde{u}_1(\%) \\ \tilde{u}_2(\%) \end{bmatrix}$$ or:

$$\begin{bmatrix} \tilde{y}_1(\%) \\ \tilde{y}_2(\%) \end{bmatrix}_{Steady-State} = \lim_{s\to 0}\begin{bmatrix} \dfrac{44.74s^2 + 96.35s}{s^2 + 56.83s + 117.6} & \dfrac{17.35s}{s^2 + 56.83s + 117.6} \\ 0 & \dfrac{2.15s^2 + 117.6s}{s^2 + 56.83s + 117.6} \end{bmatrix}.\begin{bmatrix} \tilde{u}_1(\%) \\ \tilde{u}_2(\%) \end{bmatrix} \tag{3.76}$$

For 1% changes, on each of the two inputs, simultaneously, the steady state outputs will be:

$$\left[\begin{matrix}\tilde{y}_1(\%)\\ \tilde{y}_2(\%)\end{matrix}\right]\Big|_{Steady-State} = \lim_{s\to 0}\left[\begin{matrix}\dfrac{44.74s^2+96.35s}{s^2+56.83s+117.6} & \dfrac{17.35s}{s^2+56.83s+117.6}\\ 0 & \dfrac{2.15s^2+117.6s}{s^2+56.83s+117.6}\end{matrix}\right]\cdot\left[\begin{matrix}\dfrac{1}{s}\\ \dfrac{1}{s}\end{matrix}\right]$$

Or:

$\tilde{y}_1(\%)\big|_{Steady-State} = 0.966\%$ and $\tilde{y}_2(\%)\big|_{Steady-State} = 1\%$

These results are the same as those obtained from the Simulink model, simulating the performance of the system using the transfer function for percent changes, shown in figure A.4.

A MATLAB program is attached to this work. This program builds the system using different approaches, draws the output responses for precentage changes on each of the two inputs and plots the system poles.

From figure 3.6, it can be seen that, for the change of the motor aramature voltage, the change of the motor angular speed has an overdamped character, with a settling time of about 0.12 seconds. A 1% change of the motor armature voltage causes around 0.82% change of the motor angular speed, but no change in the motor field current.

Figure 3.7 shows that for the change in the motor field voltage, the system has also an overdamped behavior for both outputs, and a settling time of about 2.5 seconds. A 1% change of the motor field voltage causes 1% change of the motor field current, and almost 0.15% change of the motor angular speed.

Even though the system is stable and well behaved, there is a cross coupling between the system outputs. Therefore, the objective of the controller will be to reduce the steady-state output cross coupling, as much as possible. A ten percent limit of cross coupling between the system outputs will be acceptable. Reducing the steady-state error and increasing the system speed, while maintaining an over-damped condition, will be another objective of the controller. Since random disturbances are expected, the ability of the system to suppress these disturbance will be studied. Another important issue that will be studied in this research work is the energy consumed by the control action itself.

Chapter (4)

The Least-Effort Feedback Controller

4.1 Introduction

In the least-effort feedback controller, a dual-loop approach is proposed. The inner loop ensures stable dynamics and the outer loop, in combination, ensures steady state interactions with necessary disturbance suppression. By this manner, the system dynamics and the steady state response can be adjusted to reach the required performance characteristics.

The generalized block diagram of a two-input, two-output system with a least effort feedback controller is shown in figure 4.1. The P controllers correspond to the outer loop and are represented by proportional gains. The H controllers correspond to the inner loop and are represented by the feedback loops. In this chapter, a least effort controller for a separetly-excited DC motor, as described by Whalley, R. and Ebrahimi, M. will be designed. The proposed controller will enable simultaneous regulation of the motor angular speed and the motor field current. The responses of the closed loop system will also be analyzed.

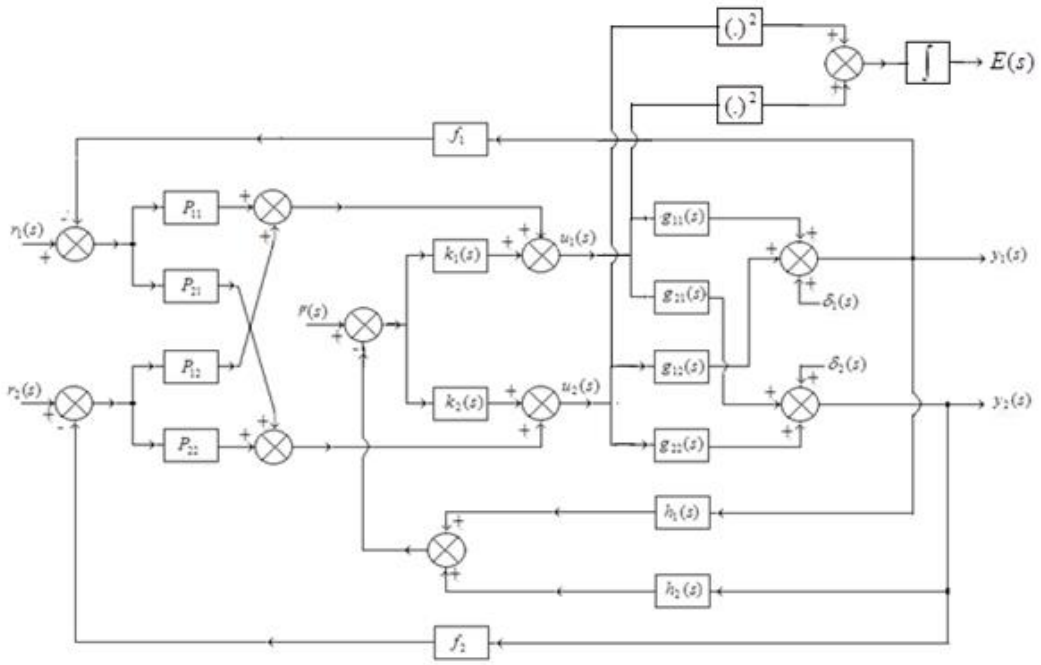

Figure 4.1: Generalized block diagram of a two-input two-output system with a least-effort controller.

As from figure 4.1, for system with m inputs, m outputs and disturbances, the system equation is:

$$y(s) = G(s).u(s) + \delta(s) \tag{4.1}$$

and the the control law is described as:

$$u(s) = k(s).[\bar{r}(s) - h(s).y(s)] + P[r(s) - F.y(s)] \tag{4.2}$$

In the above equation, the inner loop is represented by $k(s).[\bar{r}(s) - h(s).y(s)]$ and it satisfies the required system dynamics in the closed loop condition. The outer loop, represented by $P[r(s) - F.y(s)]$, handles steady state output interactions and recovery from undesired disturbances.

4.2 Outer-Loop Analysis

The outer loop feedbak matrix, F, is a diagonal matrix with elements of the main diagonal are less than one, or:

$$F = (f_1, f_2, ..., f_m), \quad 0 < f_j < 1, \quad 1 \le j \le m \tag{4.3}$$

With $\bar{r}(s) = 0$, the system closed loop equation becomes:

$$y(s) = \{I_m + G(s)[k(s) >< h(s) + PF]\}^{-1}[G(s)\,\mathrm{Pr}(s) + \delta(s)] \tag{4.4}$$

If a steady-state matrix, S_S, is chosen, such that:

$$y(0) = S_S.r(0) \tag{4.5}$$

then equation (4.4), with no disturbances, can be written as:

$$P = [G(0)^{-1} + k(0) >< h(0)]S_S(I_m - FS_S)^{-1} \tag{4.6}$$

For low steady-state output coupling, the diagonal elements of the steady-state matrix, S_S, must have unity values and the off-diagonal elements must have absolute values that are much less than unity. Or:

$$s_{j,j} = 1, \quad 1 \le j \le m \tag{4.7}$$

And:

$$|s_{i,j}| << 1, \quad 1 \le i, j \le m, \quad i \ne j \tag{4.8}$$

For the case of low steady-state interaction of the closed-loop system, and after substituting P , from equation (4.6) in equation (4.4), equation (4.4) becomes:

$$y(s) = \left\{I_m + G(s)\left[k(s) >< h(s) + \left(G(0)^{-1} + k(s) >< h(s)\right)\left(I_m - F\right)^{-1} F\right]\right\}^{-1}\left[G(s)\,\mathrm{Pr}(s) + \delta(s)\right] \tag{4.9}$$

At low frequencies, as:

$$G(s) \cong G(0)$$

or:

$$G(s).G(0)^{-1} \cong I_m$$

equation (4.9) becomes:

$$y(s) = \left\{\left[I_m + G(s)k(s) >< h(s)\right]\left[I_m + \left(I_m - F\right)^{-1} F\right]\right\}^{-1}\left[G(s)\,\mathrm{Pr}(s) + \delta(s)\right] \tag{4.10}$$

If the elements of the diagonal matrix F are equal and are less than unity, or if:

$$f_1 = f_2 = \ldots = f_m = f \qquad and \qquad 0 < f < 1$$

equation (4.10) is reduced to:

$$y(s) \cong (1 - f)\left[I_m + G(s)k(s) >< h(s)\right]^{-1}\left[G(s)\,\mathrm{Pr}(s) + \delta(s)\right] \tag{4.11}$$

As:

$$G(s)P = G(s)\left[G(0)^{-1} + k(0) >< h(0)\right]\left(I_m - F\right)^{-1}$$

and at low frequencies:

$$G(s)P \cong \frac{1}{1 - f}\left[I_m + G(s)k(0) >< h(0)\right]$$

Then equation (4.11) can be written as:

$$y(s) = I_m r(s) + S(s)\delta(s) \tag{4.12}$$

where:

$$S(s) = (1 - f)\left[I_m + G(s)k(s) >< h(s)\right] \qquad and \qquad 0 < f < 1 \tag{4.13}$$

Equation (4.12) shows that low steady state interaction, caused by reference input changes, can be realized. Also, equation (4.13) shows that as f is increased, the steady state disturbance rejection is increased.

From equation (4.4), it becomes evident that if a conventional multivariable regulator structure, having a forward path matrix $K(s)$ and a feedback matrix $H(s)$, is required, then the closed-loop input-output relation would be:

$$y(s) = \left[I_m + G(s)K(s)H(s)\right]^{-1}\left[G(s)K(s)r(s) + \delta(s)\right] \tag{4.14}$$

From equations (4.4) and (4.14), it can be concluded that:

$$K(s) = P \tag{4.15}$$

and:

$$H(s) = P^{-1}\left[k(s) >< h(s)\right] + F \tag{4.16}$$

4.3 Inner-Loop Analysis

As in equation (4.2), the inner-loop is represented by:

$$u(s) = k(s).\left[\bar{r}(s) - h(s).y(s)\right] \tag{4.17}$$

and its function is to satisfy the required system dynamics for closed loop conditions.

By Whalley et al. (2001), for the purpose of inner-loop analysis, the pre-compensated system transfer function $G(s)$ can be factorized as:

$$G(s) = L(s).\frac{A(s)}{d(s)}.R(s).\Gamma(s) \tag{4.18}$$

Where $L(s)$, $R(s)$ and $\Gamma(s)$ are diagonal matrices of order m, in which $L(s)$ and $R(s)$ contain the left (row) factors and the right (column) factors of $G(s)$, respectively, and $\Gamma(s)$ contains the transformed, actuator finite time delays of $G(s)$. With:

$$L(s) = diag\left(\frac{\lambda_i(s)}{p_j(s)}\right) \tag{4.19}$$

$$R(s) = diag\left(\frac{\rho_j(s)}{q_j(s)}\right) \tag{4.20}$$

$$\Gamma(s) = diag\left(e^{-sT_j}\right), \qquad 1 \le j \le m \tag{4.21}$$

The matrix $A(s)$ is a non-singular matrix of rational functions, with elements:

$$a_{ij}(s) = a_{ij}s^m + b_{ij}s^{m-1} + \ldots + \gamma_{ij}, \qquad 1 \le i, j \le m \tag{4.22}$$

Combining system input-output-disturbance relationship, as in equation (4.1), with the inner-loop control law, equation (4.17), yields:

$$y(s) = \left[I_m + G(s)k(s) >< h(s)\right]^{-1}\left[G(s)k(s)r(s) + \delta(s)\right] \tag{4.23}$$

The time delays in matrix $\Gamma(s)$ can be arranged such that $T_i \ge T_j$ for $\mathbf{1} \le \boldsymbol{j} \le \boldsymbol{m}$, $\boldsymbol{i} \ne \boldsymbol{j}$ and the forward path gain vector can be arranged as:

$$k(s) = \left[k_1(s)e^{-s(T_i - T_1)} \quad k_2(s)e^{-s(T_i - T_2)} \quad \ldots \quad k_i(s) \quad \ldots \quad k_m(s)e^{-s(T_i - T_m)}\right]^T \tag{4.24}$$

And as:

$$h(s) = \left[h_1(s) \quad h_2(s) \quad \ldots \quad h_m(s)\right] \tag{4.25}$$

Then if $k_j(s) = k_j\phi_j(s)$ and $h_j(s) = h_j\chi_j(s)$, $\mathbf{1} \le \boldsymbol{j} \le \boldsymbol{m}$, where $\phi_j(s)$ and $\chi_j(s)$ are proper or strictly proper, stable, realisable, minimunum phase, rational functions. They can be chosen such that equation (4.23) becomes:

$$y(s) = \left[I_m + e^{-sT_i}n(s)\frac{A(s)}{d(s)}k >< h\right]^{-1}\left[n(s)\frac{A(s)}{d(s)}ke^{-sT_i}r(s) + \delta(s)\right] \tag{4.26}$$

where, in this equation:

$$k = \left[k_1 \quad k_2 \quad \ldots \quad k_m\right]^T \tag{4.27}$$

and:

$$h = \left[h_1 \quad h_2 \quad \ldots \quad h_m\right] \tag{4.28}$$

$$d(s) = s^K + a_1s^{K-1} + \ldots + a_0 \tag{4.29}$$

and:

$$\deg\left[n(s)a_{ij}(s)\right] < K, \qquad 1 \le i, j \le m \tag{4.30}$$

The determinant required in equation (4.26), as shown in Whalley (1991) is:

$$\det\left[I_m + e^{-sT_i}n(s)\frac{A(s)}{d(s)}k >< h\right] = 1 + e^{-sT_i}n(s)\left\langle h(s)\frac{A(s)}{d(s)}k(s)\right\rangle \tag{4.31}$$

The inner product in this equation, can be written as:

$$\langle h(s)A(s)k(s)\rangle = \begin{bmatrix}1 & s & \dots & s^{m-1}\end{bmatrix}\begin{bmatrix}\gamma_{11} & \gamma_{12} & \dots & \gamma_{mm}\\ \dots & \dots & \dots & \dots\\ b_{11} & b_{12} & \dots & b_{mm}\\ a_{11} & a_{12} & \dots & a_{mm}\end{bmatrix}\begin{bmatrix}k_1h_1\\ k_2h_1\\ \dots\\ k_mh_m\end{bmatrix} \tag{4.32}$$

If in this equation, the gain ratios are represented as:

$$k_2 = n_1k_1,\ \ k_3 = n_2k_1,\ \dots,\ k_m = n_{m-1}k_1 \tag{4.33}$$

and:

$$\langle h(s)A(s)k(s)\rangle = b(s) \tag{4.34}$$

then this equation implies that:

$$k_1[Q]h = \begin{pmatrix}b_m & b_{m-1} & \dots & b_0\end{pmatrix}^T \tag{4.35}$$

where:

$$Q = \begin{bmatrix}\gamma_{11}+\gamma_{12}n_1+\dots+\gamma_{1m}n_{m-1} & \dots & \gamma_{21}+\gamma_{22}n_1+\dots+\gamma_{2m}n_{m-1} & \dots & \gamma_{m1}+\gamma_{m2}n_1+\dots+\gamma_{mm}n_{m-1}\\ \dots & \dots & \dots & \dots & \dots\\ b_{11}+b_{12}n_1+\dots+b_{1m}n_{m-1} & \dots & b_{21}+b_{22}n_1+\dots+b_{2m}n_{m-1} & \dots & b_{m1}+b_{m2}n_1+\dots+b_{mm}n_{m-1}\\ a_{11}+a_{12}n_1+\dots+a_{1m}n_{m-1} & & a_{21}+a_{22}n_1+\dots+a_{2m}n_{m-1} & \dots & a_{m1}+a_{m2}n_1+\dots+a_{mm}n_{m-1}\end{bmatrix} \tag{4.36}$$

and b_j, $0 \le j \le m-1$, are the coefficients of $b(s)$, given by equation (4.34). Taking into consideration the constraint, that $n_1, n_2, ..., n_{m-1}$ can be chosen in equation (4.35) so that the matrix is invertible, then a unique solution for $\begin{bmatrix}h_1 & h_2 & \dots & h_m\end{bmatrix}k_1$ exists.

The dynamics of the closed-loop system, arising from equation (4.25), could be improved by selecting an appropriate $b(s)$ function and gain ratios $n_1, n_2, ..., n_{m-1}$. The vector h is found by solving equation (4.35), after selecting an arbitray value for the parameter k_1.

4.4 Least-Effort Optimization

As mentioned earlier, the values of the gain ratios $n_1, n_2, ..., n_{m-1}$ can be chosen arbitrarily. This provides us with the ability to select these values, such that the energy consumed is minimized. For this purpose a performance index, representing the

control effort is defined. The minimum of this performance index, against the values of the gain ratios, $n_1, n_2, ..., n_{m-1}$, is looked for.

The control effort required to suppress disturbances, with zero set-point changes is proportional to:

$$\left(|k_1 h_1| + |k_2 h_1| + ... + |k_m h_1|\right)|y_1(t)| + \left(|k_1 h_2| + |k_2 h_2| + ... + |k_m h_2|\right)|y_2(t)| + ...$$
$$+ \left(|k_1 h_m| + |k_2 h_m| + ... + |k_m h_m|\right)|y_m(t)|$$

or, the control energy costs are proportional to:

$$E(t) = \int_{t=0}^{t=T} \left(\sum_{i=1}^{m} k_i^2 \sum_{j=1}^{m} h_j^2 y_j^2 \right) dt \tag{4.37}$$

Hence, for arbitrary changes in the transformed output vector $y(t)$, following arbitrary disturbance changes, minimising the performance index, defined as:

$$J = \sum_{i=1}^{m} k_i^2 \sum_{j=1}^{m} h_j^2 \tag{4.38}$$

would minimize the required control effort, defined by equation (4.37).

If the relationships:

$k_2 = n_1 k_1$, $k_3 = n_2 k_1$, ..., $k_m = n_{m-1} k_1$

are proposed, then equation (4.38) becomes:

$$J = (k_1)^2 \left(1 + n_1^2 + n_2^2 + ... + n_{m-1}^2\right)\left(h_1^2 + h_2^2 + ... + h_m^2\right) \tag{4.39}$$

where: $h_1^2 + h_2^2 + ... + h_m^2 = \langle h, h \rangle$.

The closed loop determinant is given by equation (4.31). With the inner product equated to $b(s)$, as in equation (4.34), then from equation (4.35), it can be found that:

$$h = k_1^{-1} Q^{-1} b \tag{4.40}$$

Upon substitution of h from equation (4.40), equation (4.39) becomes:

$$J = \left(1 + n_1^2 + n_2^2 + ... + n_{m-1}^2\right) b^T \left(Q^{-1}\right)^T Q^{-1} b \tag{4.41}$$

Assuming, for example, that $m = 3$, this equation becomes:

$$J = \left(1 + n_1^2 + n_2^2\right) b^T \left(Q^{-1}\right)^T Q^{-1} b$$

Where J is minimized, when:

$$\frac{\partial J}{\partial n_1} = 0, \quad \frac{\partial J}{\partial n_2} = 0 \text{ and } \frac{\partial^2 J}{\partial n_1^2}\frac{\partial^2 J}{\partial n_2^2} - \left(\frac{\partial^2 J}{\partial n_1 \partial n_2}\right) > 0, \text{ if } \frac{\partial^2 J}{\partial n_1^2} > 0$$

For $m > 3$ a numerical minimization technique, such as the algorithim of Nedler or the genetic algorithm could be employed to find the values of $n_1, n_2, ..., n_{m-1}$ which minimize J.

4.5 Stability of the Complete System

The stability of the complete system, system with inner and outer feedback loops, depends on the denominator of equation (4.14), describing the input-output relationship of the system with these two feedback loops.

As the outer-loop feedback gain matrix F is given by:

$$F = diag(f_j, f_j, ..., f_j), \quad 0 < f_j < 1, \quad 1 \leq j \leq m$$

then the denominator of equation (4.14) can be computed from:

$$\det\left\{ I_m + G(s)\left[\frac{k(s) >< h(s)}{1-f} + \frac{G(0)^{-1} f}{1-f} \right] \right\}$$

From this, it is clear that the elements of the feedback-compensator matrix $\left[\frac{k(s) >< h(s)}{1-f} + \frac{G(0)^{-1} f}{1-f} \right]$ become infinite as $f \to 1$. Or in other words, as $f \to 1$ the closed-loop system becomes unstable.

In addition to that, the characteristic locus method, presented by Macfarlane, can be used to confirm the relative stability of the closed-loop system. This can be seen from equations (4.15) and (4.16) of the forward path matrix $K(s)$ and the feedback matrix $H(s)$ and then, the conevtional structure of the multivariable feedback ssystem, indicated by equation (4.14) (Whalley, R. and Ebrahimi, M., 2006).

It has to be mentioned that, in general, disturbance rejection would not be achieved by the minimum control effort. To achieve that, the outer-loop feedback gain f should satisfy the condition $0 < f < 1.0$. Equation (4.13) shows that as f is increaed, the steady state disturbance rejection is inceased. For further analysis see Whalley and Ebrahimi (2006).

4.6 Least Effort Controller For the Separetly-Excited DC Motor

From equation (3.63), the transfer function of the separately-excited DC motor, in percent terms, is given by:

$$G_N(s) = \begin{bmatrix} \dfrac{44.74s + 96.35}{s^2 + 56.83s + 117.6} & \dfrac{17.35}{s^2 + 56.83s + 117.6} \\ 0 & \dfrac{2.15s + 117.6}{s^2 + 56.83s + 117.6} \end{bmatrix} \tag{4.42}$$

Comparing the above equation with the form $G(s) = L(s).\dfrac{A(s)}{d(s)}.R(s).\Gamma(s)$, and selecting:

$$L(s) = R(s) = \Gamma(s) = I \tag{4.43}$$

It is found that:

$$A(s) = \begin{bmatrix} 44.74s + 96.35 & 17.35 \\ 0 & 2.15s + 117.6 \end{bmatrix} \tag{4.44}$$

And:

$$d(s) = s^2 + 56.83s + 117.6 \tag{4.45}$$

The inner product is:

$$< h.A(s).k >= \begin{bmatrix} h_1 & h_2 \end{bmatrix}.\begin{bmatrix} 44.74s + 96.35 & 17.35 \\ 0 & 2.15s + 117.6 \end{bmatrix}.\begin{bmatrix} k_1 \\ k_2 \end{bmatrix} \tag{4.46}$$

Or:

$$< h.A(s).k >= (44.74s + 96.35)k_1h_1 + 17.35k_2h_1 + (2.15s + 117.6)k_2h_2 \tag{4.47}$$

Or, in matrix form:

$$< h.A(s).k >= \begin{bmatrix} 1 & s \end{bmatrix}.\begin{bmatrix} 96.35 & 17.35 & 0 & 117.6 \\ 44.74 & 0 & 0 & 2.15 \end{bmatrix}.\begin{bmatrix} k_1.h_1 \\ k_2.h_1 \\ k_1.h_2 \\ k_2.h_2 \end{bmatrix} \tag{4.48}$$

With the gain ratio n, substituting $k_2 = n.k_1$ and with $k_1 = 1$, the inner product becomes:

$$< h.A(s).k >= \begin{bmatrix} 1 & s \end{bmatrix} \begin{bmatrix} 96.35 & 17.35 & 0 & 117.6 \\ 44.74 & 0 & 0 & 2.15 \end{bmatrix} . \begin{bmatrix} h_1 \\ n.h_1 \\ h_2 \\ n..h_2 \end{bmatrix} \quad (4.49)$$

$$< h.A(s).k >= \begin{bmatrix} 96.35 + 44.74s & 17.35 & 0 & 117.6 + 2.15s \end{bmatrix} . \begin{bmatrix} h_1 \\ n.h_1 \\ h_2 \\ n.h_2 \end{bmatrix} \quad (4.50)$$

Hence:

$$Q = \begin{bmatrix} 96.35 + 17.35n & 117.6n \\ 44.74 & 2.15n \end{bmatrix} \quad (4.51)$$

In order to design the inner loop for the system that takes the form $< h.\frac{A(s)}{d(s)}.k >= \frac{b(s)}{d(s)}$, the roots of denominator, $d(s)$, and the numerator, $b(s)$, should be calculated. Assuming that $b(s)$ has the form $b(s) = b_0(s + x)$, in order to find b_0 and x, the root locus diagram of $\frac{b(s)}{d(s)} = -1$ should be plotted. However, as b_0 and x are unknown, the root locus diagram is initially plotted with unity as numerator and $d(s)$ as the denominator. Such a plot is performed by the MATLAB® program, attached to this thesis, and is shown in figure 4.2.

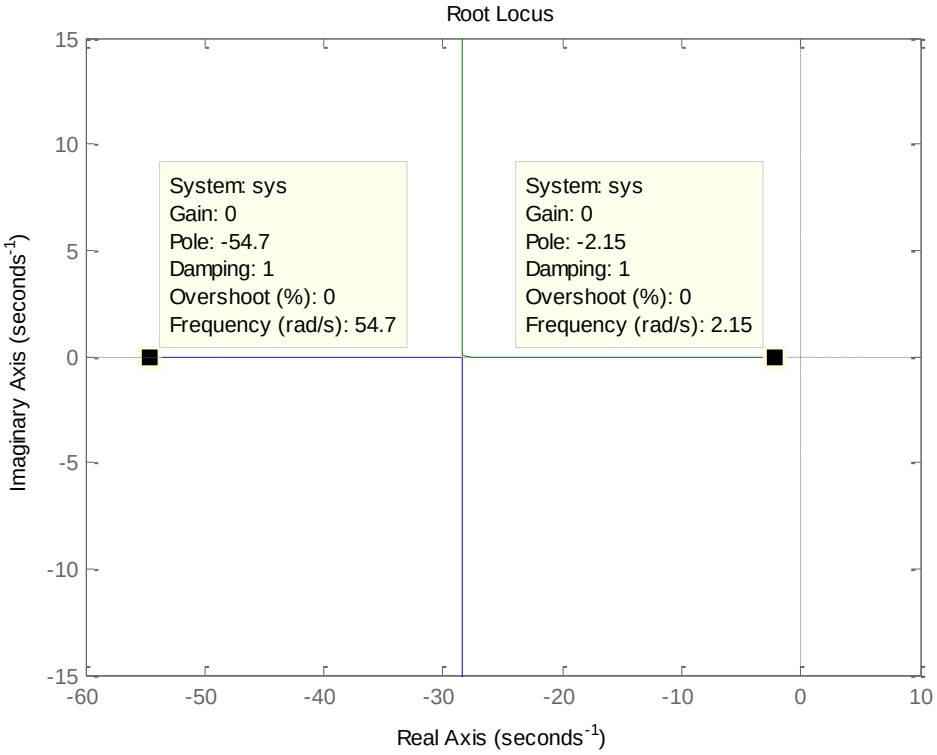

Figure 4.2: Root locus of $\frac{b(s)}{d(s)} = -1$.

From the root locus diagram, shown in figure 4.2, it can be noted that the poles of the system lie at -54.7 and at -2.15. As the slowest pole is located at -2.15, a zero at -2.5 would attract this pole more efficiently and helps in reducing the settling time. Thus, χ is chosen as 2.5 and b_0 as 1. For the chosen χ and b_0, the equation $\frac{b(s)}{d(s)}$ becomes:

$$\frac{b(s)}{d(s)} = \frac{s + 2.5}{s^2 + 56.83s + 117.6}.$$

Hence:

$$b = \begin{bmatrix} 1 \\ 2.5 \end{bmatrix} \tag{4.52}$$

To determine k_2, the specific gain ratio n, corresponding to minimum effort control, should be calculated. As the performance index J is given by:

$$J = \left(1+n^2\right) b^T .\left(Q^{-1}\right)^T .Q^{-1}.b \tag{4.53}$$

substituting the values of Q and b, from equations (4.51) and (4.52), respectively, in equation (4.53), we find that:

$$J = \frac{100\left(n^2+1\right)\left(3482312525n^2+680588450n+1538757529\right)}{n^2\left(74605n-10108543\right)^2} \tag{4.54}$$

The plot of the performance index J versus the gain ratio n is shown in figure 4.3.

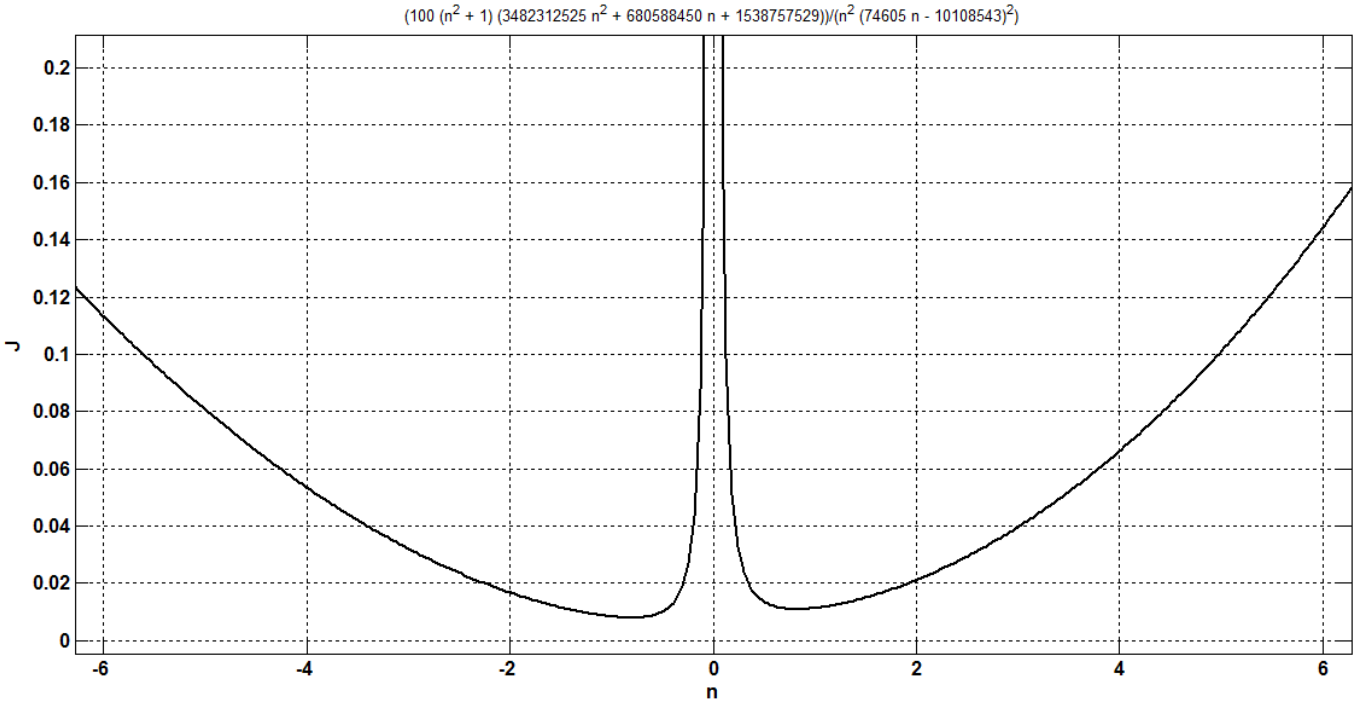

Figure 4.3: The performance index J as a function of the gain ratio n.

In order to find the absolute minimum value of the performnce index, J, the value of n should be calculated by letting

$$\frac{\partial J}{\partial n} = 0 .$$

The solutions of $\frac{\partial J}{\partial n} = 0$ are -0.80669, 0.82128, $-0.061438 + j0.81407$ and $-0.061438 - j0.81407$. The corresponding values of J are: 0.0079873,

0.010935, $0.00033489 + j0.00026885$ and $0.00033489 - j0.00026885$. From the values of J, it can be noted that $J_{\min} = 0.0079873$ and it occurs at $n = -0.80669$. Alternatively, the graph of J in Figure 4.3 confirms an absolute minimum exists when $n = -0.80669$.

Substituting the value of n in Q matrix (equation 4.51), thus:

$$Q = \begin{bmatrix} 82.354 & -94.867 \\ 44.74 & -1.7344 \end{bmatrix} \tag{4.55}$$

$h(s)$ is given by:

$$h(s) = \frac{Q^{-1}}{k_1}.b \tag{4.56}$$

Substituting the value of Q and b in the abBZove equation and assuming $k_1 = 1$

$$h(s) = \begin{bmatrix} 82.354 & -94.867 \\ 44.74 & -1.7344 \end{bmatrix}^{-1} . \begin{bmatrix} 1 \\ 2.5 \end{bmatrix} = \begin{bmatrix} 0.057401 \\ 0.039289 \end{bmatrix} \tag{4.57}$$

$$h(0) = \begin{bmatrix} 0.057401 \\ 0.039289 \end{bmatrix} \tag{4.58}$$

As $k_2 = n.k_1$, and as $k_1 = 1$, thus $k_2 = -0.80669$, and:

$$k = \begin{bmatrix} k_1 \\ k_2 \end{bmatrix} = \begin{bmatrix} 1 \\ -0.80669 \end{bmatrix} \tag{4.59}$$

Also, as $K(s)$ is given by $K(s) = k.R(s)$, and as $R(s) = 1$, thus:

$$K(s) = k = \begin{bmatrix} 1 \\ -0.80669 \end{bmatrix} \tag{4.60}$$

And:

$$K(0) = \begin{bmatrix} 1 \\ -0.80669 \end{bmatrix} \tag{4.61}$$

The steady state value of the transfer function is found as $G(0)$, where $G(s)$ is as defined by equation (4.42), or:

$$G(0) = \begin{bmatrix} 0.8193 & 0.14753 \\ 0 & 1 \end{bmatrix} \tag{4.62}$$

In order to minimize the closed loop steady state interaction of the system due to coupling, the steady state value is assumed as:

$$S_S = \begin{bmatrix} 1 & 0.1 \\ 0.1 & 1 \end{bmatrix} \tag{4.63}$$

The final step in the calculation is to choose the value of f, such that $0 < f < 1$. In order to achieve the shortest response time and maximum disturbance rejection while minimizing the percentage overshoot, the values of the feed forward and feedback loop gains will be calculated with three different values of f from 0.1 to 0.9 and the most optimized value will be selected.

For $f = 0.1$,

$$F = \begin{bmatrix} 0.1 & 0 \\ 0 & 0.1 \end{bmatrix} \tag{4.64}$$

The feed forward gain of the outer loop is calculated by substituting the values of $G(0)$, $K(0)$, $h(0)$, S_S and F, as found before, in the equation:

$$P = \left(G(0)^{-1} + K(0) >< h(0)\right) S_S . (I - F.S_s)^{-1} \tag{4.65}$$

Or:

$$P = \left(\begin{bmatrix} 0.8193 & 0.14753 \\ 0 & 1 \end{bmatrix}^{-1} + \begin{bmatrix} 1 \\ -0.80669 \end{bmatrix} >< \begin{bmatrix} 0.057401 \\ 0.039289 \end{bmatrix} \right) . \begin{bmatrix} 1 & 0.1 \\ 0.1 & 1 \end{bmatrix} . \left(\begin{bmatrix} 1 & 0 \\ 0 & 1 \end{bmatrix} - \begin{bmatrix} 0.1 & 0 \\ 0 & 0.1 \end{bmatrix} . \begin{bmatrix} 1 & 0.1 \\ 0.1 & 1 \end{bmatrix} \right)^{-1}$$

$$P = \begin{bmatrix} 1.4043 & 0.0011718 \\ 0.068045 & 1.0715 \end{bmatrix} \tag{4.66}$$

The feedback gain matrix, H , can be calculated from the equation:

$$H = P^{-1}.K(0) >< h(0) + F \tag{4.67}$$

Or:

$$H = \begin{bmatrix} 1.4043 & 0.0011718 \\ 0.068045 & 1.0715 \end{bmatrix}^{-1} . \begin{bmatrix} 1 \\ -0.80669 \end{bmatrix} >< \begin{bmatrix} 0.057401 \\ 0.039289 \end{bmatrix} + \begin{bmatrix} 0.1 & 0 \\ 0 & 0.1 \end{bmatrix}$$

$$H = \begin{bmatrix} 0.14091 & 0.028003 \\ -0.045813 & 0.068643 \end{bmatrix} \tag{4.68}$$

By similar calculation, it can found that the values of P and H at $f = 0.5$ are:

$$P = \begin{bmatrix} 2.5507 & 0.22909 \\ 0.29675 & 1.957 \end{bmatrix} \tag{4.69}$$

$$H = \begin{bmatrix} 0.52497 & 0.017091 \\ -0.027447 & 0.48121 \end{bmatrix} \tag{4.70}$$

Similarly for $f = 0.9$

$$P = \begin{bmatrix} 65.904 & 59.184 \\ 48.307 & 53.113 \end{bmatrix} \tag{4.71}$$

$$H = \begin{bmatrix} 0.90903 & 0.0061782 \\ -0.0090814 & 0.89378 \end{bmatrix} \tag{4.72}$$

4.7 Simulations and Results

Based on the obtained values of the feed-forward and feedback gains (P and H matrices), the open loop system model is modified to include the least effort controller, as shown in figure 4.4.

Simulink models, as shown in figure A.5, were built for all the values of P and H matrices, obtained for three different values of f ($0.1, 0.5$ and 0.9). Each of these models was simulated separately and their responses were analyzed to compare the

performance factors, such as speed of response, overshoot, steady state error, steady state output interaction, disturbance rejection and energy consumed by the controller. To analyze the steady state output interactions, the responses of the system, with different values of f, for a unit step input on each of the two inputs individually, have been obtained. Disturbances of unit steps were added to the two system outputs, to simulate the disturbance rejection capability of the system. To analyze the energy consumed by the controller, for different values of f, random disturbances were added to the two system outputs. This section explains the dynamic responses, steady state interactions, disturbance rejection capability and energy consumed by the controller for the closed-loop system, with different values of f.

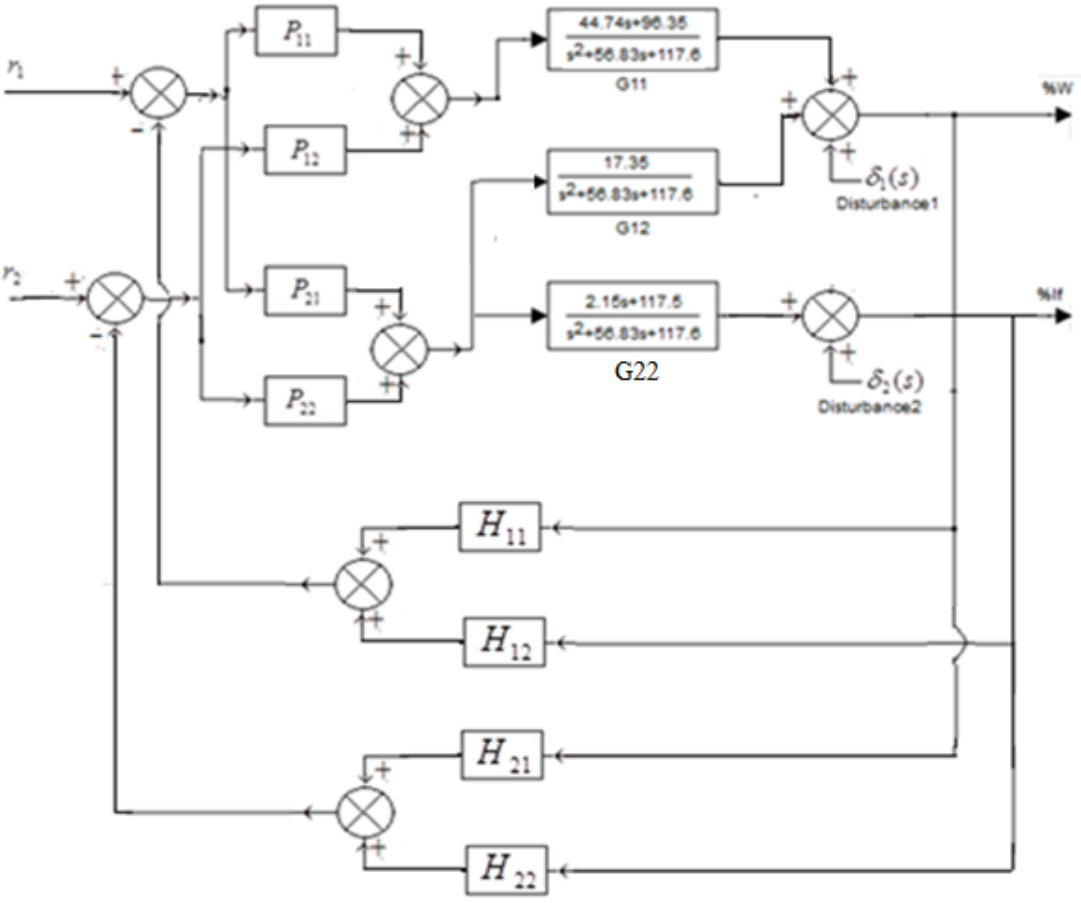

Figure 4.4: Block diagram of the separately-excited DC motor with a least-effort controller.

The percentage changes in the motor angular speed and the motot field current, caused by a 1% step input on $r_1(t)$, with $r_2(t) = 0$, for different values of f, are shown in figures 4.5 and 4.6, respectively.

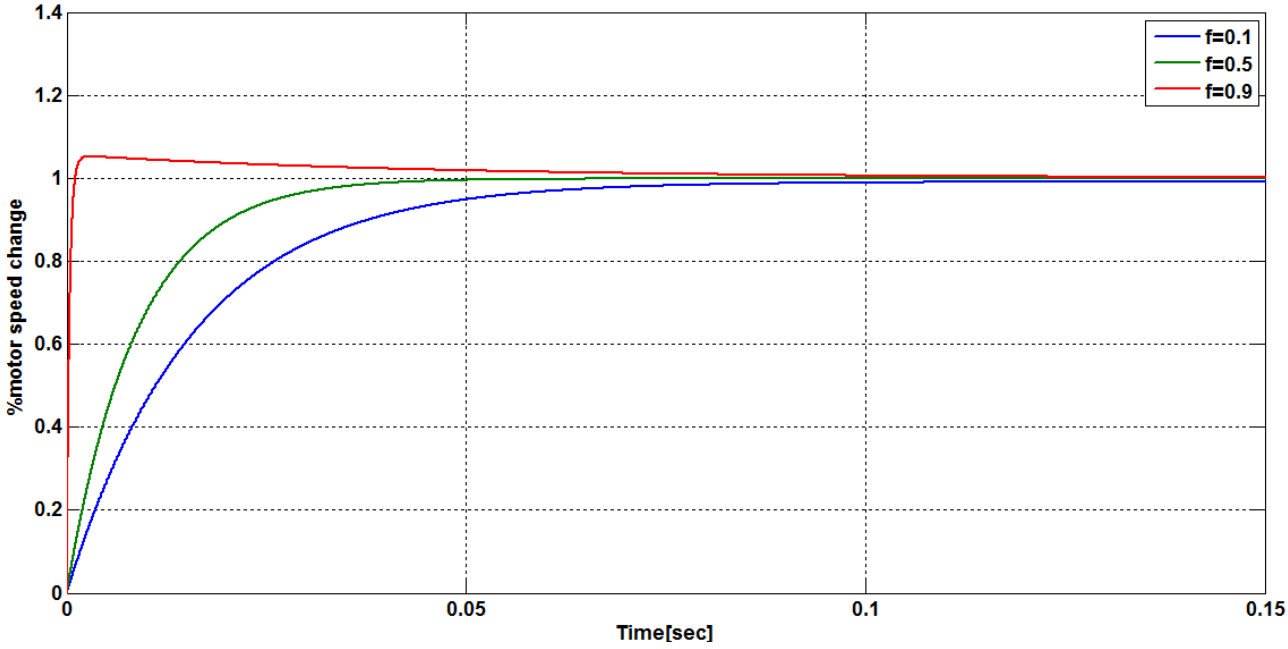

Figure 4.5: Percentage change in the motor angular speed, as a result of a unit step input on $r_1(t)$, with $r_2(t) = 0$, for different values of f.

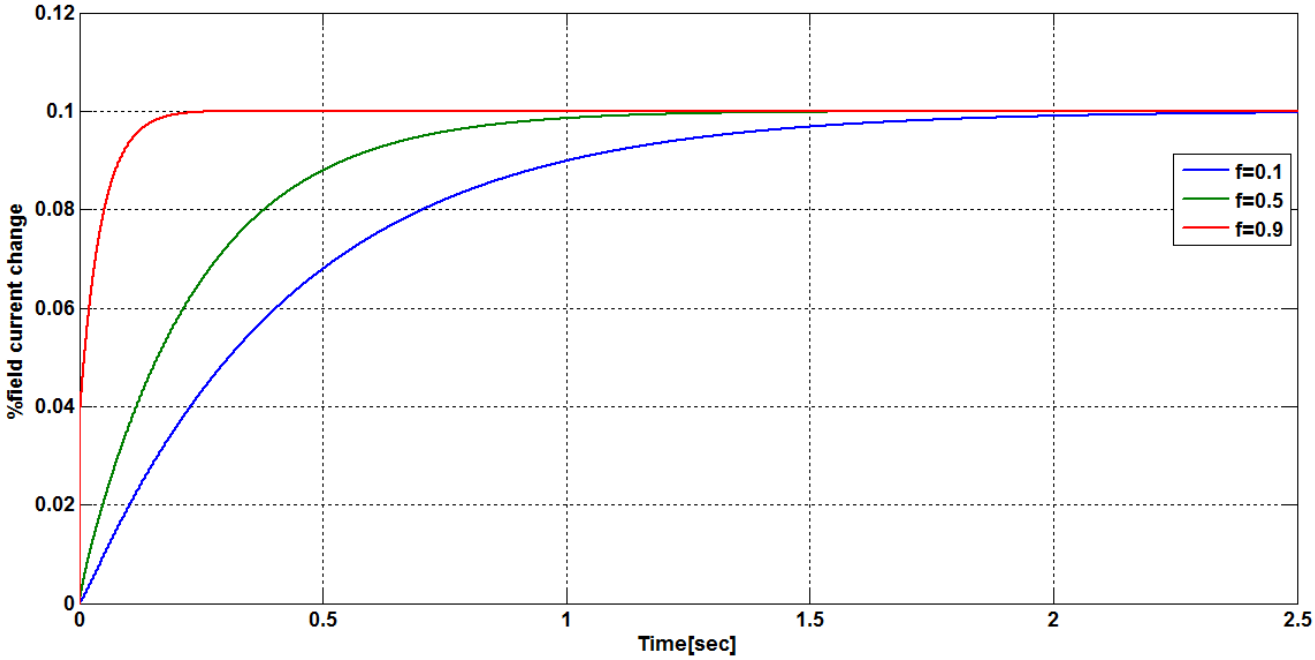

Figure 4.6: Percentage change in the motor field current, as a result of a unit step input on $r_1(t)$, with $r_2(t) = 0$, for different values of f.

Figures 4.7 and 4.8 show the system responses for a unit step input on $r_2(t)$ with $r_1(t) = 0$, for different values of f.

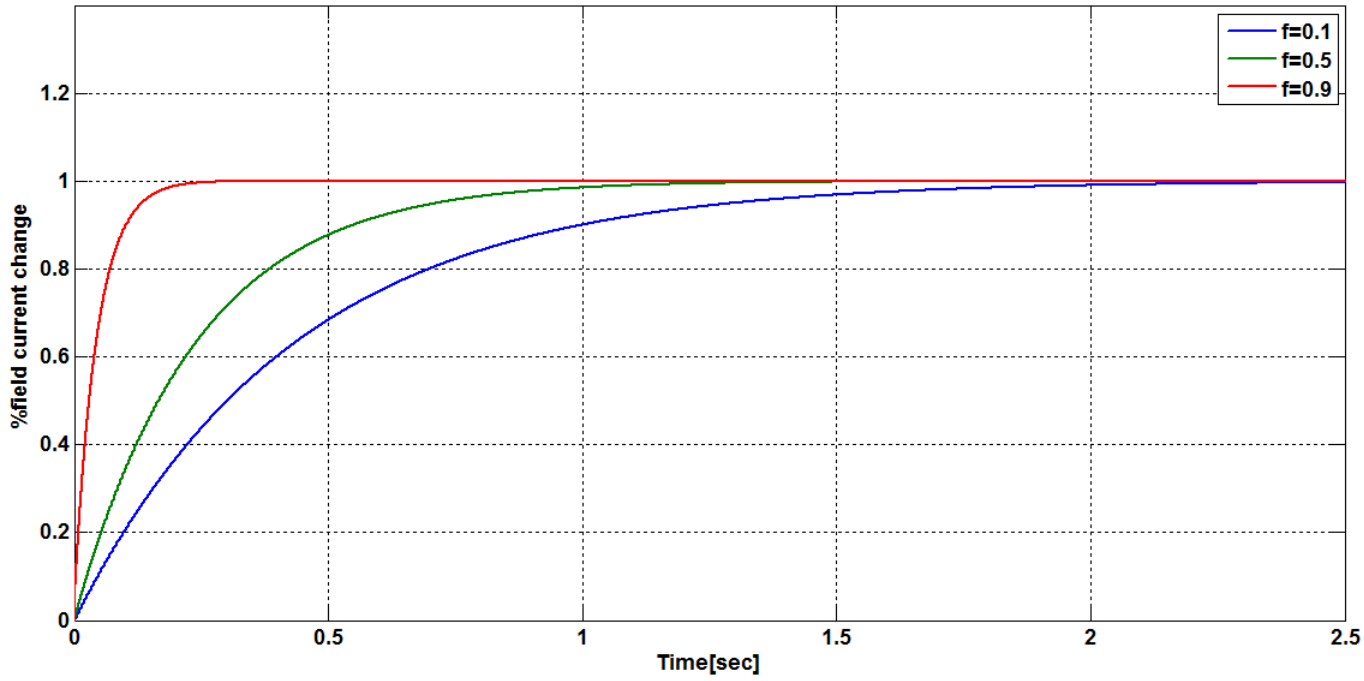

Figure 4.7: Percentage change in the motor field current, as a result of a unit step input on $r_2(t)$, with $r_1(t) = 0$, for different values of f.

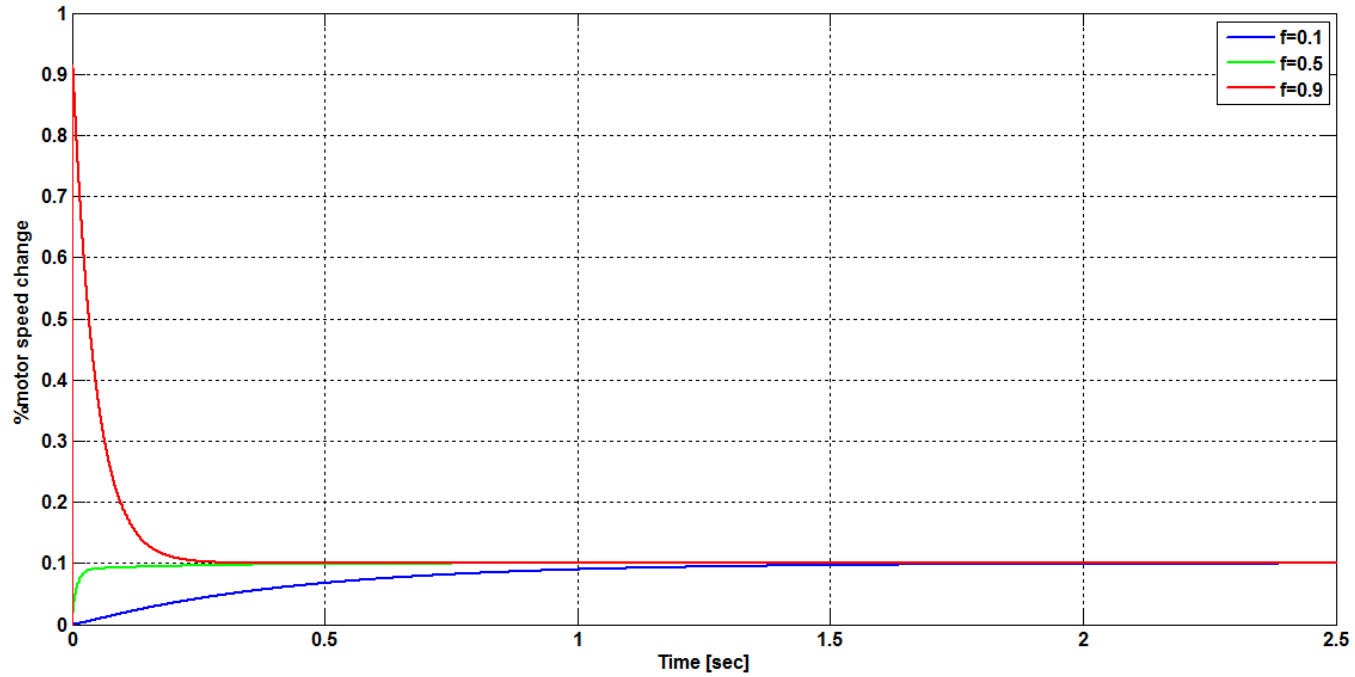

Figure 4.8: Percentage change in the motor angular speed, as a result of a unit step input on $r_2(t)$, with $r_1(t) = 0$, for different values of f.

From figure 4.5, it is clearly seen that following a unit step change on the first reference input, the first output, which is the motor angular speed, changes by almost 1%. This means that the steady state error is almost zero. Also it can be clearly noted that incresaing the outer loop feedback gain, f, decreases the rising time, with a slight over shoot when $f = 0.9$.

Figure 4.6 shows that, a unit step change on the first reference input causes only a 0.1% change of the second system output, which is the motor field current. This means that the steady state output interaction is limited to 10%. Again, incresaing the outer loop feedback gain, f, decreases the system rising time.

Figures 4.7 and 4.8 show the effect of a unit step change on the second reference input. It can be seen from figure 4.7, that a unit step change on the second reference input causes almost a unit change on the second output, which is the motor field current. This means that the steady state error is again almost zero. Also, it can be seen, from figure 4.8, that a 10% output coupling is reached, as a a unit step change on the second reference input causes only a 0.1% change of the first system output, which is the motor angular speed. Again, incresaing the outer loop feedback gain, f, decreases the system rising time, but with a large overshoot when $f = 0.9$.

The effect of the outer loop feedback gain, f, on the system disturbance recovery, following unit step changes on each of the first disturbance $\delta_1(t)$ and the second disturbance $\delta_2(t)$, are studied for three system designs, using $f = 0.1$, $f = 0.5$ and $f = 0.9$. These system responses are shown in figures 4.9, 4.10, 4.11 and 4.12.

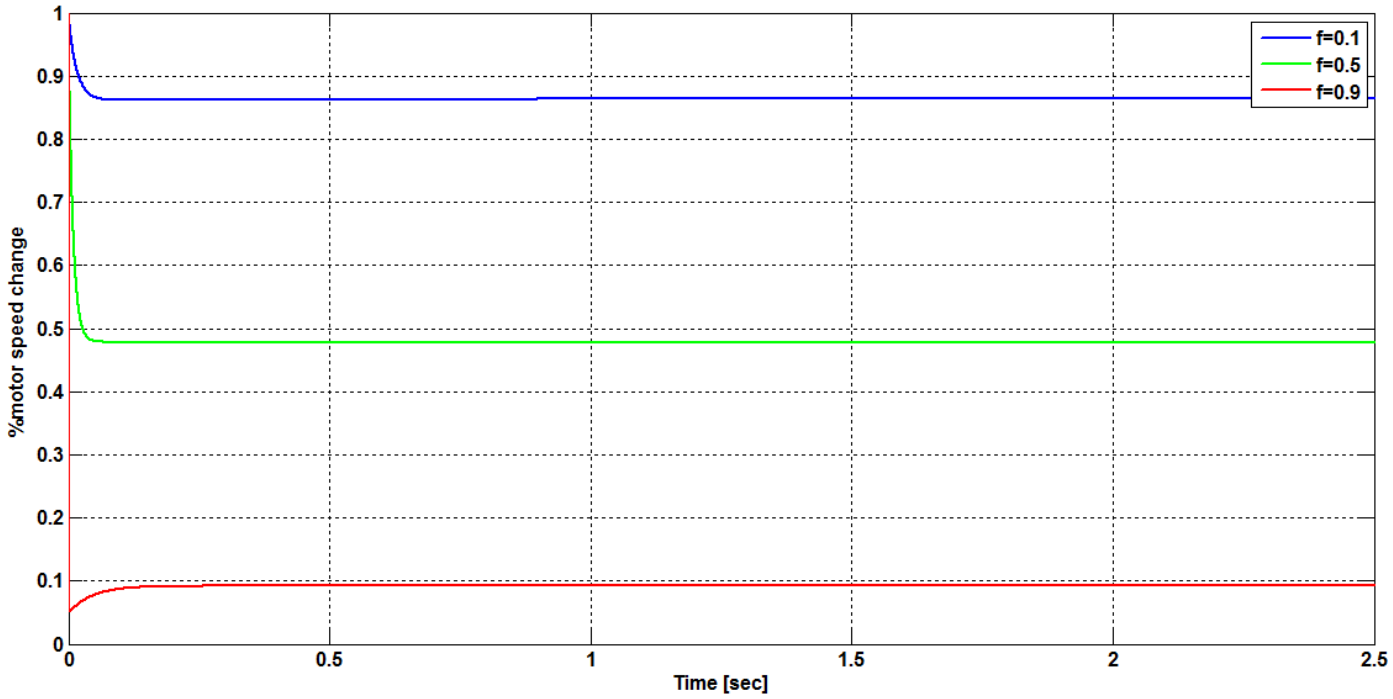

Figure 4.9: Percentage change in the motor angular speed, as a result of a unit step change on $\delta_1(t)$, for different values of f.

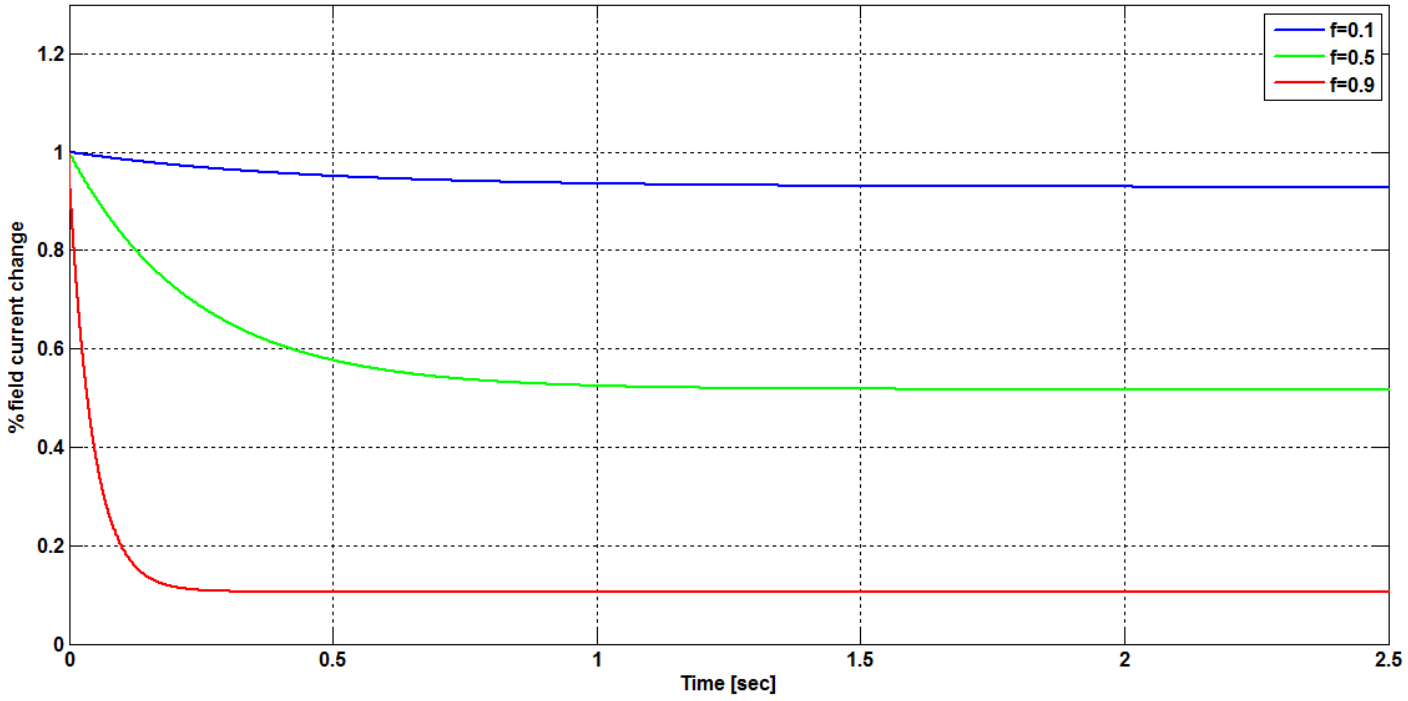

Figure 4.10: Percentage change in the motor field current, as a result of a unit step change on $\delta_2(t)$, for different values of f.

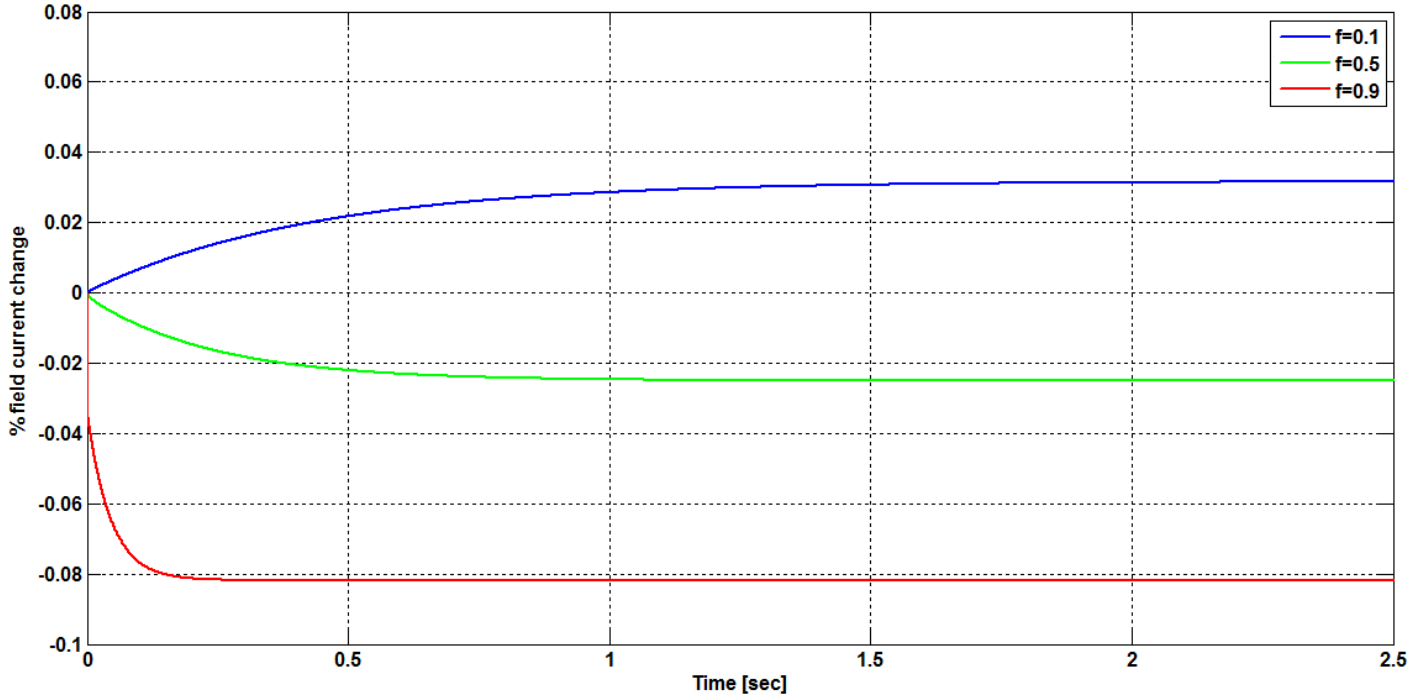

Figure 4.11: Percentage change in the motor field current, as a result of a unit step change on $\delta_1(t)$, for different values of f.

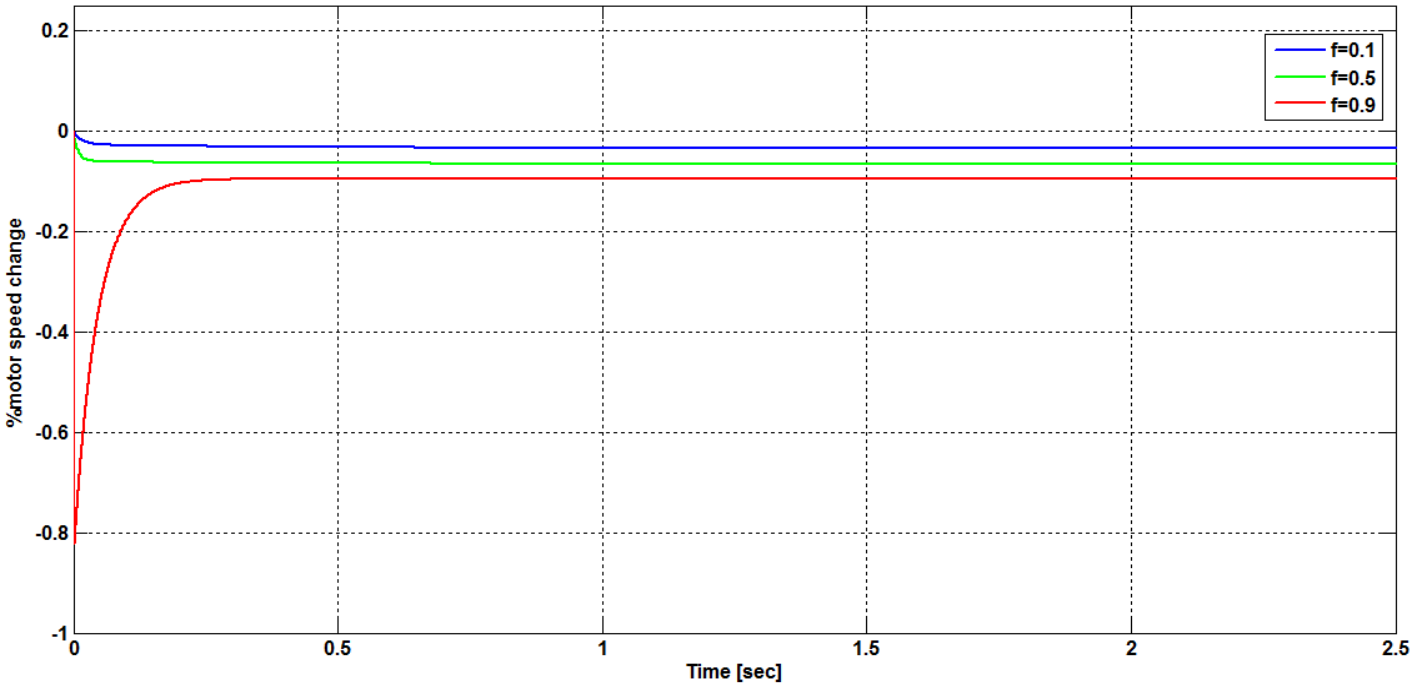

Figure 4.12: Percentage change in the motor angular speed, as a result of a unit step change on $\delta_2(t)$, for different values of f.

From these figures, it is obviously seen that increasing the outer loop feedback gain, f , increases the disturbance recovery rates. Figures 4.9 and 4.10 show that with $f = 0.1$ the disturbance recovery rate is poor, and it is about 10% only. With $f = 0.5$ an almost 50% disturbance recovery rate, with settling time about 0.1 seconds for the motor angular speed and about a second for the motor field current, is achieved. The best disturbance recovery rate, where about 90% of the disturbance is eliminated in a very short time, is achieved when $f = 0.9$.

Figures 4.11 and 4.12 show that a disturbance on one output also affects the second output responses; however these effects are very small and could be neglected.

The energy consumed by the controller can be computed from:

$$E(t) = \int_0^T \left({u_1}^2(t) + {u_2}^2(t) \right) dt \qquad (4.73)$$

Figure 4.13 shows the energy consumed by the controller, following the imposition of random disturbances of the both outputs with $f = 0.1$ and 0.5, for a period of 100sec. It can be noticed from this figure that with increasing the value of f , the control energy increases very rapidly.

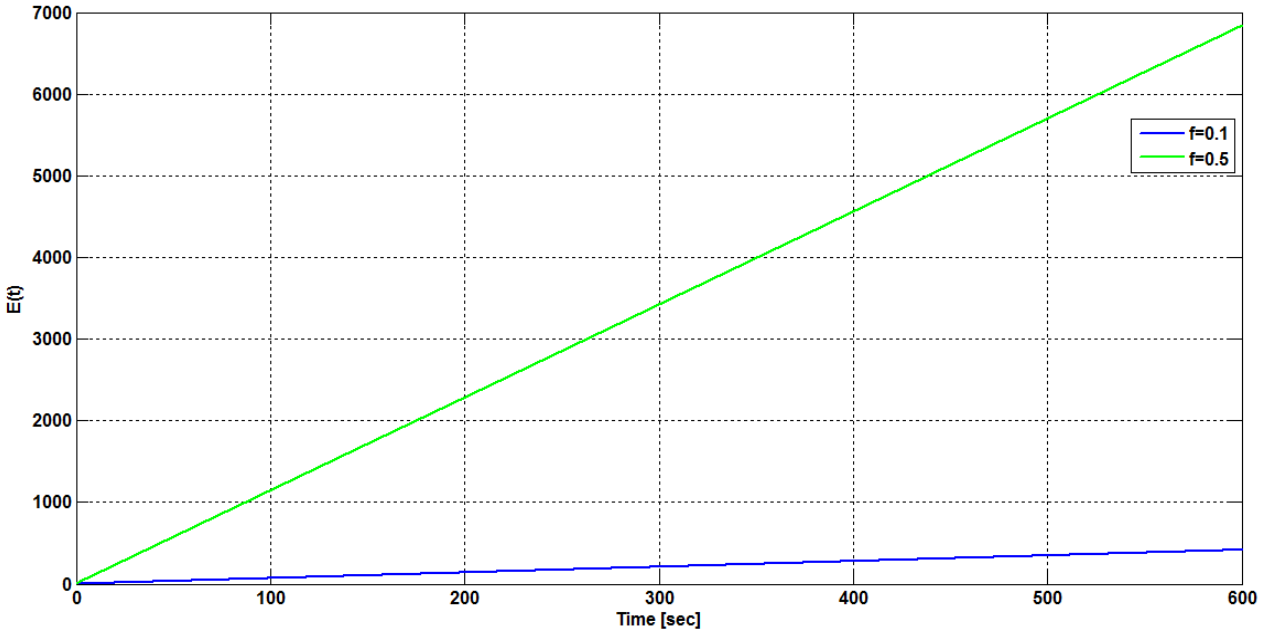

Figure 4.13: Control energy with random disturbances on the two outputs, with $r_1(t) = r_2(t) = 0$.

By analyzing the performance of the compensated system for all values of f, it can be noted that the system shows excellent integrity. The presence of steady state errors is almost negligible and the system achieves steady state rapidly. The steady state interactions due to output coupling are also maintained at 10%. Further, by analyzing the response of the closed-loop system, with different values of f, it can be seen that increasing the value of f improves the performance of the system but increases the energy consumed by the controller. Thus, in order to maintain stability and to meet the design criteria of less steady state interaction, acceptable response and settling time, reduced or almost negligible steady state error, with no overshoot in the output responses and minimum control effort, $f = 0.1$ is chosen.

Chapter (5)

The Inverse-Nyquist Array Controller

5.1 Introduction

In this chapter a feedback controller, using the second approach, the Inverse Nyquist Array (INA) approach will be designed. In order to compare the performance of this controller with that designed using the least effort approach, as in the previous chapter, the designed feedback controller will be simulated and its performance will be analyzed.

The INA method was developed by Rosenbrock in 1969 and was used for designing controllers for multivariable systems. In this method and in order to decrease the system output interaction, a diagonally-dominant closed-loop transfer function has to be found. This will reduce the design process to designing a set of independent single loops.

In the INA method, the multivariable system is assumed to be represented by a square mxm transfer function matrix $G(s)$, which is controlled by an mxm pre-compensator matrix $K(s)$ and closing m feedback SISO loops, as shown in figure (5.1), below.

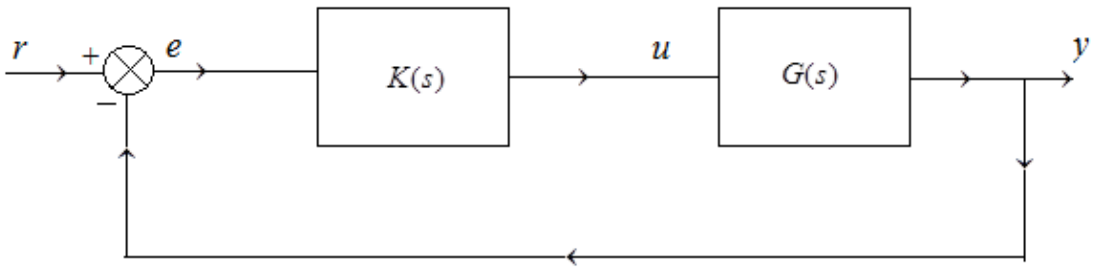

Figure 5.1: Generalized block diagram of a multivariable control system.

Here, it is assumed that all the elements of $G(s)$ and $K(s)$ are rational polynomials in the Laplace variable, s, and both $G(s)$ and $K(s)$ are invertible matrices. Also it

is assumed that the system $G(s)$ is stable and all the elements of the pre-compensator matrix $K(s)$ have their zeroes and poles in the left-half plane. These assumptions will provide a diagonal dominance of the open-loop system, $G(s).K(s)$, which in turn will reduce the system output coupling, hence single-input single-output (SISO) controllers can be used for each loop independently, to provide the required closed loop response.

From figure (5.1), the open-loop transfer function matrix is:

$$Q(s) = G(s).K(s) \tag{5.1}$$

And the system output is:

$$y(s) = Q(s).e(s) = Q(s).[r(s) - y(s)] \tag{5.2}$$

So the closed-loop transfer function is:

$$H(s) = [I_m + Q(s)]^{-1} Q(s) \tag{5.3}$$

Or:

$$H^{-1}(s) = I_m + Q^{-1}(s) \tag{5.4}$$

For notation, inverted matrices will be denoted as:

$G^{-1} = \hat{G}$, $K^{-1} = \hat{K}$, $Q^{-1} = \hat{Q}$ and $H^{-1} = \hat{H}$

and their elements as $\hat{g}_{ij}$, $\hat{k}_{ij}$, $\hat{q}_{ij}$ and $\hat{h}_{ij}$, respectively.

then, equation (5.4) can be written as:

$$\hat{H}(s) = I_m + \hat{Q}(s) \tag{5.5}$$

A more general approch of the closed-loop system will be when the function $F(s)$ is introduced in the feedback path, as shown in figure (5.2).

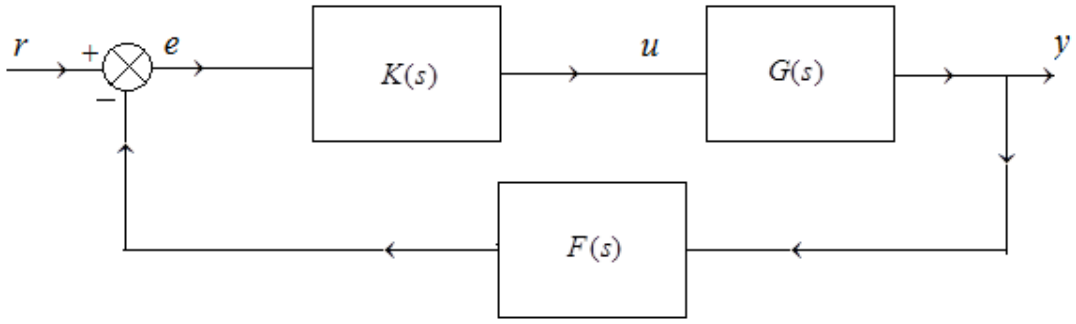

Figure 5.2: Closed-loop multivariable control system with feedback $F(s)$.

For this system, the transfer function relating system output to system input is:

$$R(s) = \left[I_m + Q(s)F(s)\right]^{-1} Q(s) \tag{5.6}$$

And:

$$R^{-1}(s) = Q^{-1}(s) + F(s) \tag{5.7}$$

Or in the form:

$$\hat{R}(s) = \hat{Q}(s) + F(s) \tag{5.8}$$

Note that, when $F = I_m$,

$$\hat{R}(s) = \hat{H}(s) \tag{5.9}$$

5.2 Diagonal Dominance

A rational mxm matrix $\hat{Q}(s)$ is said to be row diagonal dominant on the Nyquist D-contour if:

$|\hat{q}_{ii}(s)| > \sum_{\substack{j=1 \\ j\neq i}}^{m} |\hat{q}_{ij}(s)|$, for all s on the D-contour.

Where:

$\hat{q}_{ij}(s)$ are the elements of $\hat{Q}(s)$.

Similarly, the matix is said to be column dominance if:

$|\hat{q}_{ii}(s)| > \sum_{\substack{i=1 \\ i\neq j}}^{m} |\hat{q}_{ij}(s)|$, for all s on the D-contour.

The diagonal dominance of a given matrix $\hat{Q}(s)$ can be tested graphically by constructing a set of Gershgorin circles, having centers the elements of the main diagonal and a radius:

$$d_i(s) = \sum_{\substack{j=1 \\ j\neq i}}^{m} |\hat{q}_{ij}(s)| \qquad (5.10)$$

According to (Munro, 1972), if the origin is not included in any of the bands generated by theses Gershgorin circles, at any frequency; then $\hat{Q}(s)$ is row or column dominant.

As the pre-compensator $K(s)$ ensures the diagonal dominance of the open-loop system, a controller can be designed for each loop independently from other loops.

Also, the system stability is ensured if the Gershgorin's bands does not enclose the (-1,0) point (Munro, 1972).

One method of dertermining the precompensator $K(s)$, which has proved useful, is to try to diagonalize the system at one frequency, for example at zero or at infinity, and hope that the effect will be sufficiently beneficial over a wide range of frequencies. For example we can choose $K(s) = G^{-1}(0)$. Here $K(s)$ is a matrix of real

constants which simply diagonalizes $Q(s)$ at zero frequency, (Munro, 1972). It has to be mentioned also that in some cases diagonal dominance of the transfer function matrix can be achieved by re-ordering of the inputs and/or the outputs.

5.3 Controller For the Separetly-Excited DC Motor by Inverse Nyquist Array

From equation (3.63), the input-output description, in percent changes, of the separately excited DC motor is given by:

$$\begin{bmatrix} \tilde{y}_1(\%) \\ \tilde{y}_2(\%) \end{bmatrix} = \begin{bmatrix} \dfrac{44.74s + 96.35}{s^2 + 56.83s + 117.6} & \dfrac{17.35}{s^2 + 56.83s + 117.6} \\ 0 & \dfrac{2.15s + 117.6}{s^2 + 56.83s + 117.6} \end{bmatrix} \begin{bmatrix} \tilde{u}_1(\%) \\ \tilde{u}_2(\%) \end{bmatrix} \tag{5.11}$$

Or in the general form:

$$\tilde{Y}(\%) = G_N(s)\tilde{U}(\%) \tag{5.12}$$

Where:

$$\tilde{Y}(\%) = \begin{bmatrix} \tilde{y}_1(\%) \\ \tilde{y}_2(\%) \end{bmatrix} = \begin{bmatrix} \omega(\%) \\ i_f(\%) \end{bmatrix} \tag{5.13}$$

$$\tilde{U}(\%) = \begin{bmatrix} \tilde{u}_1(\%) \\ \tilde{u}_2(\%) \end{bmatrix} = \begin{bmatrix} v_a(\%) \\ v_f(\%) \end{bmatrix} \tag{5.14}$$

and:

$$G_N(s) = \begin{bmatrix} \dfrac{44.74s + 96.35}{s^2 + 56.83s + 117.6} & \dfrac{17.35}{s^2 + 56.83s + 117.6} \\ 0 & \dfrac{2.15s + 117.6}{s^2 + 56.83s + 117.6} \end{bmatrix} \tag{5.15}$$

As seen from the system description above, a decoupling is already existing between the motor field current, i_f , and the motor armature voltage, v_a , as the motor field current is controlled only by the motor field voltage, v_f .

The inverse of $G_N(s)$ is:

$$\hat{G}_N(s) = \begin{bmatrix} \dfrac{s^2 + 56.83s + 117.6}{44.74s + 96.35} & -\dfrac{17.35(s^2 + 56.83s + 117.6)}{(44.74s + 96.35)(2.15s + 117.6)} \\ 0 & \dfrac{s^2 + 56.83s + 117.6}{2.15s + 117.6} \end{bmatrix} \quad (5.16)$$

The diagonal dominance of $\hat{G}_N(s)$ can be proved by Gershgorin's bands theorem. As per this theorem, the matrix $\hat{G}_N(s)$ is column diagonally dominant if the union of Gershgorin's bands does not enclose the complex plane's origin. Also, the system stability is ensured if the Gershgorin's bands does not enclose the (-1,0) point (Munro, 1972).

The Inverse Nyquist Array for $\hat{G}_N(s)$, as described by equation 5.16, with Gershgorin circles superimposed could be plotted by an m-file program, attached in the appendix.

Figure 5.3 shows the Nyquist diagram of the element $\hat{G}_N(1,1)$, with imposed Gershgorin circles for the first column of $\hat{G}_N(s)$. It can be seen, from this figure, that the origin is not included in any of the circles, thus the system is first column diagonal dominant.

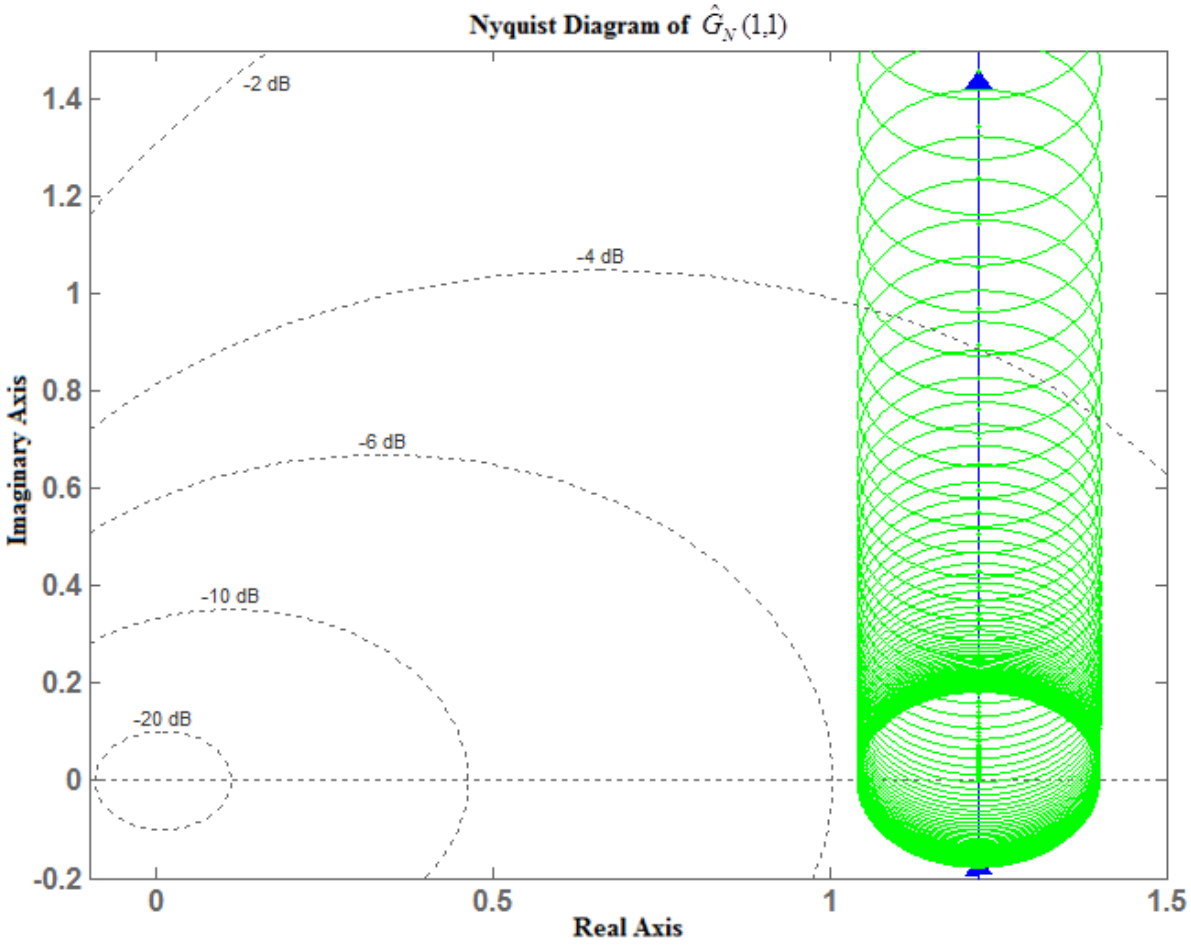

Figure 5.3: Nyquist diagram of the element $\hat{G}_N(1,1)$, with Gershgorin circles.

In the same way, Gershgorin's bands for the second column of $\hat{G}_N(s)$, superimposed on the Nyquist diagram of the $\hat{G}_N(2,2)$ element, is shown in figure 5.4. It is also seen that none of the bands include the origin, therefore diagonal dominance of the system (second column) is also achieved, hence the system is completely column dominant. This is a special case, where no diagonalising pre-compensator is required and infinite gains can be used. Since $\hat{G}_N(s)$ is already a diagonal dominant matrix, a controller for each loop could be designed independently.

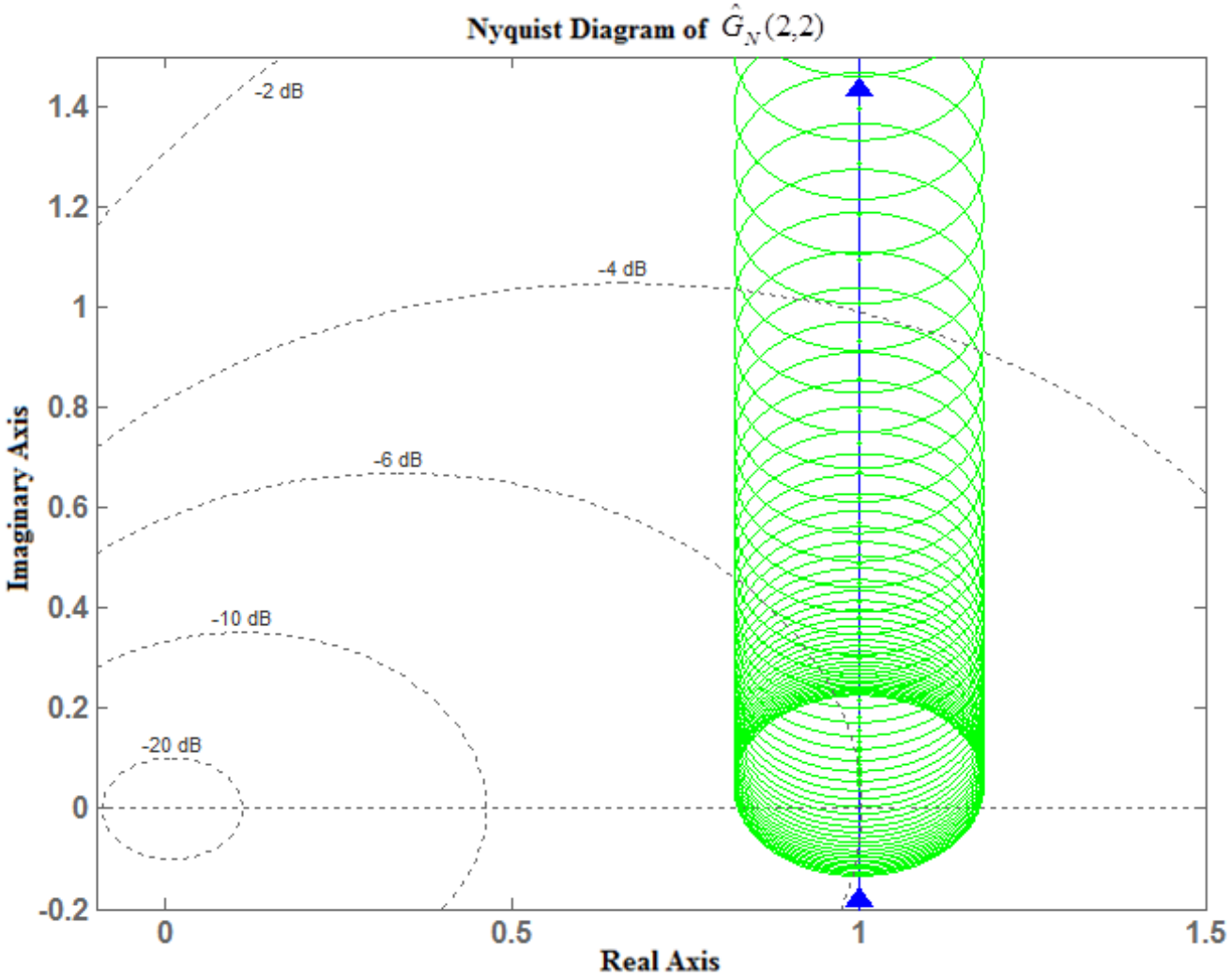

Figure 5.4: Nyquist diagram of the element $\hat{G}_N(2,2)$, with Gershgorin circles.

For the purpose of comparing the performance of this system with that of a system having a Least Effort Controller, a pre-compensator, $K(s)$, with gain elements equal to that of the feed-forward gain matrix, P, in the least-effort controller, is added to the system. Or the pre-compensator matrix is:

$$K(s) = P = \begin{bmatrix} 1.4043 & 0.0011718 \\ 0.068045 & 1.0715 \end{bmatrix}$$

The open-loop transfer function matrix is:

$$Q(s) = G(s).K(s)$$

$$Q(s)=\begin{bmatrix} \dfrac{44.74s+96.35}{s^2+56.83s+117.6} & \dfrac{17.35}{s^2+56.83s+117.6} \\ 0 & \dfrac{2.15s+117.6}{s^2+56.83s+117.6} \end{bmatrix}\cdot\begin{bmatrix} 1.4043 & 0.0011718 \\ 0.068045 & 1.0715 \end{bmatrix}$$

$$=\begin{bmatrix} \dfrac{62.828s+136.48}{s^2+56.83s+117.6} & \dfrac{0.0524s+18.703}{s^2+56.83s+117.6} \\ \dfrac{0.1463s+8.0021}{s^2+56.83s+117.6} & \dfrac{2.3037s+126.01}{s^2+56.83s+117.6} \end{bmatrix}$$

and its inverse is:

$$\hat{Q}(s)=\frac{s^2+56.83s+117.6}{144.73s^2+8228.2s+17048}\begin{bmatrix} 2.3037s+126.01 & -(0.0524s+18.703) \\ -(0.1463s+8.0021) & 62.828s+136.48 \end{bmatrix}$$

The Nyquist diagrams, with imposed Gershgorin circles, for the elements $\hat{Q}(1,1)$ and $\hat{Q}(2,2)$ are shown in figures 5.4 and 5.5, respectively. From these figures, it can be seen that the origin is not included in any of the circles, thus the system is first and second column diagonally dominant, and decoubling between the outputs is existing in the closed-loop system. Also, the system stability is ensured as the Gershgorin's bands does not enclose the point (-1,0).

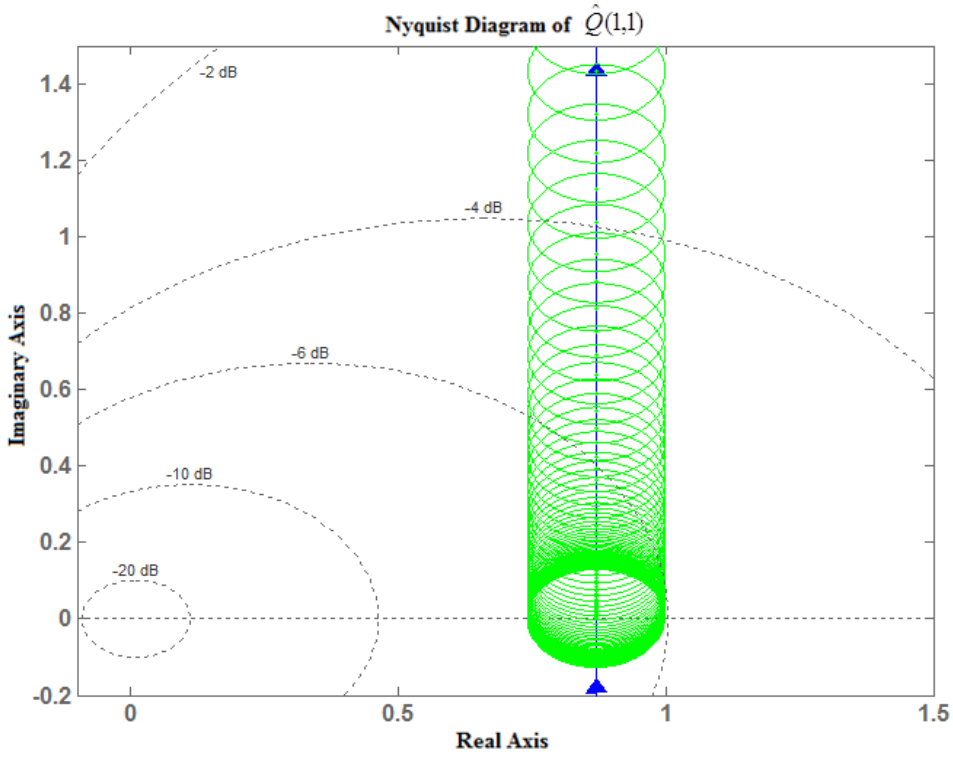

Figure 5.5: Nyquist diagram of the element $\hat{Q}(1,1)$, with Gershgorin circles.

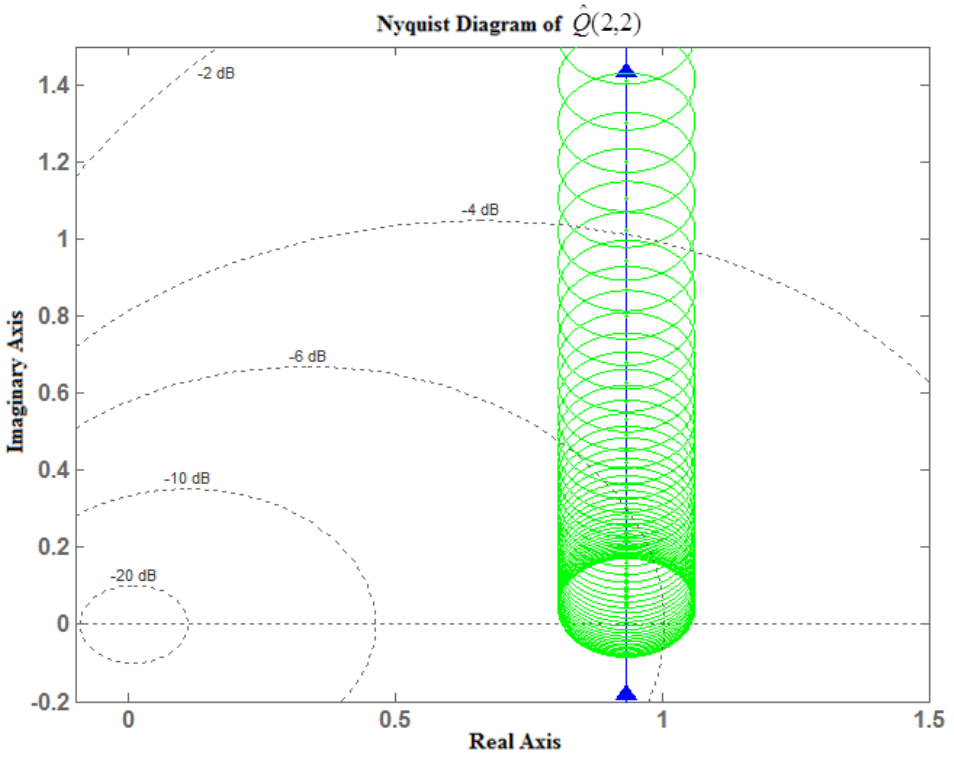

Figure 5.6: Nyquist diagram of the element $\hat{Q}(2,2)$, with Gershgorin circles.

The figure below shows the block diagram of the closed-loop system with unity feedback for each of the two independent loops.

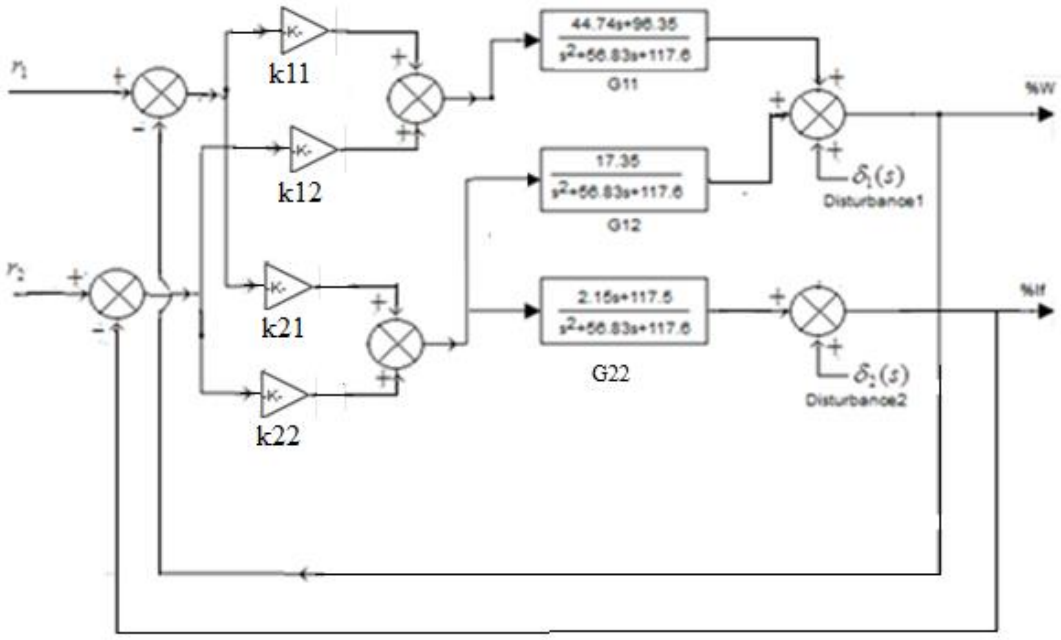

Figure 5.7: Block diagram of the system with a closed-loop controller using the inverse Nyquist array method.

A MATLAB®/Simulink® model of the closed-loop system was built, and is shown in figure A.6.

5.4 Simulations and Results

The model shown in figure A.6 was simulated, following a unit step changes on each of the two inputs, in turn. These responses are shown in figures 5.8 and 5.9, below.

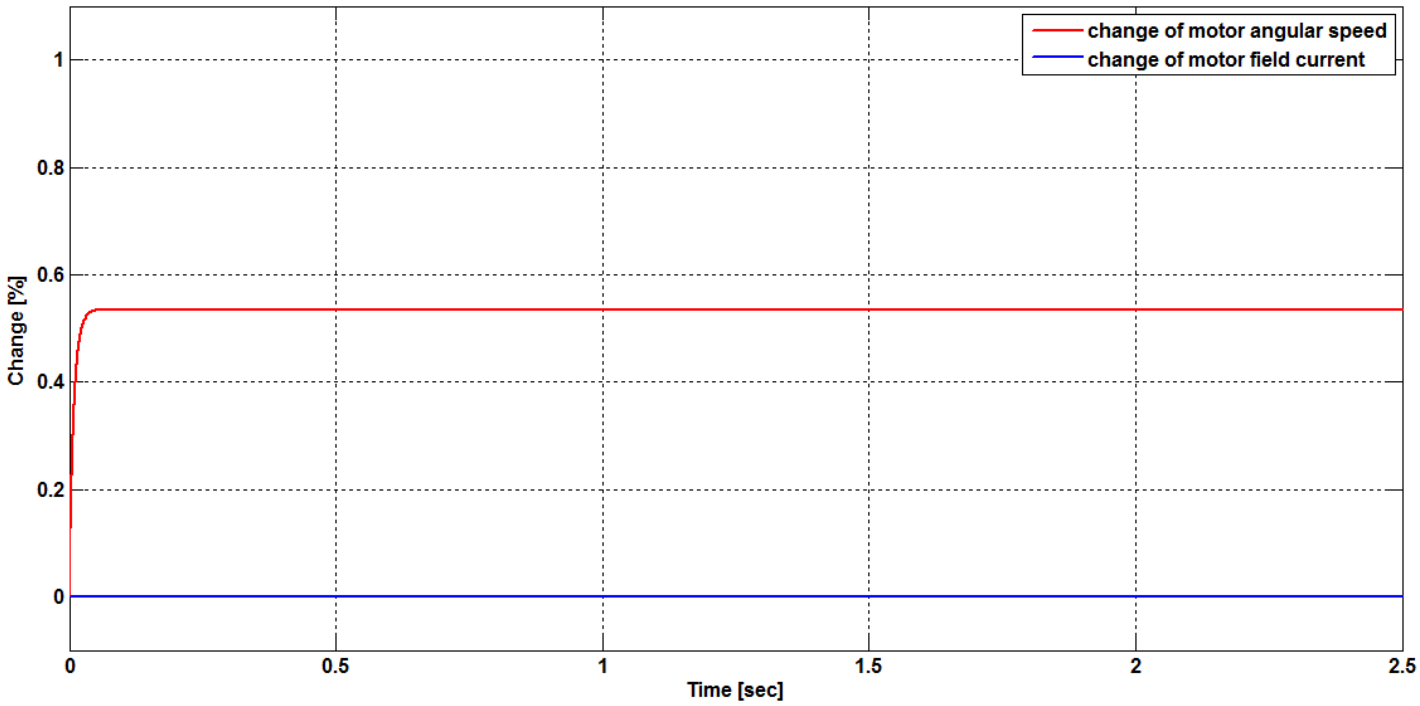

Figure 5.8: Percentage changes in the motor angular speed and the motor field current, as a result of a unit step input on $r_1(t)$, with $r_2(t) = 0$.

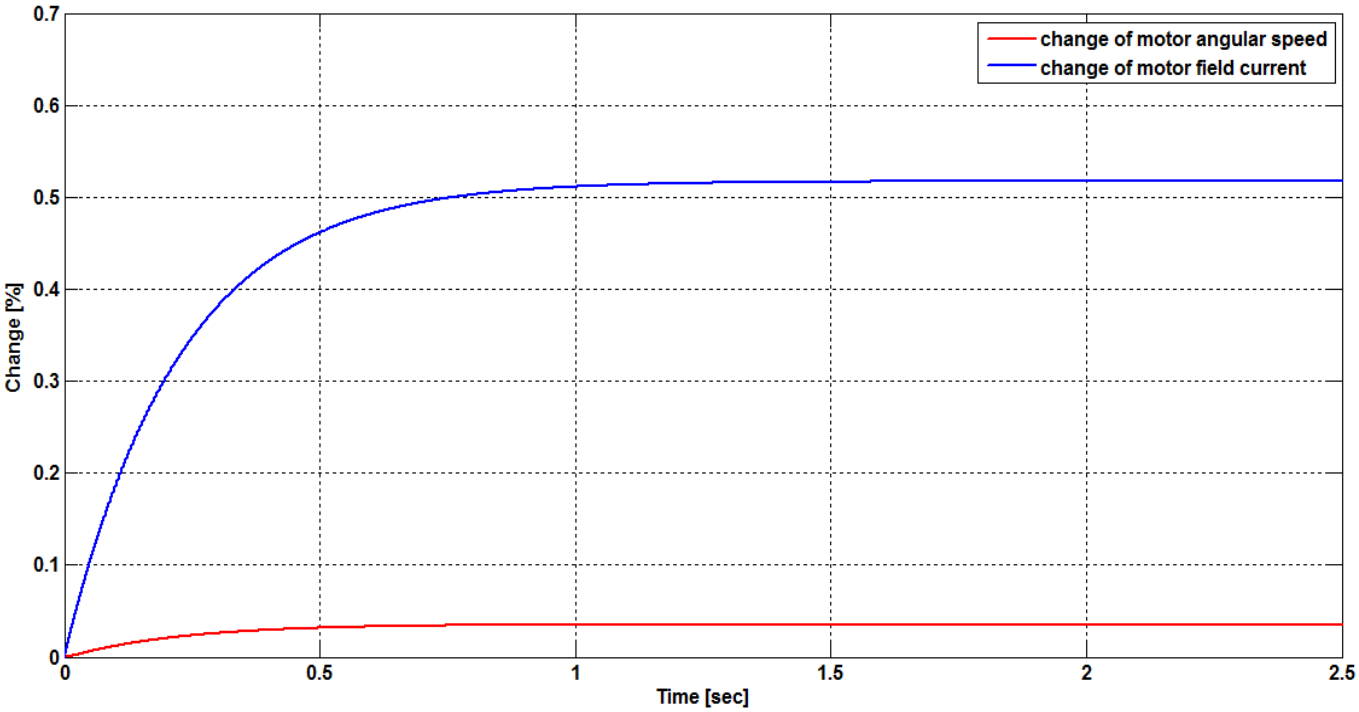

Figure 5.9: Percentage changes in the motor angular speed and the motor field current, as a result of a unit step input on $r_2(t)$, with $r_1(t) = 0$.

Figure 5.8, shows that following a unit step change on the first reference input, the first output, which is the motor angular speed, changes only by around 0.55%. This means that the steady state error is very large, as it is around 45%. At the same time, the motor field current doesn't change, which means that a complete decoupling is exising.

From figure 5.9, it can be also seen that, following a unit step change on the second reference input, the second output, which is the motor field current, changes only by around 0.52%. This means that the steady state error is also very large, as it is around 48%. At the same time, the motor speed changes by around 0.035%, which means that a coupling of aound 3.5% is existing.

The responses of the closed-loop system, following unit step changes on each of the first disturbance $\delta_1(t)$ and the second disturbance $\delta_2(t)$, are shown in figures 5.10 and 5.11, respectively. It can be seen from these two figures that the disturbance suppression for each of $\delta_1(t)$ and $\delta_2(t)$ is around 50%, which is poor.

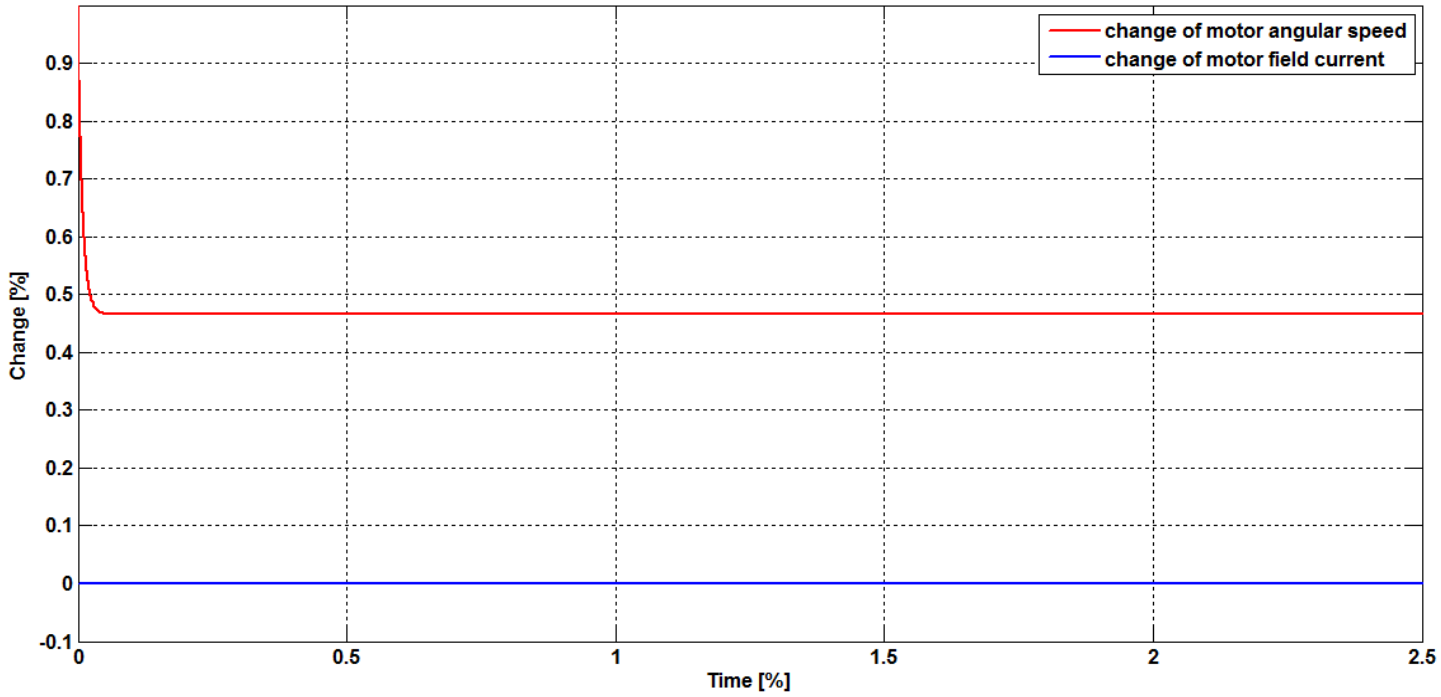

Figure 5.10: Percentage changes in the motor angular speed and the motor field current, as a result of a unit step input on $\delta_1(t)$.

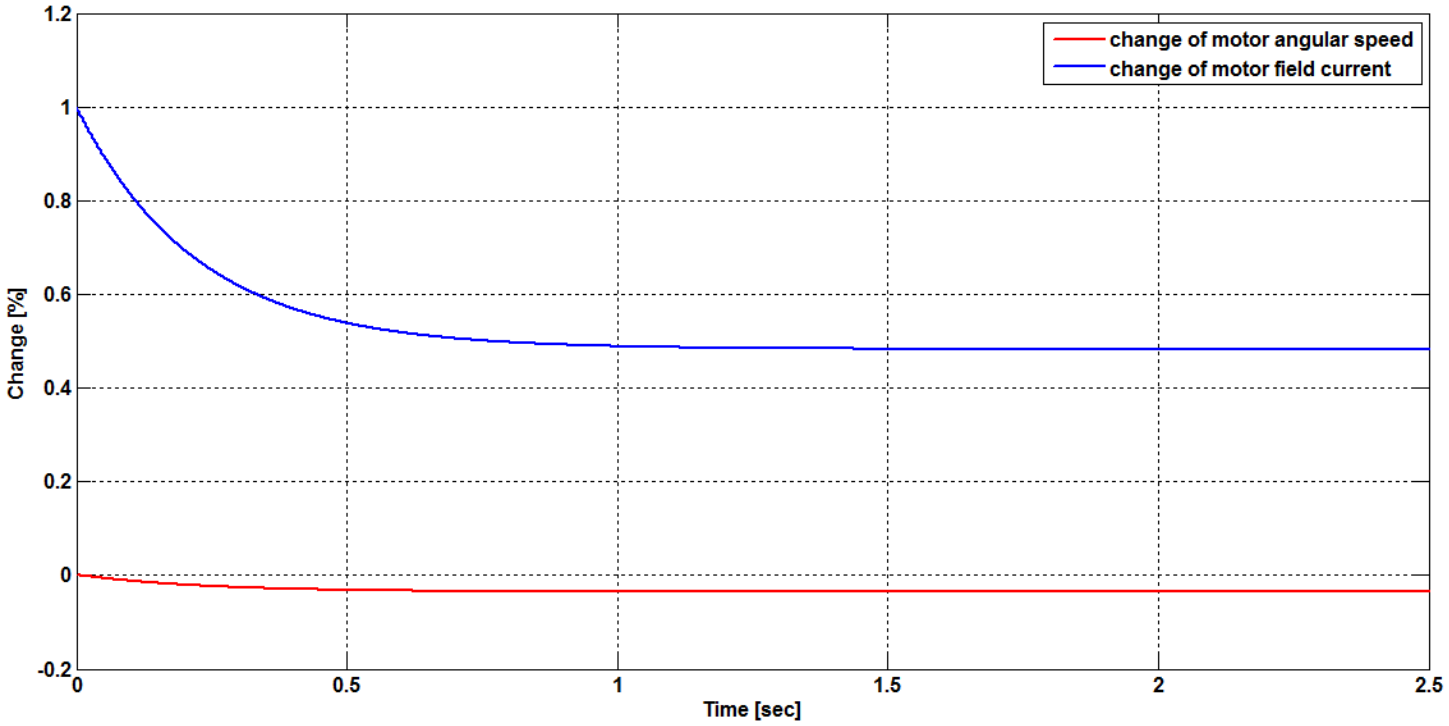

Figure 5.11: Percentage changes in the motor angular speed and the motor field current, as a result of a unit step input on $\delta_2(t)$.

In the same way, as the case with the Least Effort Controller, the control energy can be computed from:

$$E(t) = \int_0^T \left({u_1}^2(t) + {u_2}^2(t) \right) dt \qquad (5.17)$$

Figure 5.12 shows the energy consumed by the controller, following the imposition of random disturbances on the both outputs, for a period of $10\,\text{min}$.

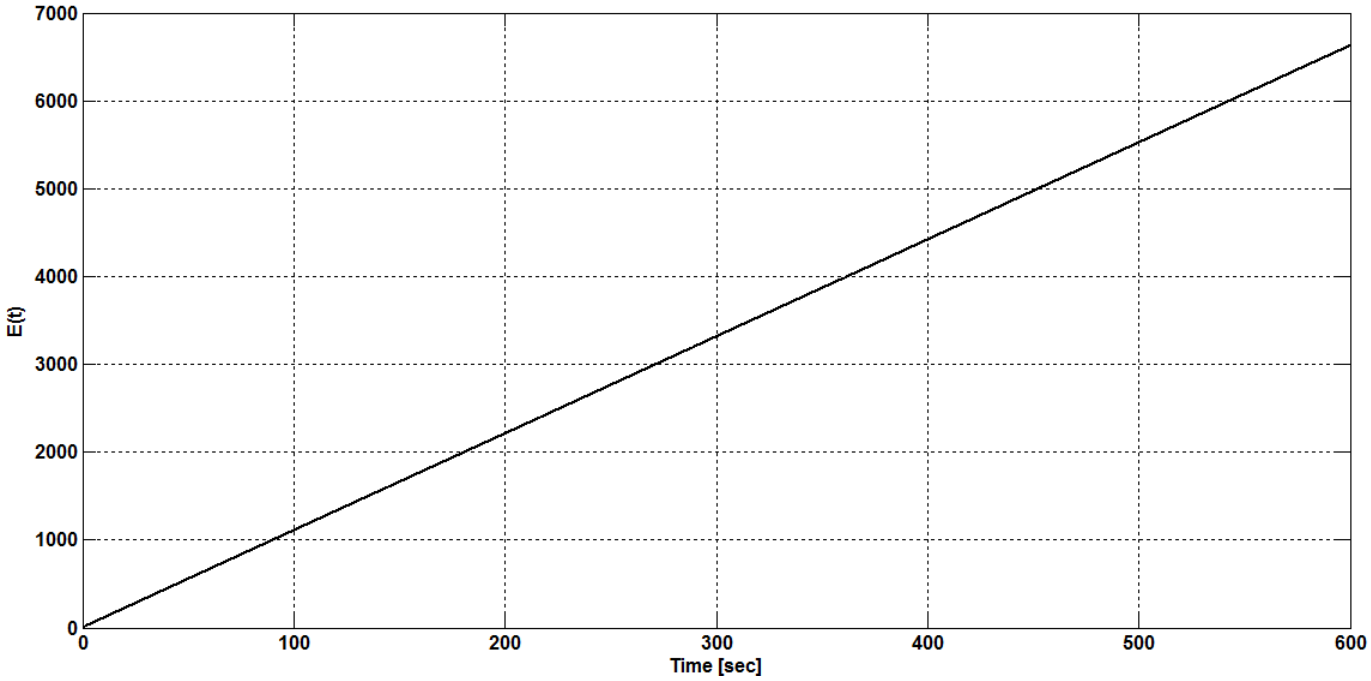

Figure 5.12: Control energy with random disturbances on the two outputs, with $r_1(t) = r_2(t) = 0$.

5.5 Effect of the Forward Gains on the Performance of The System

Figures 5.8 – 5.12 show the performance of the system with an Inverse Nyquist Array Controller with forward gains the same as that of the Least Effort Controller, i.e., $K(s) = P = \begin{bmatrix} 1.4043 & 0.0011718 \\ 0.068045 & 1.0715 \end{bmatrix}$.

To invistigate the effect of the values of the forward gains on the performance of the system, the system was simulated for different values of forward gains.

Figures 5.13 and 5.14 show the percentage changes in system outputs following a 1% step change on each of the two inputs, respectively, for different values of the forward

gains. These figures show that increasing the forward gains decreases the steady state error and increases the system response speed.

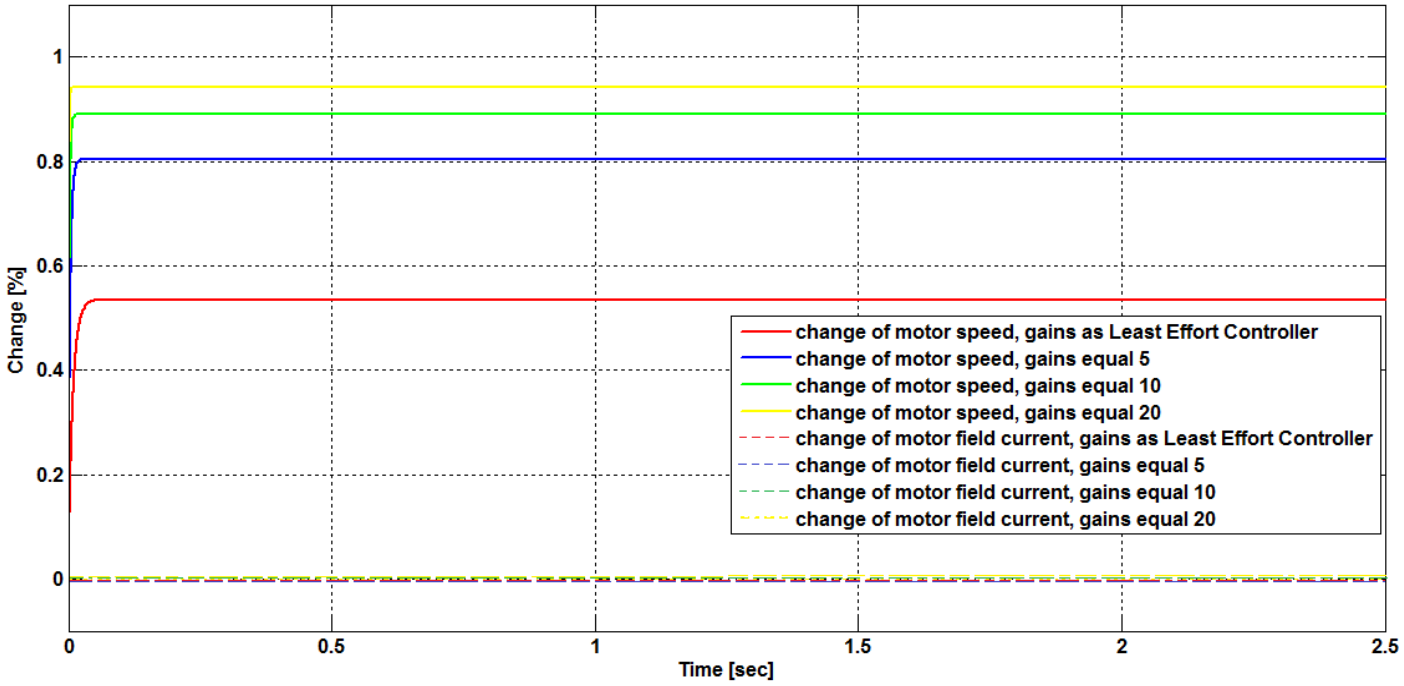

Figure 5.13: Percentage changes in the motor angular speed and the motor field current, as a result of a unit step input on $r_1(t)$, with $r_2(t) = 0$, for different gains.

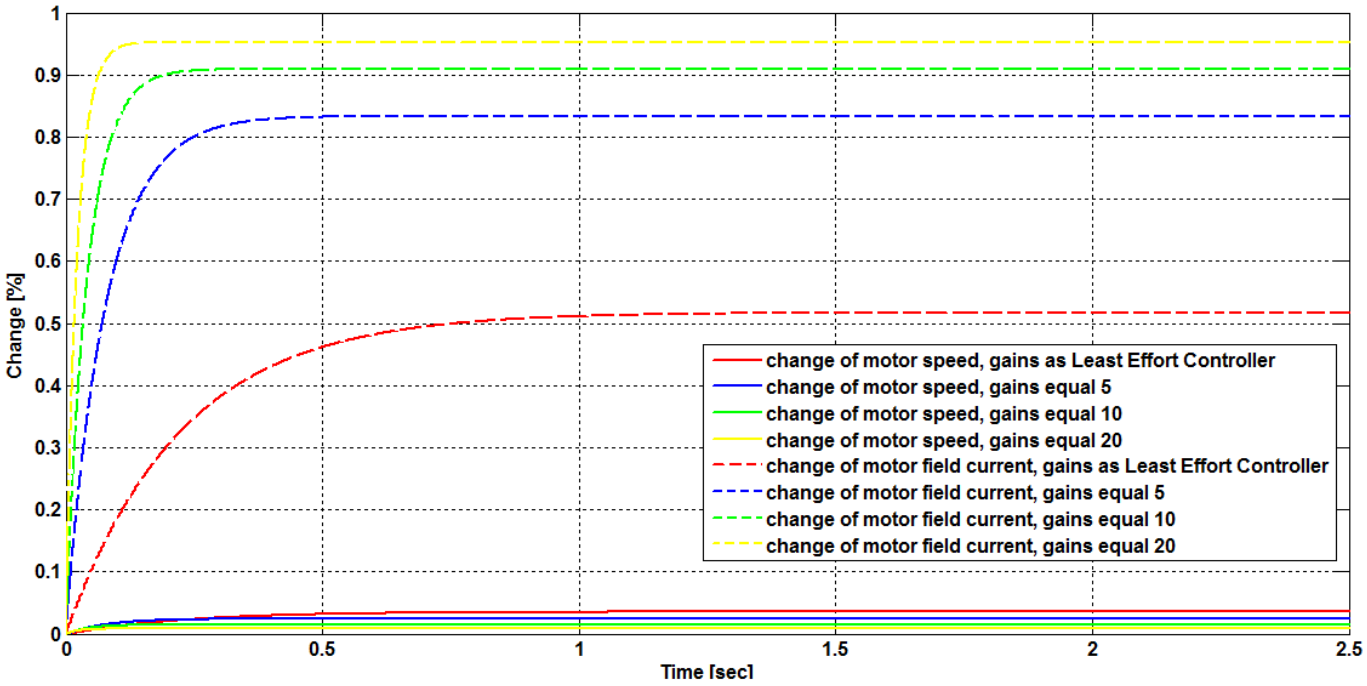

Figure 5.14: Percentage changes in the motor angular speed and the motor field current, as a result of a unit step input on $r_2(t)$, with $r_1(t) = 0$, for different gains.

To investigate the effect of the forward gains on the system disturbance rejection, the responses of the system, following unit step changes on each of the first disturbance $\delta_1(t)$ and the second disturbance $\delta_2(t)$, are simulated for different values of the forward gains. These system responses are shown in figures 5.15 and 5.16.

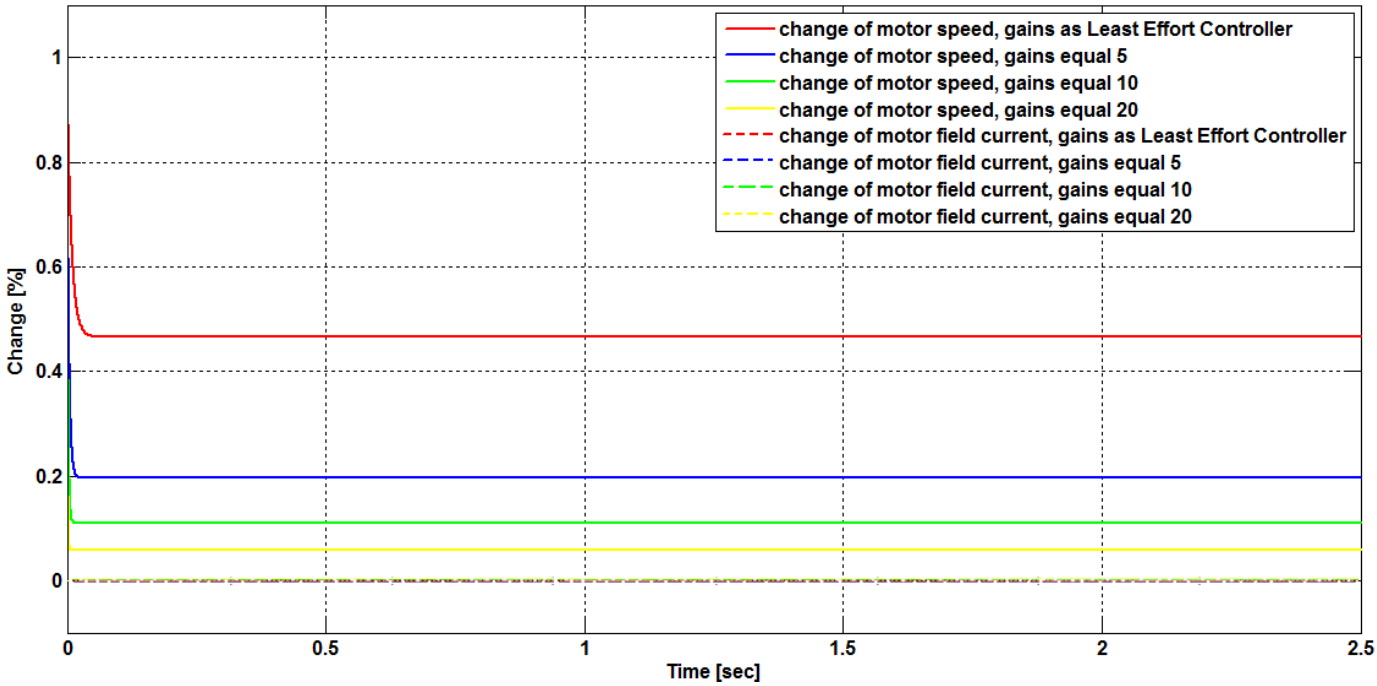

Figure 5.15: Percentage changes in the motor angular speed and the motor field current, as a result of a unit step change on $\delta_1(t)$, for different gains.

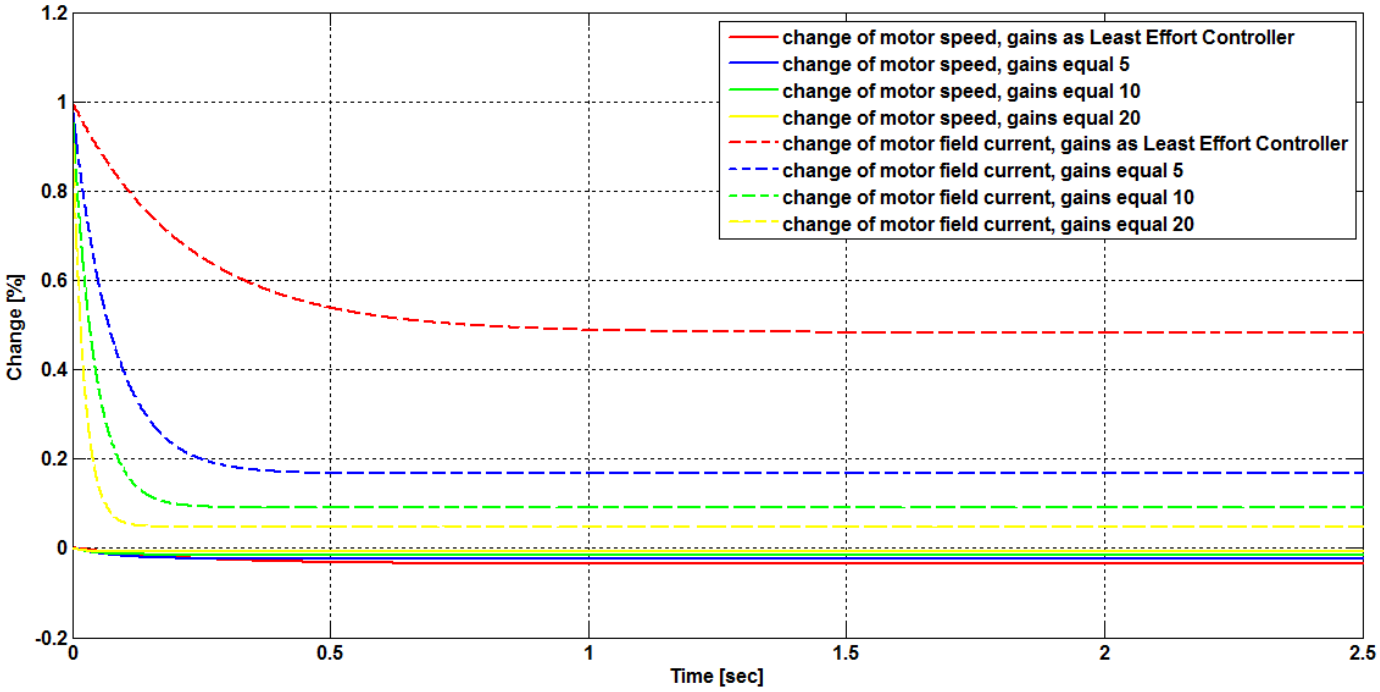

Figure 5.16: Percentage changes in the motor angular speed and the motor field current, as a result of a unit step change on $\delta_2(t)$, for different gains.

It is clearly seen from these figures that increasing the forward gains increases the disturbance recovery rates.

Figure 5.17 shows the energy consumed by the controller, following the imposition of random disturbances on the both outputs, for different values of the forward gains. It

can be noticed from this figure that with increasing the value of forward gains, the control energy increases very rapidly.

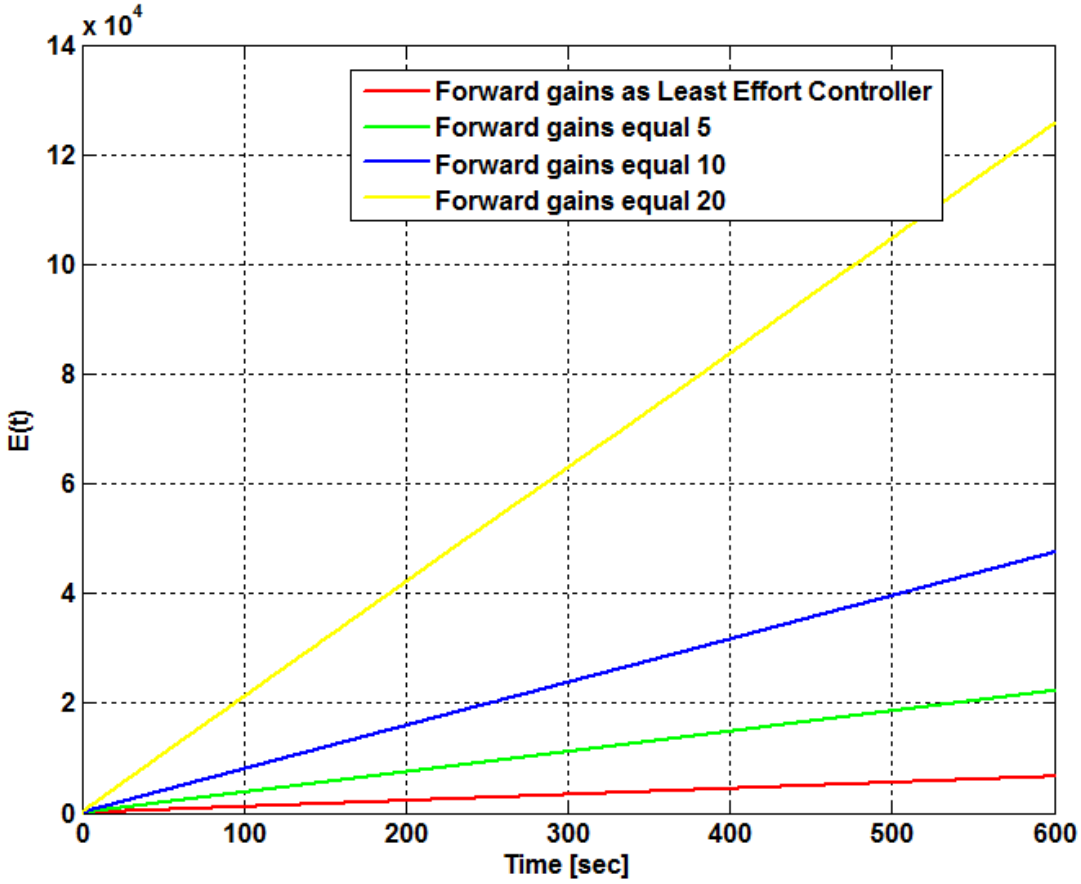

Figure 5.17: Control energy with random sisturbances on the two outputs, with $r_1(t) = r_2(t) = 0$, for different gains.

Chapter (6)

The Optimal Controller

6.1 Introduction

According to the modern control theory, founded by Kalman, the continuous linear time-invariant system can be represented by the state-space equations. These equations are:

$$\dot{X}(t) = A.X(t) + B.U(t) \tag{6.1}$$

$$Y(t) = C.X(t) + D.U(t) \tag{6.2}$$

The first equation is called the state equation, while the second equation is called the output equation.

In these equations, A is a square matrix of order n and is called the state (or system) matrix, B is nxm matrix and is called the input matrix, C is rxn matrix and is called the output matrix, D is rxm matrix and is called the feedthrough (or feedforward) matrix, while X is $nx1$ state vector, U is $mx1$ input vector and Y is $rx1$ output vector.

The system transfer function can be found from the system state-space eqution, defined above.

Laplace transforming, with zero initial conditions, for each of the state equation (6.1) and the output equation (6.2) give, respectively:

$$s.X(s) = A.X(s) + B.U(s) \tag{6.3}$$

and:

$$Y(s) = C.X(s) + D.U(s) \tag{6.4}$$

From these two equations, it is found that:

$$Y(s) = \left[C.(s.I - A)^{-1}.B + D\right]U(s)$$

Or, the system transfer function is:

$$G(s) = \frac{Y(s)}{U(s)} = C.(s.I - A)^{-1}.B + D \tag{6.5}$$

In this equation, matrix I is the identity matrix of order as that of matrix A.

For a strictly proper system, $D = 0$, and the system transfer function becomes:

$$G(s) = \frac{Y(s)}{U(s)} = C.(s.I - A)^{-1}.B \qquad (6.6)$$

This chapter will include the design of a feedback controller for the SEDM using the third approach, namely, the Optimal Control approach. The designed feedback controller will also be simulated and its performance will be analyzed.

6.2 Controllability and Observability

The concepts of contrllability and observability, introduced first by Kalman, paly an important role in the design of the optimal controller. In order to be able to design a feedback controller for a given system, the systen must be controllable and observable.

The condition of controllability of the system is closely related to the existance of a solution of the state feedback for the purpose of placing the eigenvalues of the system arbitrarily. The concept of observability relates to the condition of observing or estimating the state variables from the output variables, which are generally measurable.

A system is said to be completely controllable if every state variable of the system is controllable, or every state variable of the system can be affected to reach a certain value in a finite time by some control input. Or in other words, if any of the system state variables is independent of the control input, there will be no way to drive this particular state to the desired value by means of a control effort, and the system is said to be not completely controllable, or uncontrollable.

Controllability can be investegated by checking the rank of the controllability matrix S, defined as:

$$S = \begin{bmatrix} B & AB & A^2B & \dots & A^{n-1}B \end{bmatrix} \qquad (6.7)$$

For a system, with a state matrix A and an input matix B, to be completely state controllabe, the rank of matrix S must be equal to n.

The concept of observability is quite similar to that of controllability. A system is completely observable if every state variable of the system affects some of the system outputs. Or in other words, an information about system states can be obtained by measurement of the system outputs. If any of the system states cannot be estimated

from the system outputs, the system is said to be not completely observable , or simply unobservable.

Similar to controllability, observability can be investegated by checking the rank of the observability matrix V , defined as:

$$V = \begin{bmatrix} C^T & A^T C^T & \left(A^T\right)^2 C^T & \dots & \left(A^T\right)^{n-1} C^T \end{bmatrix} \quad (6.8)$$

For a system, with a state matrix A and an output matix C, to be completely state observable, the rank of matrix V must be equal to n .

6.3 The Optimal Control Method

The controller structure in the Optimal Control method is shown in the figure below.

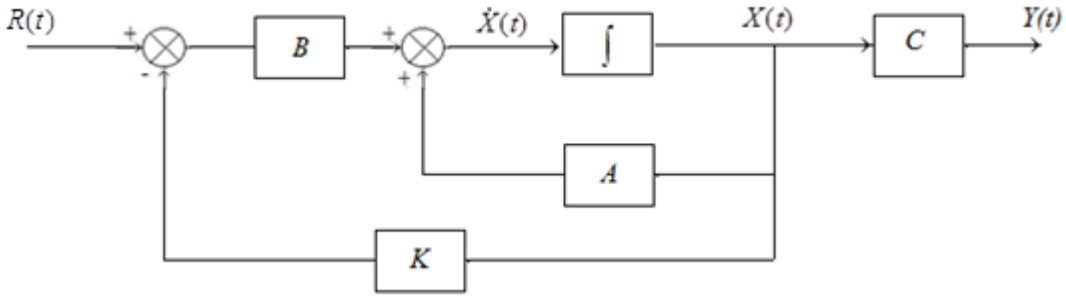

Figure 6.1: Controller structure in the optimal control method.

In this method, state feedback is used. The control law is assumed to be:

$$U(t) = -K.X(t) \quad (6.9)$$

Where K is a constant matrix.

Substituting equation 6.9 in equation 6.1 yields:

$$\dot{X}(t) = (A - B.K).X(t) \quad (6.10)$$

This equation shows that the system behavior depends on the eigen values of the matrix $(A - B.K)$, which can be found by solving the characteristic equation

$$|\lambda.I - (A - B.K)| = 0 \quad (6.11)$$

In order the closed-loop system to be stable, the roots of equation 6.11 should have negative real parts. So, for a system with A and B matrices, the design objective will be to find the matrix K that will place the poles of the closed loop system in

suitable s-plane locations and minimizes the quadratic performance index J , defined as:

$$J = \int_0^\infty \left(X^T Q.X + U^T R.U \right) dt \tag{6.12}$$

In this definition, Q and R should be square, symetric and positive definite or positive semi definite matrices. They are the weighting matrices of the state and the input vectors, respectively. J is always a scalar quantity.

An alternative definition of the performance index J , can be defined as:

$$J = \int_0^\infty \left(Y^T Q.Y + U^T R.U \right) dt \tag{6.13}$$

In this defintion, the state vector X is replaced by the output vector Y .

The gain matrix K is determined as:

$$K = R^{-1} B^T .P \tag{6.14}$$

Where P is found by solving the algebriac Riccati equration (ARE):

$$A^T P + PA - PBR^{-1} B^T P + Q = 0 \tag{6.15}$$

As said before, the weighting matrices, matrices Q and R , should be square, symetric and positive definite or positive semi definite matrices. A good intial selection of these two matrices is that:

$$Q = \begin{bmatrix} q_1 & 0 & 0 & \dots & 0 \\ 0 & q_2 & 0 & \dots & 0 \\ 0 & 0 & q_3 & \dots & . \\ . & . & . & . & . \\ 0 & 0 & 0 & \dots & q_n \end{bmatrix} \tag{6.16}$$

and:

$$R = \begin{bmatrix} r_1 & 0 & 0 & \dots & 0 \\ 0 & r_2 & 0 & \dots & 0 \\ 0 & 0 & r_3 & \dots & . \\ . & . & . & . & . \\ 0 & 0 & 0 & \dots & r_n \end{bmatrix} \tag{6.17}$$

Where:

$$q_i = \frac{1}{(x_{i,\max})^2} \tag{6.18}$$

And:

$$r_i = \frac{1}{(u_{i,\max})^2} \tag{6.19}$$

After simulating the system with these initial values of the weighting matrices, the elements of these matrices are adjusted till the required performance of the system is achieved.

6.4 Optimal Controller For the Separetly-Excited DC Motor

The design of the optimal controller requires the system to be represented in the sate-space form. From equations (3.51), the state equation of the SEDM is given by:

$$\begin{bmatrix} \dot{\omega} \\ \dot{i}_f \end{bmatrix} = \begin{bmatrix} -54.68 & 11.05 \\ 0 & -2.15 \end{bmatrix} . \begin{bmatrix} \omega \\ i_f \end{bmatrix} + \begin{bmatrix} 1.23 & 0 \\ 0 & 0.043 \end{bmatrix} . \begin{bmatrix} v_a \\ v_f \end{bmatrix} \tag{6.20}$$

And the output equation is:

$$\begin{bmatrix} y_1 \\ y_2 \end{bmatrix} = \begin{bmatrix} 1 & 0 \\ 0 & 1 \end{bmatrix} . \begin{bmatrix} \omega \\ i_f \end{bmatrix} \tag{6.21}$$

Here, the system states are the motor angular speed and the motor field current, the inputs are the motor armature voltage and the motor field voltage. The system outputs are the same as the system states.

From these equations, it can be concluded that:

$$A = \begin{bmatrix} -54.68 & 11.05 \\ 0 & -2.15 \end{bmatrix} \tag{6.22}$$

$$B = \begin{bmatrix} 1.23 & 0 \\ 0 & 0.043 \end{bmatrix} \tag{6.23}$$

$$C = \begin{bmatrix} 1 & 0 \\ 0 & 1 \end{bmatrix} \tag{6.24}$$

The system eigen values are the roots of the characteristic equation:

$$|\lambda . I - A| = 0 \tag{6.25}$$

Or:

$$\left|\lambda.\begin{bmatrix}1 & 0\\ 0 & 1\end{bmatrix}-\begin{bmatrix}-54.68 & 11.05\\ 0 & -2.15\end{bmatrix}\right|=0$$

$$\begin{vmatrix}\lambda+54.68 & -11.05\\ 0 & \lambda+2.15\end{vmatrix}=0$$

$$(\lambda+54.68).(\lambda+2.15)=0$$

Or the system eigen values are:

$$\lambda_1=-54.68\,,\ \lambda_2=-2.15$$

As all the system eigenvalues lie on the left hand complex plane, then the open-loop system of the SEDM is stable.

Testing controlability and observability of the system is the first step in designing the optimal controller. As mentioned before, the controllabilty matrix of the system is:

$$S=\begin{bmatrix}B & AB\end{bmatrix}$$

(6.26)

Substituting values of A and B matrices into the controllabilty matrix, results:

$$S=\begin{bmatrix}1.23 & 0 & -67.256 & 0.47515\\ 0 & 0.043 & 0 & -0.09245\end{bmatrix} \qquad (6.27)$$

Since the rank of the controllability matrix S is 2, i.e, matrix S is a full row rank, hence the system is completely controllable.

System observability is tested by finding the rank of the observabilty matrix, defined by equation 6.8. For our system, the observabilty matrix is:

$$V=\begin{bmatrix}C^T & A^TC^T\end{bmatrix} \qquad (6.28)$$

Substituting values of A and C matrices into the observability matrix, yields:

$$V=\begin{bmatrix}1 & 0 & -54.68 & 0\\ 0 & 1 & 11.05 & -2.15\end{bmatrix} \qquad (6.29)$$

Since the rank of matrix V is 2, i.e, matrix V is a full row rank, hence the system is completely observable.

As the system is completely controllable and oservable, an optimal controller for this system can be designed.

The weighting matrices, Q and R, are selected to be diagonal and positive definite ones. Equations 6.18 and 6.19 can be used to determine the elements of these two matrices. Or:

$$Q = \begin{bmatrix} q_1 & 0 \\ 0 & q_2 \end{bmatrix} = \begin{bmatrix} \frac{1}{(\omega_{\max})^2} & 0 \\ 0 & \frac{1}{(i_{f,\max})^2} \end{bmatrix} = \begin{bmatrix} \frac{1}{10.96^2} & 0 \\ 0 & \frac{1}{8^2} \end{bmatrix} \tag{6.30}$$

$$R = \begin{bmatrix} r_1 & 0 \\ 0 & r_2 \end{bmatrix} = \begin{bmatrix} \frac{1}{(v_{f,\max})^2} & 0 \\ 0 & \frac{1}{(v_{a,\max})^2} \end{bmatrix} = \begin{bmatrix} \frac{1}{400^2} & 0 \\ 0 & \frac{1}{400^2} \end{bmatrix} \tag{6.31}$$

Here, the values of $\omega_{\max}$, $i_{f,\max}$, $v_{f,\max}$ and $v_{a,\max}$ are the ones used for scaling of the model, as in chapter 3.

Matrix P is found by solving the algebriac Riccati equration (ARE), defined by 6.15.

Substituting the values of matrices A, B, Q and R in this equation results:

$$\begin{bmatrix} -54.68 & 11.05 \\ 0 & -2.15 \end{bmatrix}^T \cdot \begin{bmatrix} p_{1,1} & p_{1,2} \\ p_{2,1} & p_{2,2} \end{bmatrix} + \begin{bmatrix} p_{1,1} & p_{1,2} \\ p_{2,1} & p_{2,2} \end{bmatrix} \cdot \begin{bmatrix} -54.68 & 11.05 \\ 0 & -2.15 \end{bmatrix} -$$
$$\begin{bmatrix} p_{1,1} & p_{1,2} \\ p_{2,1} & p_{2,2} \end{bmatrix} \cdot \begin{bmatrix} 1.23 & 0 \\ 0 & 0.043 \end{bmatrix} \cdot \begin{bmatrix} \frac{1}{400^2} & 0 \\ 0 & \frac{1}{400^2} \end{bmatrix}^{-1} \cdot \begin{bmatrix} 1.23 & 0 \\ 0 & 0.043 \end{bmatrix}^T \cdot \begin{bmatrix} p_{1,1} & p_{1,2} \\ p_{2,1} & p_{2,2} \end{bmatrix} + \begin{bmatrix} \frac{1}{10.96^2} & 0 \\ 0 & \frac{1}{8^2} \end{bmatrix} = \begin{bmatrix} 0 & 0 \\ 0 & 0 \end{bmatrix}$$

(6.32)

or:

$$\begin{bmatrix} -54.68 & 0 \\ 11.05 & -2.15 \end{bmatrix} \cdot \begin{bmatrix} p_{1,1} & p_{1,2} \\ p_{2,1} & p_{2,2} \end{bmatrix} + \begin{bmatrix} p_{1,1} & p_{1,2} \\ p_{2,1} & p_{2,2} \end{bmatrix} \cdot \begin{bmatrix} -54.68 & 11.05 \\ 0 & -2.15 \end{bmatrix} -$$
$$\begin{bmatrix} p_{1,1} & p_{1,2} \\ p_{2,1} & p_{2,2} \end{bmatrix} \cdot \begin{bmatrix} 1.23 & 0 \\ 0 & 0.043 \end{bmatrix} \cdot \begin{bmatrix} 160000 & 0 \\ 0 & 160000 \end{bmatrix} \cdot \begin{bmatrix} 1.23 & 0 \\ 0 & 0.043 \end{bmatrix} \cdot \begin{bmatrix} p_{1,1} & p_{1,2} \\ p_{2,1} & p_{2,2} \end{bmatrix} + \begin{bmatrix} 0.008325 & 0 \\ 0 & 0.015625 \end{bmatrix} = \begin{bmatrix} 0 & 0 \\ 0 & 0 \end{bmatrix}$$

(6.33)

This equation can be expressed as four simultaneous quations:

$$-242064\,p_{1,1}^2 - 109.36\,p_{11} - 295.84\,p_{12}\,p_{21} + 0.0083249 = 0 \quad (6.34)$$

$$11.05\,p_{11} - 242064\,p_{11}\,p_{12} - 56.83\,p_{12} - 295.84\,p_{12}\,p_{22} = 0 \quad (6.35)$$

$$11.05\,p_{11} - 242064\,p_{11}\,p_{12} - 56.83\,p_{12} - 295.84\,p_{12}\,p_{22} = 0 \quad (6.36)$$

$$-295.84\,p_{22}^2 - 4.3\,p_{22} + 11.05\,p_{12} + 11.05\,p_{21} - 242064\,p_{12}\,p_{21} + 0.015625 = 0 \quad (6.37)$$

Since P is symmetric, $p_{21} = p_{12}$, and as equations 6.35 and 6.36 are the same, the system of the above four equations is reduced to:

$$-242064\,p_{1,1}^2 - 109.36\,p_{11} - 295.84\,p_{12}\,p_{21} + 0.0083249 = 0 \quad (6.38)$$

$$11.05\,p_{11} - 242064\,p_{11}\,p_{12} - 56.83\,p_{12} - 295.84\,p_{12}\,p_{22} = 0 \quad (6.39)$$

$$-295.84\,p_{22}^2 - 4.3\,p_{22} + 22.1\,p_{12} - 242064\,p_{12}^2 + 0.015625 = 0 \quad (6.40)$$

Solving these equations and using only the positive values of the variables, results:
$p_{11} = 0.0000663725$, $p_{12} = p_{21} = 0.0000099384$ and
$p_{22} = 0.0030424091$

Or the Riccati matrix is:

$$P = \begin{bmatrix} 0.0000663725 & 0.0000099384 \\ 0.0000099384 & 0.0030424091 \end{bmatrix} \quad (6.41)$$

The gain matrix K is calculated using equation 6.14, or:

$$K = \begin{bmatrix} 13.062 & 1.9559 \\ 0.068376 & 20.932 \end{bmatrix} \quad (6.42)$$

To achieve output decoupling at steady state, this loop-gain matrix is decompsed into a forward path gain matrix, K_e, and a backward path gain matrix, H. Or:

$$K = K_e.H \tag{6.43}$$

Where, K_e is found from the equation:

$$K_e = G^{-1}(0)\left[I + G(0).K_e..H\right]S_S \tag{6.44}$$

In this equation S_S is the steady state matrix. For zero steady state interaction, the matrix S_S is the identity matrix. Otherwise, it would have small off-diagonal elements. From equations (6.44) and (6.43) , and for steady state matrix $S_S = \begin{bmatrix} 1 & 0.1 \\ 0.1 & 1 \end{bmatrix}$, as the case with the least-effort controller in chapter 4, it is found that:

$$K_e = \begin{bmatrix} 56.903 & -1.2872 \\ 7.1658 & 70.981 \end{bmatrix} \tag{6.45}$$

and:

$$H = K_e^{-1}.K = \begin{bmatrix} 0.2291 & 0.041 \\ -0.02216 & 0.2908 \end{bmatrix} \tag{6.46}$$

The block diagram of the closed loop system with the optimal controller is shown in figure 6.2.

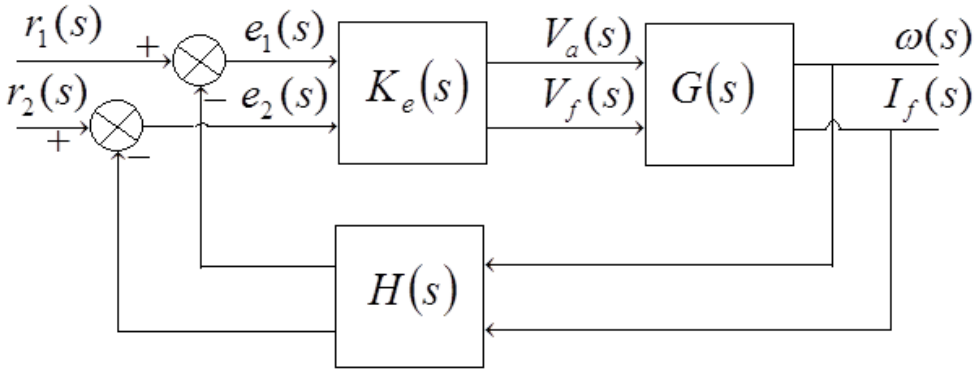

Figure 6.2: Block diagram of the closed-loop system with the optimal control approach.

6.5 Simulations and Results

A MATLAB®/SIMULINK® model, to simulate the performance of the closed loop system, with the values of matrices K_e and H , as given by 6.45 and 6.46, , was built and is shown in figure A.7. This model was simulated for unit step on each of the two inputs, respectively. The simulation results are shown in figures 6.3 and 6.4.

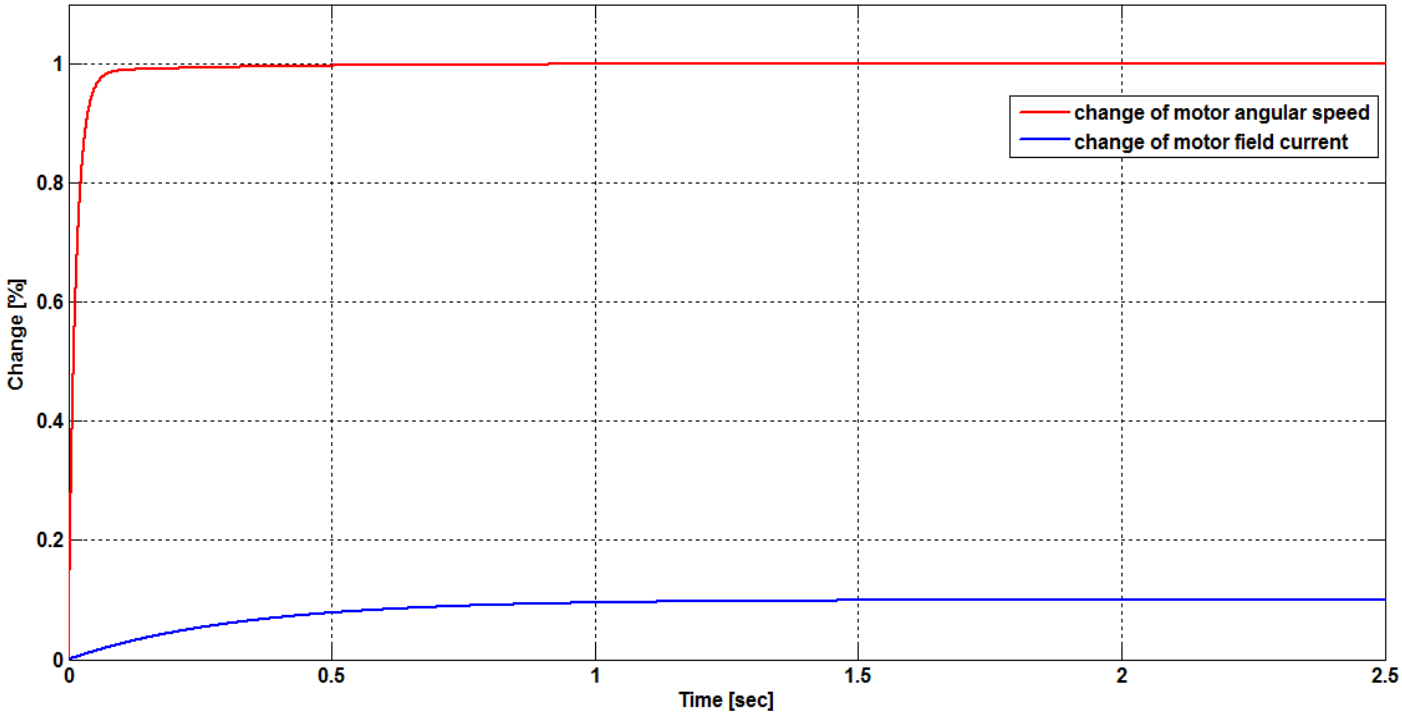

Figure 6.3: Closed-loop response caused by a unit step change on $r_1(t)$, with $r_2(t) = 0$.

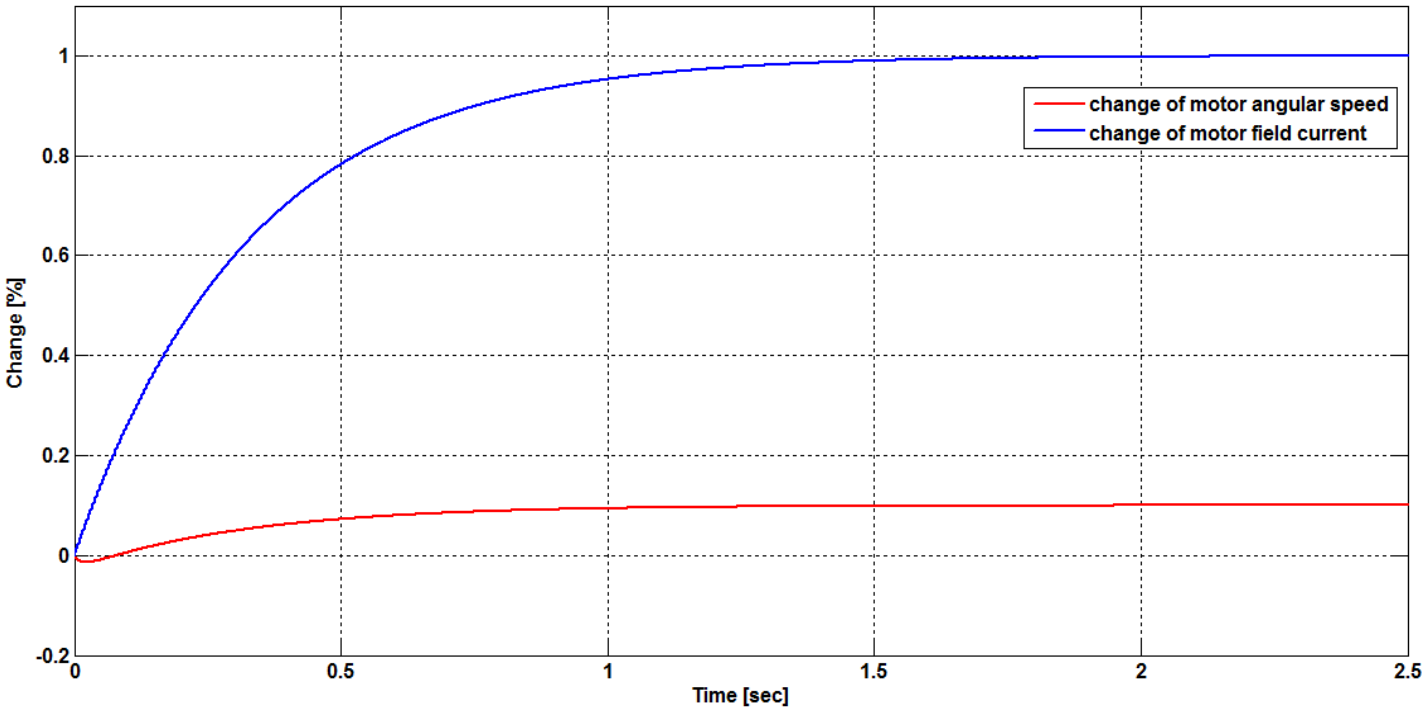

Figure 6.4: Closed-loop response caused by a unit step change on $r_2(t)$, with $r_1(t) = 0$.

Figure 6.3 shows that, a unit step change on the first reference input causes the first output (the motor angular speed) to change by 1%, or no steady state error exists. While, at the same time, the motor field current changes by 0.1% , which means that a 10% coupling is existing between the two outputs.

In the same way, figure 6.4 shows that, following a unit step change on the second reference input, the second output, which is the motor field current, changes by 1%, which means that also no steady state error exists. While, the first output, which is the motor angular speed, changes by 0.1%, which means that a coupling of 10% is also existing between the two system outputs.

The responses of the closed-loop system, caused by unit step changes on each of the first and the second disturbances, $\delta_1(t)$ and $\delta_2(t)$ respectively, are shown in figures 6.5 and 6.6, respectively. It can be seen from these two figures that the disturbance suppression for each of $\delta_1(t)$ and $\delta_2(t)$ is around 25%, which is very poor.

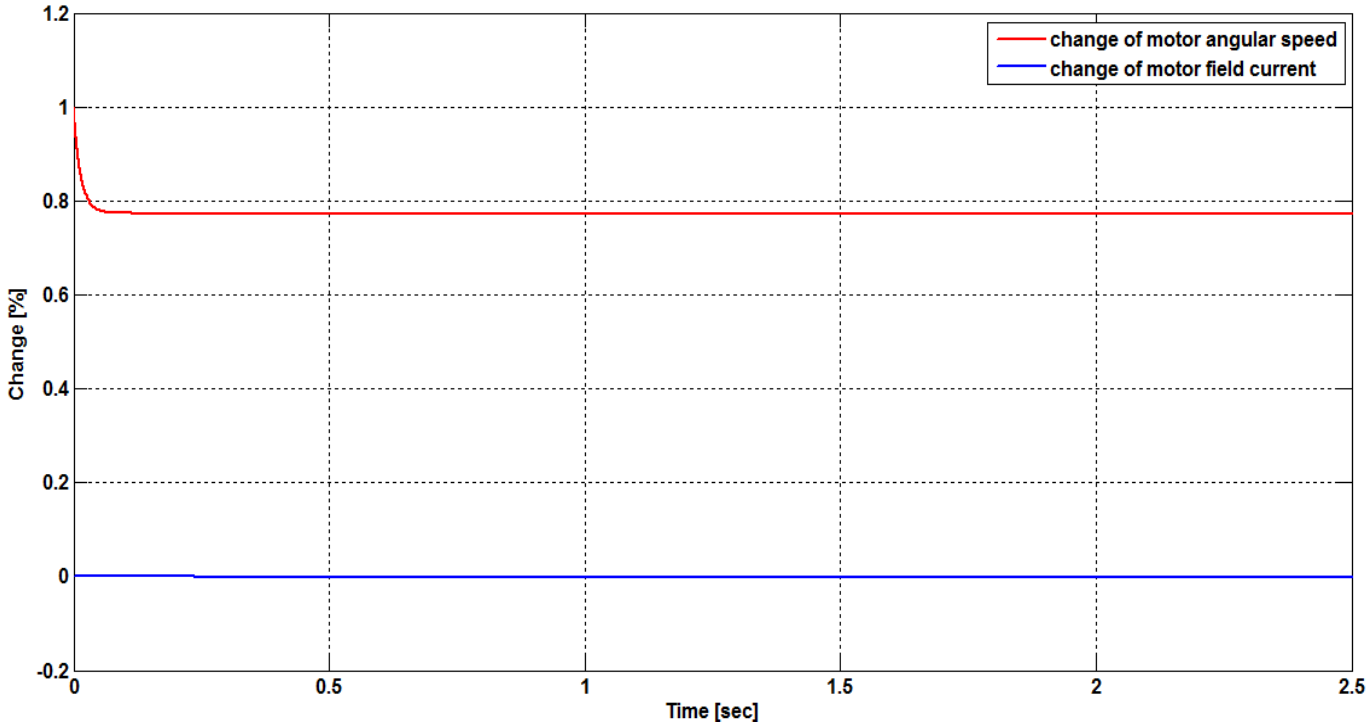

Figure 6.5: Percentage changes in the motor angular apeed and the motor field current, as a result of a unit step input on $\delta_1(t)$.

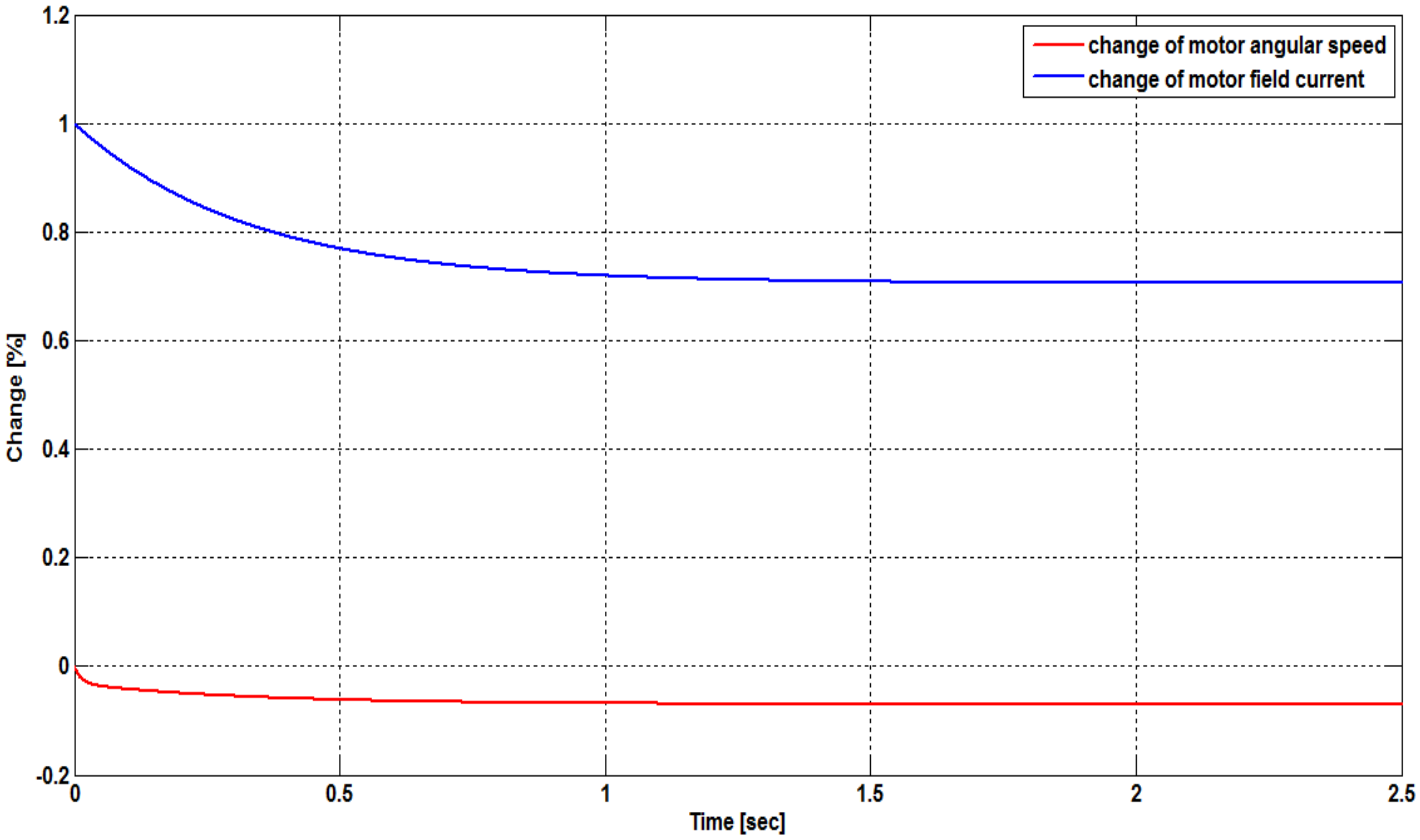

Figure 6.6: Percentage changes in the motor angular speed and the motor field current, as a result of a unit step input on $\delta_2(t)$.

The control energy is computed from:

$$E(t) = \int_0^T \left({u_1}^2(t) + {u_2}^2(t) \right) dt \tag{6.55}$$

Figure 6.7 shows the energy consumed by the controller, following the imposition of random disturbances of the both outputs, for a period of $10\,\text{min}$.

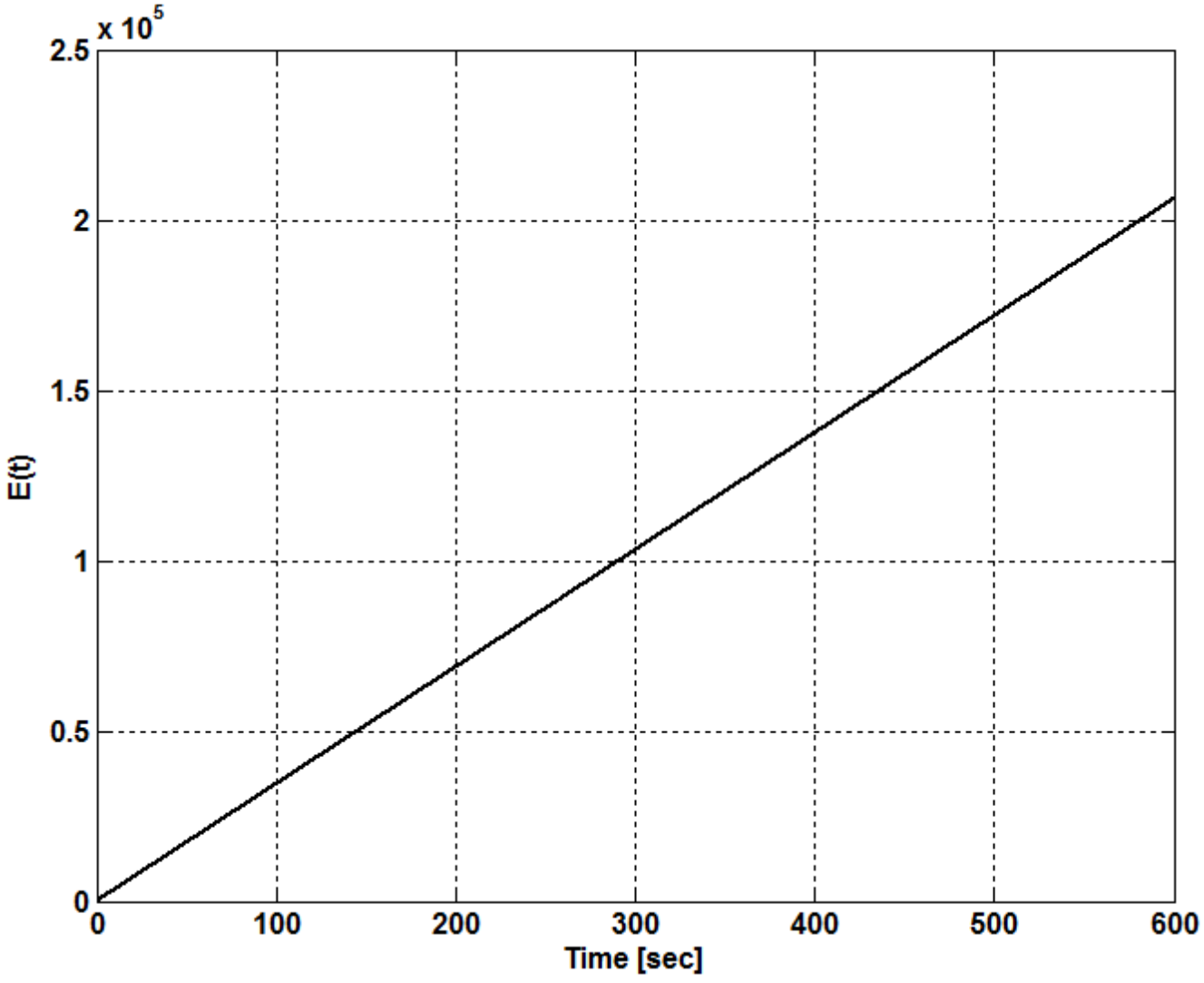

Figure 6.7: Control energy with random disturbances on the two outputs and $r_1(t) = r_2(t) = 0$.

Chapter (7)

Comparative Study and Discussion

7.1 Introduction

In this research, three approaches were used to design a controller for a separately excited DC motor. These approaches are namely the least effort approach, as outlined in Whalley, R. and Ebrahimi, M., the Inverse Nyquist Array (INA) approach, as an example from the British school, and the Optimal Control approach, as an approach from the American school. Each of the above stated approaches found to have its advantages and disadvantages.

The separately-excited DC motor is represented as a multi-input, multi-output (MIMO) system. The armature voltage V_a and the field voltage V_f are the control inputs, while the controlled outputs are the motor angular speed ω and the motor field current I_f.

This chapter includes a detailed comparative study between the three above mentioned approaches. The comparison covers four important aspects:

1. The practicality of the controllers and the difficulties of application.
2. The responses of the closed-loop systems, caused by a unit step change on each of the two inputs, separately.
3. Disturbance recovery, following a unit step change disturbing each output.
4. The energy consumed by the controller.

7.2 Practicality of the Controller and Difficulties of Application

In the least-effort approach, which is a new method from the British school, the system for which the feedback controller has to be designed, is required to be represented by its transfer function matrix. The controller designed by this approach, as outlined by Whalley, R. and Ebrahimi, M. has two loops. The inner loop ensures stable dynamics, while the outer loop ensures steady state interactions with necessary disturbance rejections. The generalized block diagram of a two-input, two-output

system with a least effort feedback controller is shown in figure 4.1. In this method a performance index, representing the energy consumed by the controller, is defined. The parameters of the controller are selected such that the mimimum of this performance index is achieved. For further analysis of this approach, see Whalley, R. and Ebrahimi, M. (2006). This approach is relativey easy and can be applied for complicated systems with many inputs and output. A MATLAB® program for designing a least-effort controller for a separetly-excied DC motor is attached in the appendix.

The Inverse Nyquist Array (INA) method, developed by Rosenbrock in 1969, is another method from the British school, which also requires the multivariable system to be represented by its transfer function matrix. In this method, the system is controlled by a pre-compensator matrix $K(s)$ with closing single-input, single-output (SISO) feedback loops, as shown in figure (5.1).

In order to decrease the system output interaction, a diagonally-dominant closed-loop transfer function has to be found. This will reduce the design process to designing a set of independent single loops. The diagonal dominance of a given transfer function matrix can be checked graphically by superimposing a set of Gershgorin bands, with centers on the diagonal elements of the transfer function matrix. A MATLAB® program for building such diagrams is attached in the appendix.

In the literature different methods are suggested to help finding the pre-compensator matrix $K(s)$, that induces diagonal dominance, . One method, which has proved useful, is to try to diagonalize the system at one frequency, for example at zero or at infinity, and hope that the effect will be sufficiently beneficial over a wide range of frequencies. Here, $K(s)$ will be a matrix of real constants, (Munro, 1972). It has to be mentioned also that in some cases diagonal dominance of the transfer function matrix can be achieved by re-ordering the inputs and/or the system outputs.

The optimal control is an approach from the American school. It requires the system to be represented in a state-space form. State feedback is used in this approach, as shown in figure 6.1. In order to apply this approach, the system must be completely controllable and completely observable. Controllability and oservability of a given

system are ensured by checking the ranks of the controllability and the observability matrices of the system. In this method a quadratic performance index is built, using two weighting matrices, determining the closed loop response of the system. These two matrices are selected in some arbitrary manner as no direct guidance are existing for their selection. Moreover, if non-measurable states are existing, an observer to estimate these states will be needed. This adds complexity to the control system design.

From the above, it can be concluded that the controller by the least effort control is the simplest and the most direct one.

7.3 Closed-Loop Responses

Closed-loop responses following a unit step change on each of the two reference inputs, for the system with different types of controllers are shown in figures 7.1 and 7.2.

Figure 7.1, shows the closed-loop responses, following a unit step change on the first reference input for the different types of controllers.

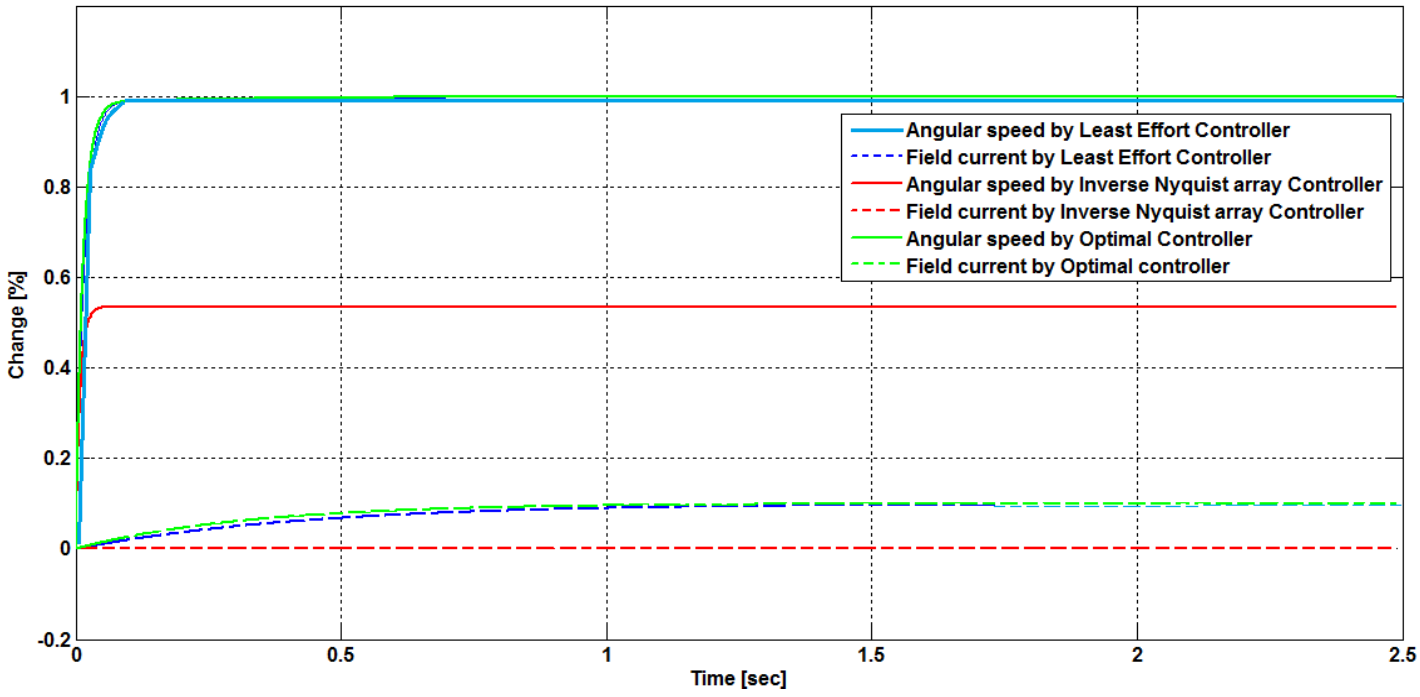

Figure 7.1: Closed-loop responses caused by a unit step change on $r_1(t)$, with $r_2(t) = 0$, for the different types of controllers.

From this figure, it is clearly seen that for the system with a Least Effort controller or the system with an Optimal controller, no steady state error exists in the motor angular speed. While for the system with Inverse Nyquist Array Controller, having forward gains the same as that for the Least Effort Controller, a large steady stare error (around 45%) exists. Moreover, the coupling with the second output (motor field current) is removed in a system with the Inverse Nyquist Array Controller, compared with almost 10 percent coupling, by the Least Effort Controller and by the Optimal Controller. The figure also shows that no overshoots are existing in the system outputs for the three different types of controllers.

In the same way, figure 7.2, shows the closed-loop responses, following a unit step change on the second reference input, for the different types of controllers.

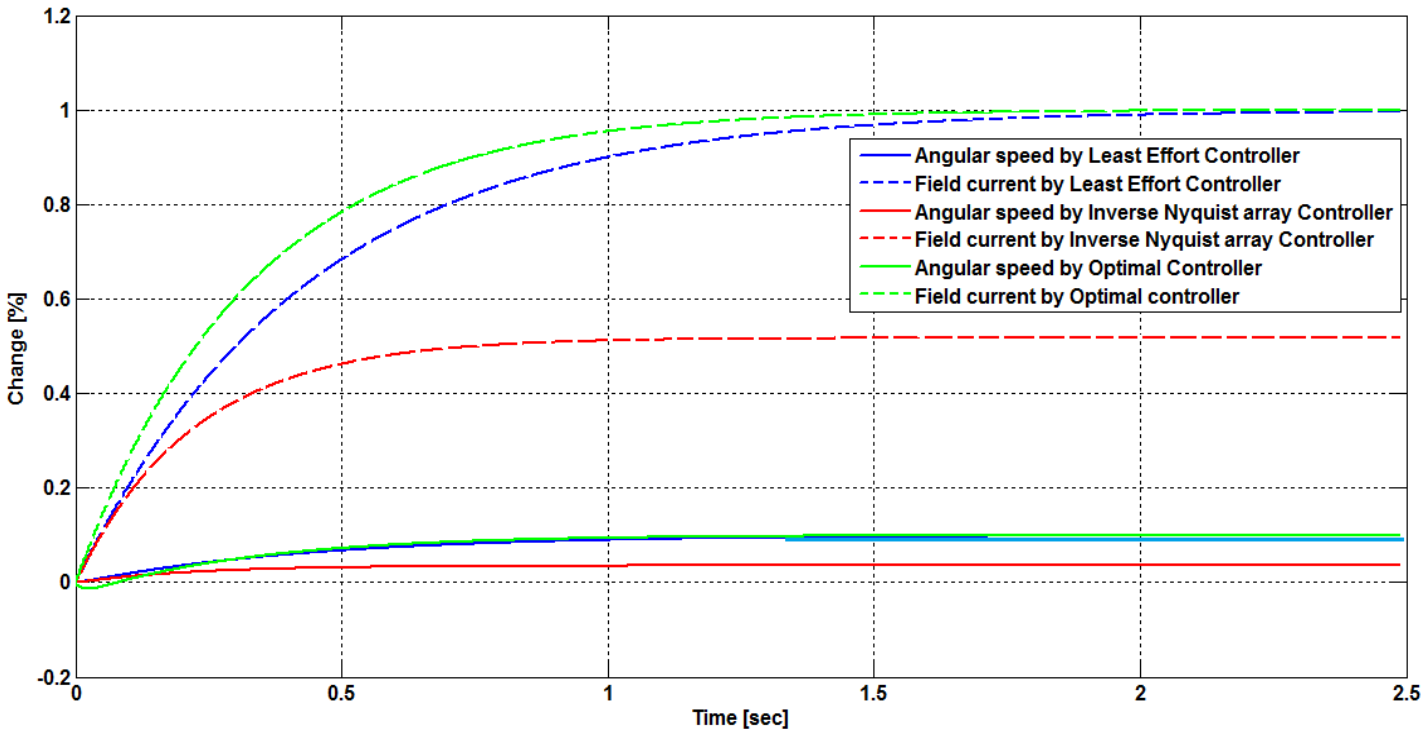

Figure 7.2: Closed-loop responses as a result of a unit step change On $r_2(t)$, with $r_1(t) = 0$, for the different types of controllers.

From this figure, it is seen that for the system with Least Effort controller or the system with Optimal controller, no steady state error exists in the motor field current. While for the system with Inverse Nyquist Array Controller, a large steady state error (around 48%) exists. The interaction of the first output (motor angular speed) is

almost 10 percent for the systems with a Least Effort Controller or with an Optimal Controller. The output interaction in the system with Inverse Nyquist Array controller is less and it is around 2.5 percent only. Again, no overshoots are existing in the system outputs for the three different types of controllers.

From the above, it can be concluded that the Inverse Nyquist Array controller, having forward gains the same as that for the Least Effort Controller, provides a large steady state error, while no error exists in the system with a Least Effort Controller or with an Optimal Controller. As mentioned in chapter 5, the steady state error in the system with an Inverse Nyquist Array controller can be decreased by increasing the values of the forward gains, but this will increase much the energy consumed by the controller, as was shown in chapter 5.

7.4 Disturbance Suppression Capability

Speed disturbances are usually caused by electrical supply fluctuations, loading variations and frictional changes. While, field current disturbances are caused by electrical supply fluctuations and field winding temperature that affects the value of the field winding resistance.

To analyze the capabilities of the different types of controllers to suppress disturbances on the two system outputs, the closed-loop system, with different types of controllers and unit step disturbances on each output, separately, are simulated. The simulation results are shown in figures 7.3 and 7.4.

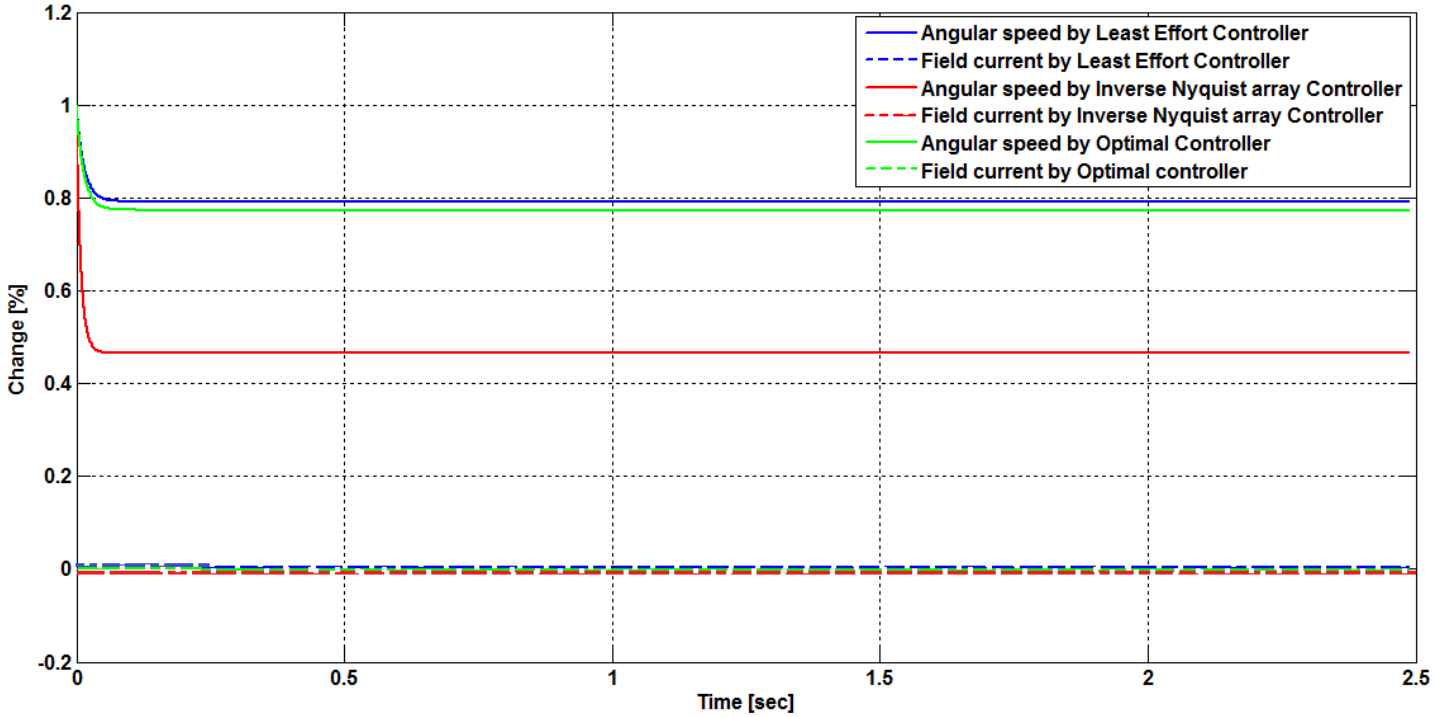

Figure 7.3: Closed-loop responses as a result of a unit step change on $\delta_1(t)$ for the different types of controllers.

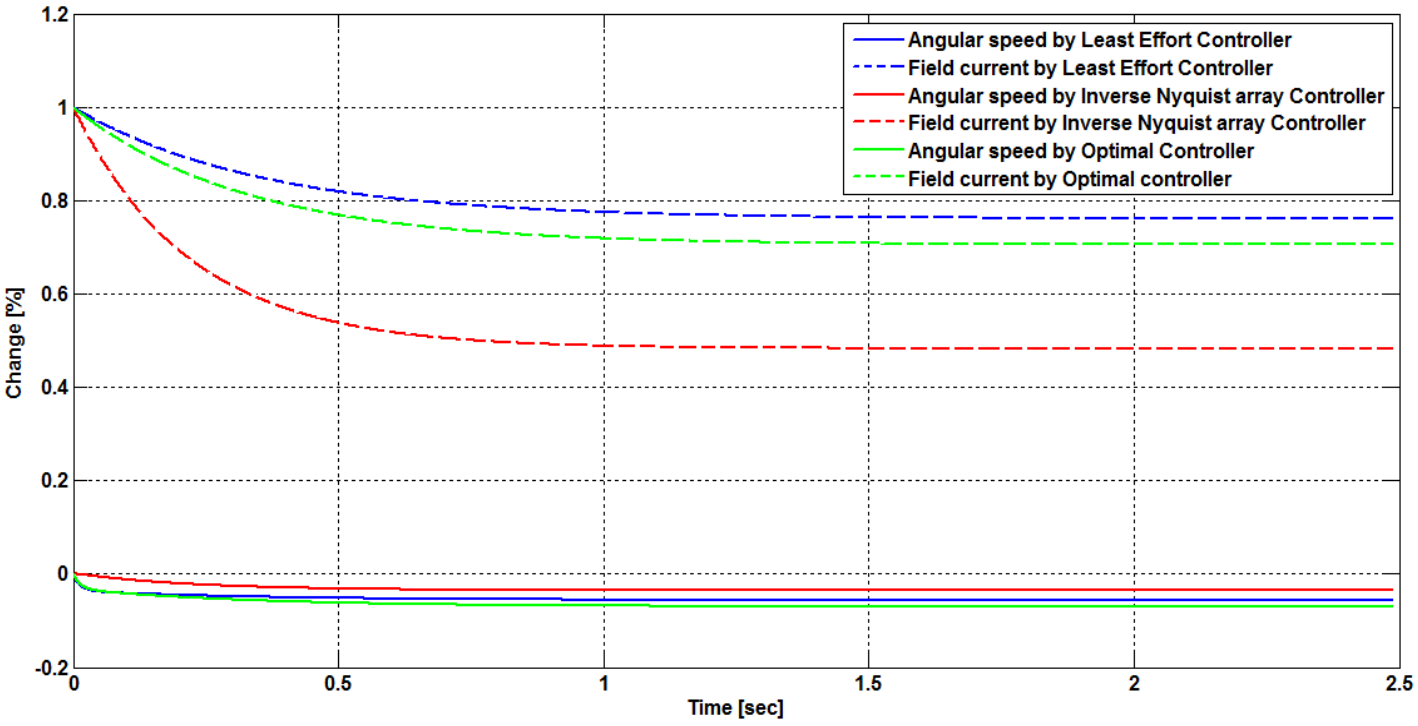

Figure 7.4: Closed-loop responses as a result of a unit step change on $\delta_2(t)$ for the different types of controllers.

Figures 7.3 and 7.4 show that following a disturbance on each of the two outputs, the disturbance suppression of the system with the Inverse Nyquist Array Controller is around 50% and can be further improved by increasing the values of the forward gains. For the system with the Least Effort Controller, the disturbance suppression capability depends on the value of the outer loop feedback gain, f. Increasing the outer loop feedback gain, f, increases the disturbance recovery rates.

For The system with the Optimal Controller, disturbance suppression is very weak and is in the range of 25% only.

7.5 Energy Consumed By The Controller

The energy consumed by the controller, following the imposition of random disturbances on the both outputs for a period of $10\,\text{min}$, could be computed according to Whally, R. and Ebrahimi, M. by:

$$E(t) = \int_0^T \left(u_1{}^2(t) + u_2{}^2(t) \right) dt \qquad (7.1)$$

Figure 7.5 shows the energy consumed by the Least Effort Controller, with $f = 0.1$, and the other two types of controllers.

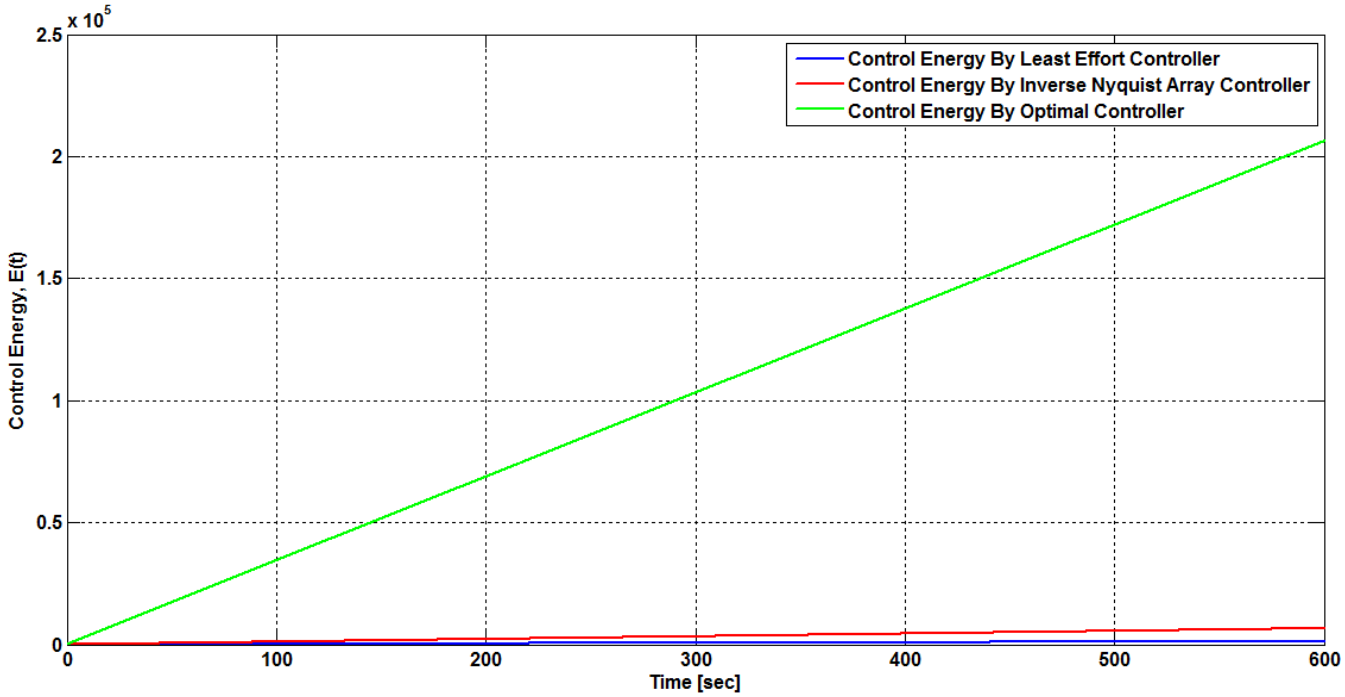

Figure 7.5: Energy consumed by the different types of controllers.

This figure shows that the Least Effort Controller consumes the least control energy, followed by the Inverse Nyquist Array Controller. The energy consumed by the Optimal controller is the highest.

7.6 Conclusions

The following table summarizes the comparisons between the three types of controllers:

Controller Type / Feature	Least Effort Controller	Inverse Nyquist Array Controller	Optimal Controller
Difficulties of Application and Practicality	Relatively easy to be designed and can be applied for complicated systems	- The closed-loop transfer function has to be diagonally dominant. - checking of diagonal dominance is by Gershgorin bands which requires graphical tools. - No systematic methods exist to find pre- or post-compensators that induces diagonal dominance.	- No direct methods are existing for selection of the weighting matrices. They are selected in some arbitrary manner. - If non-measurable states exist, an observer to estimate these states is required.
Steady State Error caused by a Unit Step Change On Each of The Two Inputs.	Zero	Large, and can be decreased by increasing the values of the forward gains.	Zero
Interaction of The First Input With The Second Output	Around 10%	No	Around 10%
Interaction of The	Around 10%	Less, around 3.5% only.	Around 10%

Controller Type / Feature	Least Effort Controller	Inverse Nyquist Array Controller	Optimal Controller
Second Input With The First Output		Can be decreased further by increasing the values of the forward gains.	
Disturbance Suppression Capability	The disturbance suppression capability depends on the value of the outer loop feedback gain. Increasing the outer loop feedback gain improves the disturbance suppression.	Around 50% of the disturbance is suppressed. Can be improved further by increasing the values of the forward gains.	Only, around 25% of the disturbance is suppressed.
Energy Consumed By The Controller	The least	Moderate	The highest

It can be concluded that:

- The Least Effort Controller satisfies all the research objectives. The response of the closed-loop system with this controller is stable and will behaved.

- The performance of the Least Effort Controller, in some aspects, is better than that for the other two types of controllers.

- The Least Effort Controller is the simplest one with the least amount of the control energy consumed.

- The design method of the Least Effort Controller gives freedom to improve the performance of the multivariable system, as it has two loops; the inner loop improves the dynamic response of the system and the outer loop improves the disturbance recovery and reduces the output interaction.

7.7 Recommendations

Because of its advantages, it is recommended to:

- Apply the Least Effort Controller for building drive systems using other types of electric motors, and compare the performance of these controllers with the existing ones.

- Build MATLAB® program(s) to automate the design of the Least Effort Controller for different plants. This will be of great benefit for complicated systems; having large number of inputs and outputs.

References

[1] Whalley, R. and Ebrahimi, M. (2006). "Multivariable System Regulation", *Proceedings of the Institution of Mechanical Engineers, Part C, Journal of Mechanical Engineering Science* May 1, 2006 vol. 220 no.5, pp. 653-667.

[2] Whalley,R., "Spectral Factorization of the Transfer Matrix", *Proc. I Mech E, vol.192*, pp.397-407.

[3] Rosenbrock,H.H., "Design of multivariable control systems using the inverse Nyquist array", *Proc.IEE*, vol.116, No.11, pp.1929-1936.

[4] Sheta, M., Agarwal, V. and Nataraj, P., "A New Energy Optimal Control Scheme for a Separately Excited DC Motor Based Incremental Motion Drive", *International Journal of Automation and Computing, August 2009.*

[5] MUTA, I and IGUCHI, M., "DC Motor Control by Model Following Controller", *Electrical Engineering in Japan, Vol. 106, No. 3, 1986.*

[6] Belletrutti, J.J. and Macfarlane, A.G.J., "Characteristic loci techniques in multivariable-control-system design", *Proc.IEE,* vol.118, No.9, pp. 1291-1297.

[7] Bryson,A.E. "Optimal Control:1950 to 1985", *IEEE Control Systems Magazine*, pp.26-33.

[8] Chin,C.T. &Desoer,C.A., "Controllability and Observability of Composite Systems", *IEEE Trans.Autamat.Cont.*, vol.AC-18, pp.74.

[9] Criss,G.B., "The Inverse Nyquist Plane in Servomechanism Theory", *Proc. I.R.E, pp.1503*-1504.

[10] Dorf,R.C. and Bishop,R.H., *"Modern Control Systems"*, Pearson Education,Inc. Dutton,K.,Thompson,S. and Barraclough ,B.(1997).

[11] Hawkins,D.J. and McMorran,P.D., "Determination of stability regions with the inverse Nyquist array", *Proc.IEE*, vol.120, No.11, pp.1445-1448.

[12] Hazen,H.L. "Theory of Servo-Mechanisms', *Journal of the Franklin Institute*, vol.218, No.3, pp.279-331.

[13] Jaw,L.C. and Garg,S., "Proportional Control Technology Development in

the United States: A Historical Perspective", *NASA/TM-2005-213978*

[14] Kalman,R.E. "On the General Theory of Control Systems", *Proceedings of the 1st International Congress of Automatic Control held in Moscow, Russia.*

[15] Kouvaritakis, B., *"Characteristic locus methods for multivariable feedback systems design*", Ph.D. thesis, University of Manchester Institute of Science and Technology, England.

[16] Sain,M.K., Peczkowski,J.L. and Melsa, J.L. eds., "Gain Design Method for Multivariable Feedback Systems in: *Alternatives for Linear Multivariable Control*", Chicago: National Engineering Consortium, pp. 299-246.

[17] Lourtie, P.M. "The Inverse Nyquist Array for Non-Square Systems", *American Control Conference,* pp.812-815.

[18] Leininger, G.G. "Diagonal Dominance for the Multivariable Nyquist Array Using Function Minimization", *Final Report, NASA Grant 3063, University* of Toledo Report TR 7701.

[19] Lewis, F.L.*" Applied Optimal Control and Estimation",* Prentice-Hall. Luenberger, D.G. (1964).

[20] Macfarlane, A.G.J. and Kouvaritakis, B., "A design technique for linear multivariable feedback systems", *ibid.*, vol. 25, 837-874.

[21] Maciejowski,J.M. *"Multivariable Feedback Design",* Addison-Wesley Publishing Company

[22] Mayr, O., "The Origins of Feedback Control", *Sci.Amer,*vol.223,pp.110-118 Maxwell, J.C.(1868). On Governors. *Proceedings of the Royal Society,* vol.16, No.100, pp.105-

[23] McMorran,P.D., "Extension of the Inverse Nyquist Method", *Electronics Letters,* vol.6, No.25, pp.800-801.

[24] Munro,N., "Design of controllers for open-loop unstable multivariable system using inverse Nyquist array", *Proc.IEE,*vol.119,No.9,pp.1377-1382.

[25] Munro, N., "Recent Extensions to the Inverse Nyquist Array Design Method", *Proc. 24th IEEE Conference on Decision & Control,* vol.24, pp.1852-1857.

[26] "IEE Colloquium on Successful Industrial Applications of Multivariable Analysis", 14th Feb. , pp.1-4

[27] Narish, K., "Modeling of DC Motors for Control Applications", *IEEE Transactions on Industrial Electronics and Control Instrumentation, 1974 (Volume:IECI-21 , Issue: 2).*

[28] Lewis F.L., *"Applied Optimal Control and Estimation", Prentice-Hall, 1992.*

[29] Whalley,R. , Abdul-Ameer,A. , Ebrahimi, M. and Nikranjbar, A., "Winder Control using a Ward-Leondard System", *Int.Journal Industrial and Systems Engineering,* vol.6, No.2, 2010, pp.129-162

[30] Vandana Jha and Dibya Bharti, "Modeling of Different Components for Speed Control of Separately Excited DC Motor", *VSRD International Journal of Electrical, Electronics & Communication Engineering, Vol. 3 No. 4 April 2013.*

[31] Ismail, K, Tuaimah. F and Hummadi, R., "DC Motor Speed Controller Design Using Pole Assignment Technique for Industrial Application", *Baghdad University, Journal of Engineering, Number 3 Volume 17 June 2011.*

[32] Hashim, A. and Obeid, A., "Optimal Speed Control for Direct Current Motors Using Linear Quadratic Regulator", *Journal of Science and Technology -Engineering and Computer Sciences, Vol. 14, No. 3, June 2013.*

[33] Hummadi R.M.K. Al-Mulla, "Simulation of optimal control for a DC motor using linear quadratic regulator (LQR)", *Baghdad University, Journal of Engineering, Vol.18, 212, pp 340-349.*

[34] Alim, A, and Abubokar, T., "Control of Separately Excited Dc Motor", Journal of Eleetrieal and Electronies Engineering, Volume 4, Number I, May 2011.

[35] Zribi, M and Al-Zamel, A., "Field-Weakening Nonlinear Control of a Separately Excited DC Motor", *Hindawi Publishing Corporation, Mathematical Problems in Engineering, Volume 2007, Article ID 58410.*

[36] Moleykutty, George., Kartik, B and Chiat, A., "Model Reference Controlled Separately Excited DC Motor", *Neural Comput & Applic, 2010.*

[37] K.Venkateswarlu, K. and Chengaiah, Ch., "Comparative Study on DC Motor Speed Control Using Various Controllers", *Research Directions, Volume 1 , Issue 6 / Dec 2013, ISSN:-2321-5488.*

[38] Ogbuka. C., "Performance Characteristics of Controlled Separately Excited DC Motor", *The Pacific Journal of Science and Technology, Volume 10. Number 1. May 2009 (Spring)*

[39] Alasooly, H and Redha.M., "Control of DC Motor Using Different Control Strategies", *Power Control and Optimization, 3rd Global Conference, 2010.*

[40] Salem, F., "Dynamic Modeling, Simulation and Control of Electric Machines for Mechatronics Applications", *International Journal of Control, Automation and Systems, Vol.1, No.2 April 2013.*

[41] Narish, K., "Modeling of DC Motors for Control Applications", *IEEE Transactions on Industrial Electronics and Control Instrumentation, 1974 (Volume:IECI-21 , Issue: 2).*

[42] Kuo, Benjamin C., "Automatic Control Systems", *Prentice-Hall, Inc., Englewood Cliffs, New Jersey, 1975.*

[43] Burns, Ronald, S., "Advanced Control Engineering", *Reed Elsevier plc group, Oxford, 2001.*

[44] Maher, Rami, A., "Optimal Control Engineering With MATLAB", Nova Science Publishers, New York. 2013.

Appendix

1) A Program for Studying the Open-Loop System of a Separately-Excited DC Motor

```
clear all
clc
disp(' A Program for Studying the Open-Loop System of a Separately-Excited DC
Motor')
disp('==================================================')
disp('This program:')
disp('   ')
disp(' 1)Represents the Open-Loop System in State-Space and Transfer function
Forms.')
disp('   ')
disp(' 2)Builds the Tranfer Function for Percent Changes')
disp('   ')
disp(' 3)Plots the output responses for step changes on each of the two inputs')
disp('   ')
disp(' 4)Displaying and Plotting System Poles')
disp('   ')
disp(' 5)Finds the Steady-State Output for Step Changes on the Two Inputs')
disp('**************************************************')
disp('   ')
disp('   ')
disp('Press Enter To Continue')
pause
disp('   ')
disp('   ')

%% The values of the system parameter
Rf=50;
Lf=23.25;
Ra=0.24;
```

```
k1=26.96;
ka=16.33;
kf=613.36;
J=55.5;
c=1200.24;
format compact
 %% Entering the inputs
 % The value of the armature voltage
 Va=input('Input the value of the armature supply voltage   ');
 disp('   ')
 % The value of the field voltage
 Vf=input('Input the value of the field supply voltage   ');
disp('   ')
disp('   ')
clc
 %% State Space Representation of the linear model of th DC motor
disp('System State Matrix is:')
A=[-ka*k1/(J*Ra)-c/J kf/J;0 -Rf/Lf]
disp('--------------------------------------------------')
disp('System Input Matrix is:')
B=[ka/(J*Ra) 0;0 1/Lf]
disp('--------------------------------------------------')
disp('System Output Matrix is:')
C=[1 0;0 1]
disp('--------------------------------------------------')
disp('==================================================')
D=zeros(2);
%% Building the system using the state-space approach
disp('Press Enter To Build The System Model Using The State-Space Approach')
pause
sys=ss(A,B,C,D)
disp('--------------------------------------------------')
disp('==================================================')
```

```
disp('Press Enter To Show The System Transfer Function')
pause
%% Finding the system transfer function
tf(sys)
%% The matrix form of the transfer function
disp('--------------------------------------------------')
disp('==================================================')
disp('Press Enter To Show The System Transfer Function in a Matrix Form')
disp(' ')
pause
syms s
G=C*inv(s*eye(2)-A)*B;
G=simple(G);
disp('The Tranfer Function is:')
pretty(G)
%% Finding the transfer function for percentage changes
disp('--------------------------------------------------')
disp('==================================================')
disp('Press Enter To Show The System Transfer Function For Percentage Changes')
GN=inv([0.1096 0;0 0.08])*G*[4 0;0 4];
GN=simple(GN);
pause
disp('The Transfer Function For Percentage Changes is:')
disp(' ')
pretty(GN)

%% Obtaining The output responses for unit step (1%) change on each input, in turn.
disp('--------------------------------------------------')
disp('==================================================')
disp('Press Enter To Draw The Output Responses For unit step (1%) change On Each
input, in turn')
pause
sys1=tf([44.74 96.35],[1 56.83 117.6]);
```

```
sys2=tf([0],[1 56.83 117.6]);
sys3=tf([17.35],[1 56.83 117.6]);
sys4=tf([2.15 117.52],[1 56.83 117.6]);

t=0:0.001:3;
y1=step(sys1,t);
y2=step(sys2,t);
y3=step(sys3,t);
y4=step(sys4,t);
subplot(2,1,1)
plot(t,y1,'b',t,y2,'r')
grid on
legend('%change of motor angular speed','%change of motor field current')
title('Responses For One Percent Step Change of Armature Voltage')
axis([0,3,-1,1.2]);
subplot(2,1,2)
plot(t,y3,'b',t,y4,'r')
grid on
legend('%change of motor angular speed','%change of motor field current')
title('Responses For One Percent Step Change of Field Voltage')
axis([0,3,-1,1.2]);
%% Obtaining System poles
disp('--------------------------------------------------')
disp('==================================================')
disp('Press Enter To Find System Poles')
pause
[P]=pole(sys)
disp('Press Enter To locate system poles')
pause
figure(2)
pzmap(sys,'k')

%% finding system steady state output for 1% changes of the two inputs
```

```
disp('-------------------------------------------------')
disp('=================================================')
disp('Press Enter To Find System Steady-State Outputs, in Percent Changes, For 1% Changes in The Two Inputs')
pause
Y=limit(s*GN*[1/s 1/s]',s,0);
Y=double(Y);
disp(' ')
disp('Percentage Steady-State Motor Angular Speed,For 1% Changes in The Two Inputs, is:')
W=Y(1)
disp(' ')
disp('Percentage Steady-State Motor Field Current,For 1% Changes in The Two Inputs, is:')
If=Y(2)
```

2) <u>A Program For Designing A Least Effort Controller For The Separately-Excited DC Motor System</u>

```
% A Program For Designing A Least Effort Controller For a
% Separately-Excited DC Motor System.
clear all
clc
disp(' Least Effort Contrller For The Separately-Excited DC Motor System')
disp('*****************************************************')
format compact
%% The Open-Loop Transfer Function
syms s
G=1/(s^2+56.83*s+117.6)*[17.35 44.74*s+96.35;2.15*s+117.5 0];
disp('The open-loop transfer function of the system, G(s), is')
pretty(G)
```

```
disp('-----------------------------------------------------')
%% Expressing G(S) as G(S)=L(s).A(s)/d(s).R(s).Gamma(s)
[A,D]=numden(G);
d=D(1,1)/2000;
A=d*G;
L=eye(2);
R=eye(2);
Gamma=eye(2);
% Displaying A(S),d(s),L(s) and R(s)
disp('Press Enter to display A(s),d(s),L(s),R(s) and Gamma(s)')
disp('-----------------------------------------------------')
pause
disp('A(s) is')
pretty(A)
disp('d(s) is')
pretty(d)
disp('L(s) is')
L
disp('R(s) is')
R
disp('Gamma(s) is')
Gamma

%% Forming the inner product <h.A(s).k>
syms h1 h2 k1 k2 n real
hak=[h1 h2]*A*[k1 k2]';
hak=subs(hak,k2,n*k1);
hak=subs(hak,k1,1);
[hak,how]=simple(hak);
disp('=================================================')
disp('Press Enter to display the inner product<h.A(s).k>')
pause
disp('The inner product is')
```

```
pretty(hak)
%% Forming the matix Q
% forming the first colum of Q
hak1=subs(hak,h2,0);
Q(1,1)=simple((subs(hak1,s,0)/h1));
Q(2,1)=simple((hak1-Q(1,1)*h1)/(s*h1));
% forming the second colum of Q
hak1=subs(hak,h1,0);
Q(1,2)=simple((subs(hak1,s,0)/h2));
Q(2,2)=simple((hak1-Q(1,2)*h2)/(s*h2));
disp('==================================================')
disp('Press Enter to display the matrix Q')
pause
disp('The Q matrix is')
Q
%% Designing the inner loop
sys=tf(1,sym2poly(d));
% Building the root locus
disp('Press Enter to display the root locus of b(s)/d(s)=-1, with unity unmerator')
pause
figure(2)
rlocus(sys)
disp('--------------------------------------------------')
display('The poles are:')
p=pole(sys)
b=[1 2.5]';
% Finding the performance index, J
J=(1+n^2)*b'*inv(Q)'*inv(Q)*b;
J=simple(J);
disp('--------------------------------------------------')
display('Press Enter to display the performance index,J')
pause
pretty(J)
```

```
disp('Press Enter to display the graph of J as a function of n')
pause
figure(3)
ezplot(J)
xlabel('n')
ylabel('J')
grid on
% Finding the minimum of J
% Finding the derivative of J
J1=diff(J);
[num,den]=numden(J1);
J1=num/den;
disp('================================================')
display('Press Enter to display the derivative of the performance index,J')
pause
pretty(J1)
% Finding the values of 'n' for which J is minimum
syms x
J1=subs(J1,n,x);
n=solve(J1);
n=double(n);
disp('=====================================================')
display('Press Enter to display the the values of n for which J has an extremum')
pause
n=sort(n)
% Findind the corresponding values of J
J1=subs(J,n)
% Finding the value of n at which J is the minimum
disp('-----------------------------------------------------------')
disp('Press Enter to display the value of n at which J is minimum')
for nn=1:length(n)
   if isreal(n(nn))==0
      n(nn)=inf;
```

```
   end
end
n=n(isfinite(n));
J=subs(J,n);
pause
n=n(find(J==min(J)))
disp('------------------------------------------------------------')
disp('Press Enter to display the cosseponding value of matrix Q')
pause
Q=subs(Q,n)
% Finding the value of h(s)
disp('------------------------------------------------------------')
disp('Press Enter to display the value of h(s)')
pause
k1=1;
hs=inv(Q)*b/k1
% Finding the value of k
disp('------------------------------------------------------------')
disp('Press Enter to display the value of vector k')
pause
k2=n*k1;
k=[k1 k2]'
% Finding the steady-state value of the transfer function
disp('------------------------------------------------------------')
disp('Press Enter to display the steady-state value of the transfer function')
pause
G0=limit(G,s,0)
% Entering Ss
disp('------------------------------------------------------------')
disp('Press Enter to display the value of Ss')
pause
Ss=[1 0.1;0.1 1]
% Entering the value of f and determining the matrix F
```

```
disp('================================================')
beep
disp('Entering the value of f')
disp('================================================')
f=input('Enter the value of f    ')
pause
F=[f 0;0 f]
% Calculating the feed-forward gain of the outer loop
disp('------------------------------------------------------------')
disp('Press Enter to display the feed-forward gain matrix of the outer loop,p')
pause
P=(inv(G0)+k*hs')*Ss*inv((eye(2)-F*Ss));
P=double(P)
% Calculating the feed-forward gain of the outer loop
disp('------------------------------------------------------------')
disp('Press Enter to display the feed-back gain matrix of the outer loop,H')
pause
H=(inv(P)*k*hs')+F;
H=double(H)
```

3) <u>A Program For Building Gershgorin circles</u>

```
function ger
% A program for building Gershgorin circles
% Inputing the tranfer function elements
g11=tf([44.74 96.35],[1 56.83 117.6]);
g12=tf(17.35,[1 56.83 117.6]);
g21=tf(0.1e-60,[1 56.83 117.6]);% The numerator of g21 is modefied from 0 t0 0.1e-
60 for calculation purposes only.
g22=tf([2.15 117.6],[1 56.83 117.6]);
% Bulding the transfer function
G=[g11 g12;g21 g22];
% Inputing the pre-compensator
K=[1.4043 0;0 1.0715];
```

```
% Calculating the Q matrix
Q=G*K;
% Finding the inverse of Q matrix
g=inv(Q);
%--------------------------------------
% Plotting Gershgorin Circles
[n,m]=size(g);
w=logspace(-1,6,200);
q=0:(pi/500):(2*pi);
for i=1:n
   for j=1:m
      if i==j
         figure(i)
         nyquist(g(i,i));
         grid on
         title(['Nyquist Diagram of G(',num2str(i),',',num2str(j),')'])
         for iest=1:n
            for jest=1:m
               if iest~=jest
                  hold on
                  C=center(g(i,j),w);
                  R=radio(g(iest,jest),w);
                  for k=1:length(C)
                     plot((R(k)*cos(q))+real(C(k)),(R(k)*sin(q))+imag(C(k)),'g-')
                  end
                  hold off
               end
            end
         end
      end
   end
axis([-0.1,1.5,-0.2 1.5])
grid on
```

```
end

%------------ Subfunction ----------
function C = center(g,w)
g=tf2sym(g);
C=subs(g,complex(0,w));
function R = radio(g,w)
g=tf2sym(g);
R=abs(subs(g,complex(0,w)));
%------------ END OF CODE ----------


function g = tf2sym(G)
%TF2SYM - Numerical to symbolic conversion of the transfer function Transfer
Function
% G is the symbolic form of the transfer function
% Syntax:  g = tf2sym(G)
% g is the numerical form of the transfer function
%
% Example:
%    g11=tf([44.74 96.35],[1 56.83 117.6]);
%    g12=tf(17.35,[1 56.83 117.6]);
%    g21=tf(0.1e-60,[1 56.83 117.6]);
%    g22=tf([2.15 117.6],[1 56.83 117.6]);
% The numerator of g21 is modefied from 0 to 0.1e-60 for calculation purposes only.
%    G=[g11 g12; g21 g22];
%    g=tf2sym(G);
%    pretty(g)
%
% Author: Oskar Vivero Osornio
% email: oskar.vivero@gmail.com
% Created: February 2006;
% Last revision: 25-March-2006;
```

```
% May be distributed freely for non-commercial use,
% but please leave the above info unchanged, for
% credit and feedback purposes

%---------- BEGIN CODE ----------
p=sym('p');
[n,m]=size(G);
g=zeros(n,m);
g=sym(g);
for i=1:n
   for j=1:m
      [num,den]=tfdata(G(i,j),'v');
      l=length(den);
      order=l;
      for k=1:l
         A(order,1)=p^(k-1);
         order=order-1;
      end
      n=num*A;
      d=den*A;
      g(i,j)=n/d;
      clear A;
   end
end
% simplifying the answer
g=simple(g);
```

4) MATLAB®/SIMULINK® Models

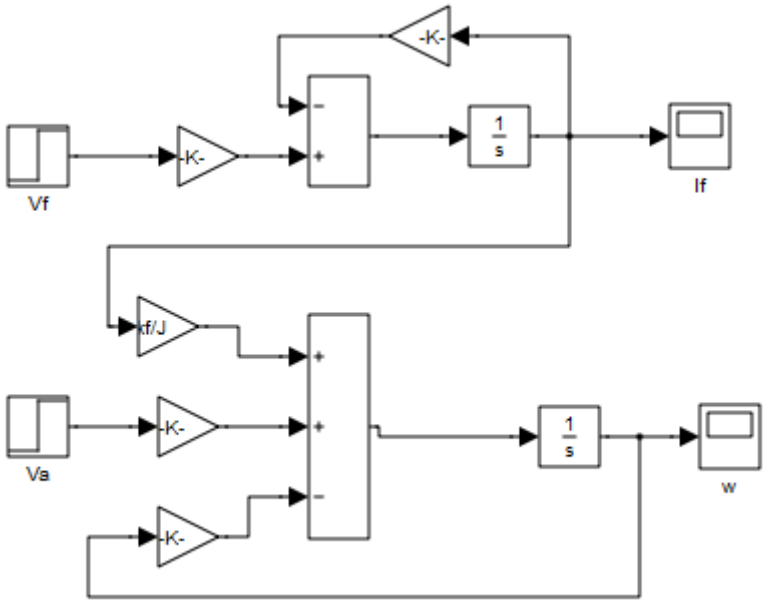

Figure A.1: A MATLAB®/Simulink® model of the separately-excited DC motor, using the state equations.

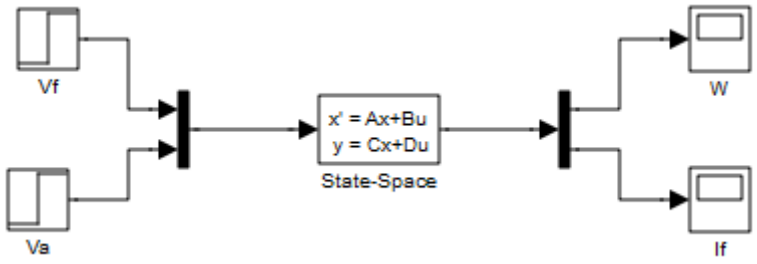

Figure A.2: A MATLAB®/Simulink® model of the separately-excited DC motor, using the state-space representation.

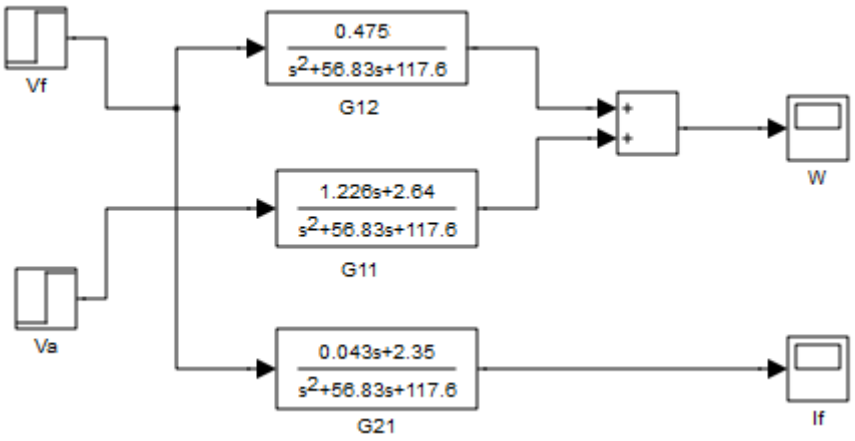

Figure A.3: A MATLAB®/Simulink® model of the separately-excited DC motor, using the transfer-function representation.

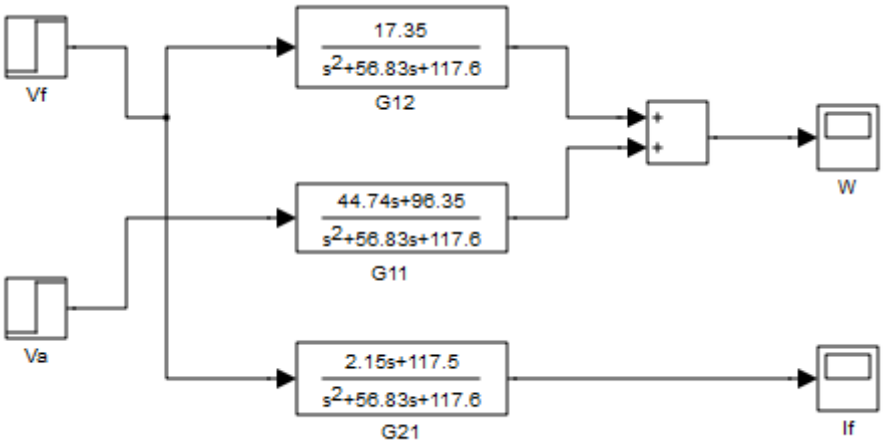

Figure A.4: A MATLAB®/Simulink® model of the separately-excited DC motor, using the transfer-function for precent changes.

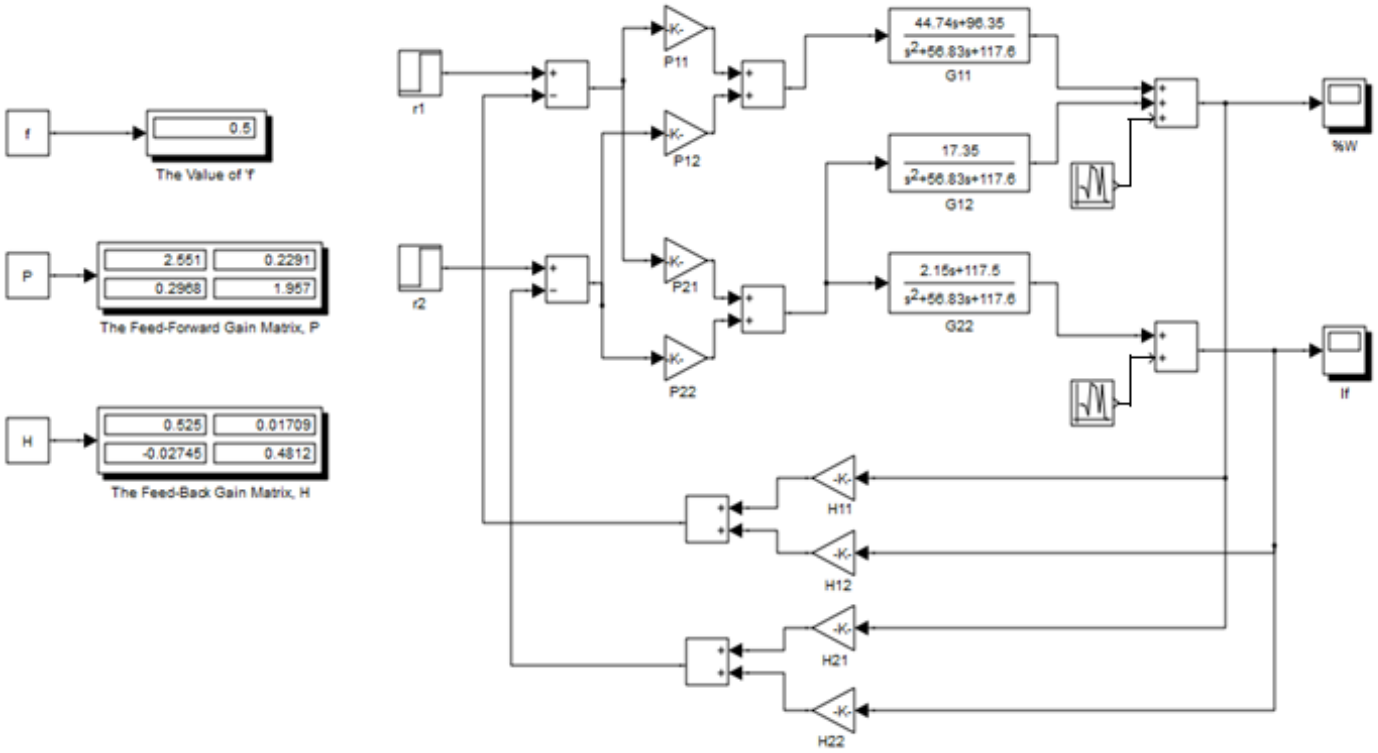

Figure A.5: A MATLAB®/Simulink® model of the separately-excited DC motor with a least-effort controller.

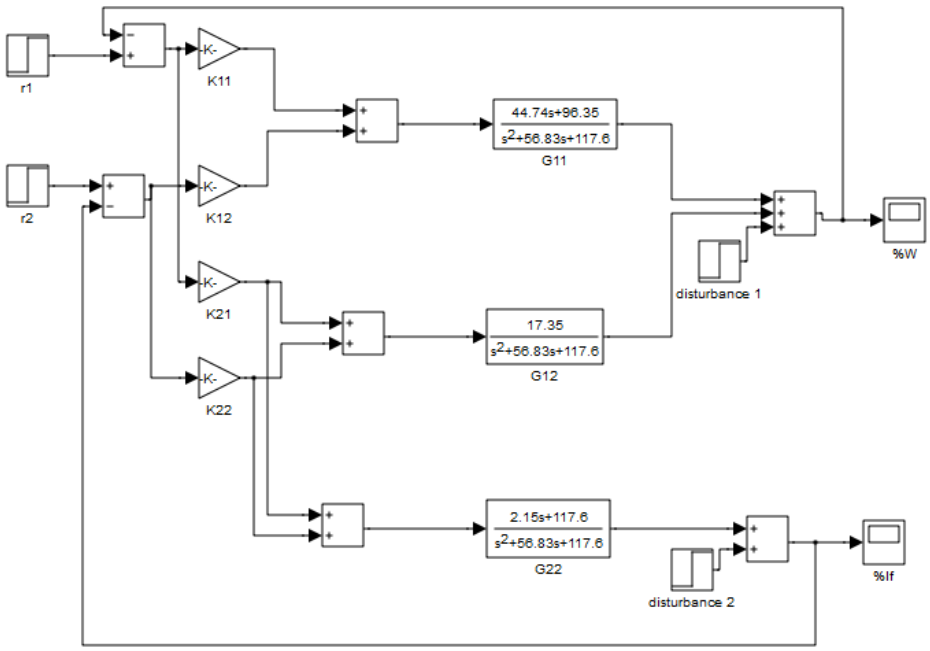

Figure A.6: A MATLAB®/Simulink® model of the separately-excited DC motor with a closed-loop controller using the inverse Nyquist array method.

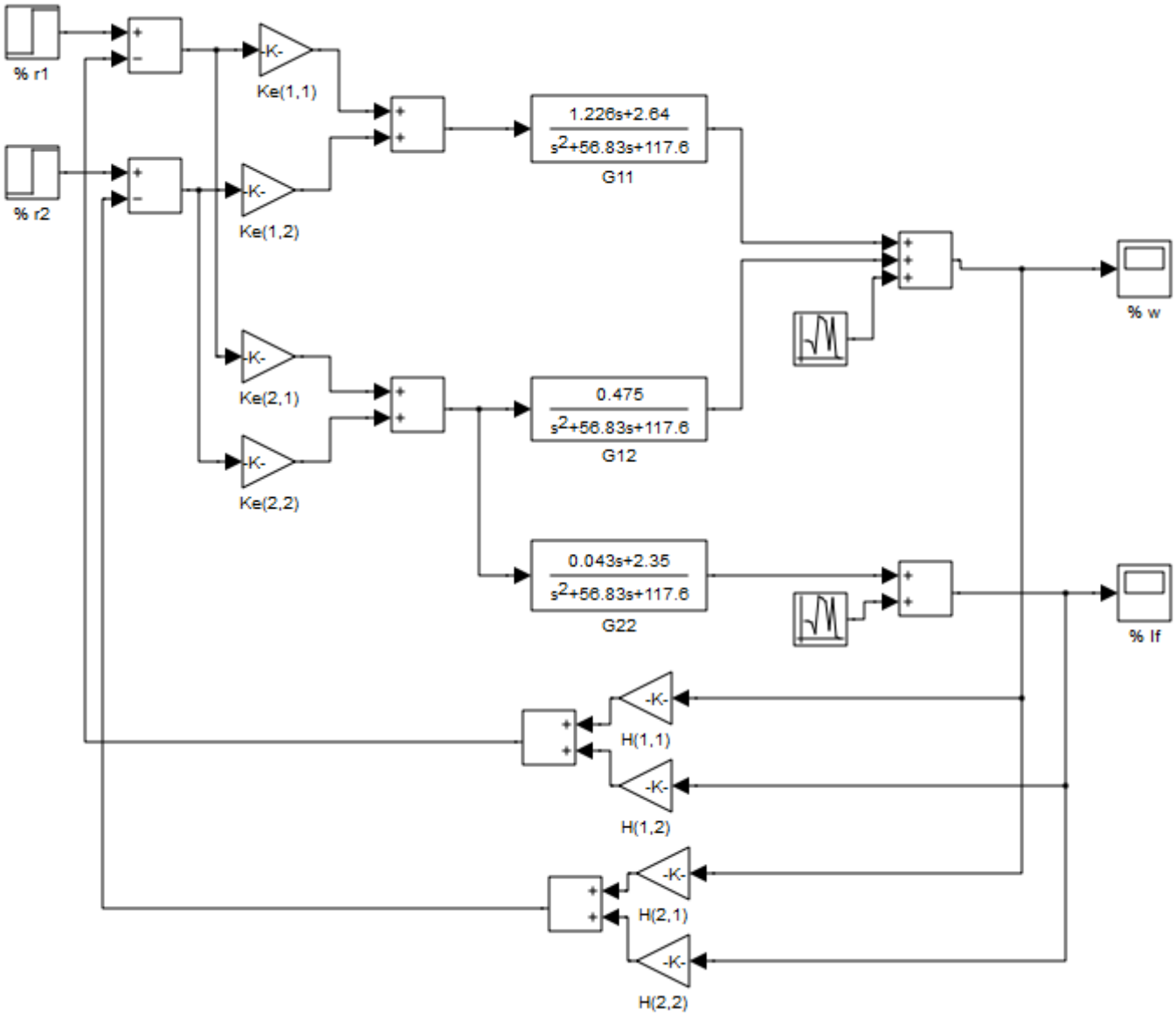

Figure A.7: A MATLAB®/Simulink® model of the closed-loop system with the optimal control approach.